UNIVERSITÀ DI PARMA

UNIVERSITA' DEGLI STUDI DI PARMA

DOTTORATO DI RICERCA IN NEUROSCIENZE

CICLO XXXV

Corticostriatal connectivity in the macaque brain

Coordinatore:
Chiar.mo Prof. Bonini Luca

Tutori:
Chiar.mo Prof. Luppino Giuseppe
Chiar.ma Prof. Borra Elena

Dottorando: Rizzo Marianna

Anni Accademici 2019/2020 – 2021/2022

SUMMARY

Abstract

In the macaque brain, projections from distant, interconnected cortical areas converge in specific zones of the striatum. For example, specific zones of the motor putamen are targets of projections from frontal motor, inferior parietal, and ventrolateral prefrontal hand-related areas and thus are integral part of the so-called “lateral grasping network.”

The present thesis presents two studies on two aspects of the corticostriatal connectivity in the macaque brain whose results extend current models of corticostriatal interactions.

In the study 1, we analyzed the laminar distribution of corticostriatal neurons projecting to different parts of the motor putamen and caudate. After injections of retrograde neural tracers in different parts of the striatum, the laminar distribution of the labeled corticostriatal neurons was analyzed quantitatively. In frontal motor areas, frontal operculum, and prefrontal cortex, where most labeled cells were located, almost everywhere the proportion of corticostriatal labeled neurons in layers III and/ or VI was comparable or even stronger than in layer V. Furthermore, within these regions, the laminar distribution pattern of corticostriatal labeled neurons largely varied independently from their density and from the projecting area/sector, but likely according to the target striatal zone. Accordingly, the present data show that cortical areas may project in different ways to different striatal zones, which can be targets of specific combinations of signals originating from the various cortical layers of the areas of a given network, suggesting more complex modes of information processing in the basal ganglia for different motor and nonmotor functions and opening new questions on the architecture of the corticostriatal circuitry.

In the study 2, again based on neural tracer injections in different parts of the striatum, we analyzed and compared qualitatively and quantitatively the distribution of labeled CSt cells in the two hemispheres in macaque brain. The results showed that crossed CSt projections to the caudate and the putamen can be relatively robust (up to 30% of total labeled cells). The origin of the direct and the crossed CSt projections was not symmetrical as the crossed ones originated almost exclusively from motor, prefrontal, and cingulate areas and not from parietal and temporal areas. Furthermore, there were several cases in which the contribution of contralateral areas tended to equal that of the ipsilateral ones. This study is the first detailed description of this anatomic pathway of the macaque brain and provides the substrate for bilateral distribution of motor, motivational, and cognitive signals for reinforcement learning and selection of actions or action sequences, and for learning compensatory motor strategies after cortical stroke.

1 INTRODUCTION

The “basal ganglia” (BG) are a group of subcortical nuclei responsible primarily for motor control, as well as other roles such as motor learning, executive functions and behaviors, and emotions (Lanciego et al, 2012). These structures are evolutionarily preserved: their basic anatomy and connectivity is conserved across most vertebrates, from the lamprey to humans (Reiner et al 1998, Stephenson-Jones et al 2012). The presence of structures at the basis of the brain has captured the attention of many scientists since antiquity. The Basal Ganglia come to light in works of classical anatomists like Galenus, Vesalius or Willis, and most of the actual nomenclature used to describe basal ganglia structures comes from authors of late 18th and early 19th century (Parent, 2013; Luys, 1868). Pivotal role in motor and non-motor functions, and the association of the basal ganglia with frontal cortical function along with its relationship to multiple neurological and psychiatric diseases, emphasizes the importance of understanding the basal ganglia with respect to cortical function. In the last half of the 20th century the basal ganglia have been a main topic of interest in the field of basic and clinical neurosciences, and the development of neuroimaging and neuroanatomical tracing techniques has allowed to get a description of basal ganglia anatomy and connectivity in different animal species.

1.1 Anatomical organization of Basal Ganglia (BG)

The main components of the Basal ganglia (BG) are: striatum, globus pallidus (GP; internal segment, Gpi, and external segment, GPe), substantia nigra (SN; pars reticulata, SNr, and pars compacta, SNpc) and subthalamic nucleus (SNT).

The striatum is formed from caudate, putamen and nucleus accumbens. Caudate and putamen have the same embryonic origin in fact present similar histological and neurochemical features. Anatomically, these two structures forming the striatum, are in some places separated thanks to the presence of white matter fibers of the internal capsule, but they remain united in some points due to presence of "cellular bridges", which give this striated aspect from which the name of the structure derives. The caudate nucleus is divided into head, body and tail, while the putamen is a large nucleus that forms the lateral portion of the BG. Antero-ventrally the putamen merges with the head of the caudate in a region called ventral striatum. The largest part of the ventral striatum is the nucleus accumbens, an important node of the limbic circuit.

In a median position relative to the putamen is located the globus pallidus, so called because this region is crossed by mostly myelin fibers. The globus pallidus consist of an internal segment and an external segment (GPi and GPe). The putamen and the GP together are called lenticular or lentiform nucleus.

The substantia nigra, so called for its pigmentation, due to the presence of neurons containing melanin, has a ventral portion called pars reticulata (SNr). This pars contains cells very similar to those found in the GPi. The most dorsal portion of the substantia nigra is the pars compacta (SNc), containing dopaminergic neurons, which are firmly packed with each other. The subthalamic nucleus is located below the thalamus and above the SN. From the anatomical point of view, it is closely connected with both segments of the GP and with the SN. Its glutamatergic cells are the only excitatory projections of the basal ganglia.

Basal Ganglia can be usually classified as input nuclei, output nuclei, and intrinsic nuclei. Input nuclei are those structures receiving incoming information from different sources, mainly cortical, thalamic, and nigral in origin. The caudate nucleus (CN), the putamen (Put), and the accumbens nucleus (Acb) are all considered input nuclei. The output nuclei are those structures that send basal ganglia information to the thalamus and pedunculopontine nucleus and consist of the internal segment of the globus pallidus (GPi) and the substantia nigra pars reticulata (SNr). Finally, intrinsic nuclei such as the external segment of the globus pallidus (GPe), the STN and the substantia nigra pars compacta (SNc) are located between the input and output nuclei in the relay of information (Lanciego 2012).

Cerebral cortex sends glutamatergic (excitatory) projections to specific areas of the striatum; it also receives excitatory signals from the thalamic intralaminar nuclei, dopaminergic afferences from the midbrain and serotoninergic projections from the Rafe nucleus. Although the striatum is a rather homogeneous structure from a cytoarchitectural point of view, the use of some specific immunohistochemical markers highlights two subdivisions (Graybiel and Ragsdale 1978; Perth et al. 1976; Desban et al. 1995) characterized by significant anatomical and functional differences: striosomes and matrix.

The matrix compartment is mainly innervated from motor and sensory areas of the cerebral cortex, thalamus and dopaminergic neurons from the SNc, whereas cortical limbic areas, the basolateral amygdala, and ventral parts of the SNc preferentially target striosomes (Graybiel 1984, 1990; Donoghue and Herkenham 1986; Ragsdale and Graybiel 1988; Gerfen 1992; Sadikot et al.,1992a,b; Kincaid and Wilson 1996) Furthermore, matrix send projections to GPe, GPi, and SNr and striosomes

preferentially project to the SNc (Gerfen 1984; Bolam et al. 1988; Kawaguchi et al. 1989; Giménez-Amaya and Graybiel 1990; Fujiyama et al. 2011). About 90% of striatal cells are gabaergic inibitory projection neurons, of medium size with dendritic spines, called medium-sized spiny neurons (MSNs); these receive from the cerebral cortex and constitute the only efferent projection. In the primate brain there are two different populations of these cells: neurons that project to GPi and SNr that produce substance P and dinorphine and neurons projecting to GPe produce encephalin and neurotensin. The two different populations generate two different BG circuits: direct and indirect (Yelnik et al, 2002). Moreover, the two populations of striatal neurons express different dopaminergic receptors: D1 receptors, excitatory, in the neurons of the direct pathway and D2 receptors, inhibitors, in those of the indirect pathway.

About 10% of the striatal neurons are interneurons. The striatal interneurons have smooth dendrites in contrast to MSNs include cholinergic interneurons (ChINs), tonically active, and a diversity of GABAergic interneurons (Assous and Tepper, 2019a; Kreitzer, 2009; Tepper and Bolam, 2004; Tepper et al., 2010). Three main groups of GABAergic interneurons have been traditionally defined: parvalbumin (PV)-expressing (also known as fast spiking interneurons or FSIs), neuropeptide Y and somatostatin (NPY/SOM)-expressing (also termed low-threshold spike or LTS interneurons), and calretinin (CR)-expressing (Kawaguchi et al., 1995) interneurons.

In the last years, genomic-based approaches have allowed to identify novel striatal cell types which are species unique. For example, a new type of striatal interneuron has been described in primates, which is not found in rodents (Krienen et al., 2020), and SPNs have been subdivided into more than the two traditional ‘direct’ and ‘indirect’ pathway categories, based on their molecular definition and anatomical localization (He et al., 2021).

1.2 Intrinsic connectivity of BG

The most basic circuit model of basal ganglia function involving the “direct” and “indirect” pathways has been originally proposed by Albin et al. (1989) and it has represented a central component of our knowledge on basal ganglia function for two decades.

The direct pathway is a mono-synaptic connection that connects the striatum to the internal segment of the globus pallidus (striato-pallidal way) and to the SNr (striato-nigral way). The indirect pathway is a poly-synaptic connection that passes through the GPe and the SNT before reaching the final output structures. Neurons in GPi and SNr are tonically active, also in the absence of cortical

input from striatum. In the direct pathway, striatal gabaergic neurons receive cortical input and project directly to GPi/SNr. An increase in direct pathway activity reduces or stops the neuronal discharge in internal pallidum and SNr, leading to a disinhibition of their projection nuclei (thalamus, pedunculopontine nucleus and superior colliculus). The result is positive feedback on the cortex (reduction of pallidal output and increase in thalamic output) with facilitation of voluntary motor activity.

Gabaergic striatal neurons of the indirect pathway receive cortical afferences and send projections to GPe, which is connected to the SNT by additional inhibitory terminals. SNT uses glutamic acid as a neurotransmitter, therefore it has an excitatory effect on the internal segment of the globus pallidus (GPi) and on the pars reticulata of the substantia nigra (SNr). Therefore, the indirect pathway generates a triple inhibition responsible for negative feedback on the cortex (increase pallidal output and reduction thalamic output), with an inhibitory effect on motor activity. Thus, activation of direct and indirect paths produces opposite effects on the movement. Dopamine release from substantia nigra pars compacta (SNc) regulates activation of these two pathways, indeed striatal neurons projecting directly to the two efferent nuclei have receptors for the neurotransmitter dopamine (D1), with facilitatory action on synaptic transmission, while those of the indirect pathway possess receptors of type D2, with inhibitory action on synaptic transmission.

More recently, a third fundamental pathway of the basal ganglia circuits, so-called "hyperdirect pathway", has been identified (Nambu et al.,2000). Although the subthalamic nucleus (STN) has for many decades been considered one of the relevant nodes of the "indirect" pathway, it also receives direct signals from the cerebral cortex, projects to GPi/SNr and consists of glutamatergic synapses. This cortico-SNT-pallidus pathway sends powerful excitatory signals, bypassing the striatum, therefore the driving times are shorter than the direct and indirect pathway.

Spatial and temporal distributions of basal ganglia activity, and involving of different pathways during voluntary movements, is described by dynamic model of BG functions (Nambu, 2004). According to this model, considering the respective axonal conduction velocities, hyperdirect pathway first inhibit thalamic neurons, then the direct pathway disinhibits them, and finally the indirect pathway inhibits them again. Thus, signals through the hyperdirect and indirect pathways, respectively during initiation and termination of the voluntary movement, inhibits large areas of the thalamus and cerebral cortex that are related to both the selected motor program and other competing programs. (Nambu et al., 2002). In addition to such a temporal aspect, pathways may work in a spatial domain as well. The center-surround model of basal ganglia functions proposes

that direct and indirect pathways work together to select an appropriate motor program and inhibit competing motor programs (Hikosaka et al., 2000; Mink JW, 1996; Nambu et al., 2002). The direct pathway inhibits a specific group of GPi neurons in the center area resulting in the release of the selected motor program; the hyperdirect and indirect pathways excite other groups of GPi neurons in the surrounding area inhibiting in this way other competing motor programs.

In addition to direct, indirect and hyperdirect pathways, in the last years the idea that several other feedback or reverberating circuit can contribute to modulate BG output has developed. A study of Naito and Kita (1994) showed the existence, in rodents, of direct connections between medial and lateral precentral cortices and GPe. Other studies based on tractography support the existence of this direct cortico-pallidal pathway in the human brain (Milardi et al., 2015; Cacciola et al.2017b, 2019; da Silva et al.,2017). Frankle et al (2006), in the macaque brain, have shown, using anterograde tracing, direct connections from orbitofrontal (OFC), and dorsolateral prefrontal cortices (dlPFC) to SN which receive direct connections also from frontal eye field (FEF) (Borra et al., 2015). Additional findings in human support direct cortico-nigral connections for several areas (Cacciola et al.,2016a, 2017b). Recent studies in monkey, with transneuronal transport of rabies virus, have demonstrated that BG communicate with cerebellum. (Hoshi et al.,2005; Dum et al.,2002; Bostan et al.2010; Neumann et al.,2015; Milardi et al, 2015; Cacciola et al.,2016a). Therefore, the BG connectome seems to be more complex than previously described.

1.3 Extrinsic connectivity of BG

The basal ganglia communicate with the cortex via cortico-BG-thalamus-cortex multisynaptic circuits. These ones are closed (segregated) parallel as well as open (split) loops.

Anatomical and physiopathological studies in non-human primates have suggested the presence of at least five different parallel circuits (Alexander et al, 1986), involving different portions of cortex, BG and thalamus, and with different functions. The circuits are parallel, but the same striatal region can receive information from different cortical areas of the same lobe or of different lobes, belonging to certain cortical circuits.

“OCULOMOTOR” CIRCUIT**:** The FEF area (Brodmann area 8) projects to the central region of the caudate body (Kunzle & Akert, 1977), which also receives projections from the dorsolateral prefrontal cortex (areas 9 and 10)and posterior parietalcortex (area 7), areas involved in the eye movement control mechanism. The caudate body projects to the caudal and dorsomedial sectors

of the internal segment of globus pallidus and to the ventrolateral region of SNr (Parent et al., 1984a)**.** These regions project directly to the thalamus, more precisely to the magnocellular portion of the anterior ventral nucleus and to the lateral portion of the mediodorsal nucleus. Both of these thalamic zones send fibers to the FEF of the cerebral cortex (Barbas & Mesulam ,1981), completing the circuit. It has been shown that part of the nigrotalamic neurons give origin to collateral fibers that project also on the superior colliculus, an important eye movement control hub.

"DORSOLATERAL PREFRONTAL" CIRCUIT**:** dorsolateral prefrontal cortex (areas 9 and 10 of Brodmann and area 46 of Walker) send fibers mainly to the dorsolateral region of the caudate head in which also fibers from posterior parietal (area 7) and premotor areas overlap. From the caudate nucleus originate projections directed to the dorsomedial region of the GP and to the rostral region of the SNr. The fibers of these projections are organized so that those coming from the dorsal lateral caudate nucleus (which receives input from dorsolateral prefrontal cortex) mostly end in the lateral regions of the GP and the SN.

The dorsomedial region of the GPi then sends fibers to the parvocellular portion of the ventral anterior thalamic nucleus (Kuo & Carpenter 1973, Kim et al 1976), from which then originate fibers returning to the dorsolateral prefrontal cortex. The rostral region of SNr, on the other hand, sends fibers to the parvocellular region of mediodorsal nucleus of the thalamus (Ilinsky et aI1985), which, subsequently, projects to dorsolateral prefrontal cortex. The dorsolateral prefrontal circuit is involved in the executive functions, which ensure the performance of cognitive tasks such as the organization of behavioral responses and the use of verbal skills in problems solving.

"LATERAL ORBITOFRONTAL" CIRCUIT**:** lateral orbitofrontal cortex (Brodmann's area 10, Walker's area 12) sends fibers to the ventromedial part of caudate nucleus. This part also receives fibers from visual and auditory associative areas, placed respectively in the superior and inferior temporal gyri. The ventromedial part of the caudate nucleus sends projections to the dorsomedial zone of the GPi and in the rostromedial area of the SNr. These structures project, in turn, to the thalamic nuclei and more precisely to the medial regions of the magnocellular part of the anterior ventral nucleus and to the magnocellular part of the mediodorsal nucleus (Carpenter et al 1976, Ilinsky et al 1985). From these thalamic regions fibers flow to the lateral orbitofrontal cortex closing the circuit (Ilinsky et aI 1985). Lateral orbitofrontal cortex is involved in the mediation of empathic and appropriate social life responses. It has been shown in primates that bilateral lesions in lateral orbitofrontal area or in the portion of the caudate to which it projects impair animal's capacity to make appropriate switches in behavioral set (Divac et a11967, Mishkin & Manning 1978).

"ANTERIOR CINGULATE" CIRCUIT**:** this circuit involves the nucleus accumbens, which receives projections from limbic structures namely hippocampus, amygdala and entorhinal (area 28) and perirhinal (area 35) cortex. Because of these connections, the ventral striatum is also defined as "limbic". The ventral striatum is also a target of the anterior cingulate cortex (area 24), frontal lobe, and posterior portion of the medial orbitofrontal area. In rats the ventral striatum projects to the ventral globus pallidus and to substantia nigra. In monkeyit has been shown that from the nucleus accumbens originate fibers directed not only to the ventral GP and the rostrodorsal region of the SNr, but also to the rostrolateral region of GPi. These two structures send projections to the thalamus, more precisely to the posteromedial region of the mediodorsal thalamic nucleus, which in turn closes the circuit projecting towards the anterior cingulate cortex (Jurgens 1983, Tobias 1975, Vogt et aI 1979). This circuit seems to play an important role in the assessment the relevance of emotions and motivational information.

"MOTOR" CIRCUIT**:** The motor circuit involves mainly the putamen, which receives projections from the supplementary motor area, the motor cortex, the somatosensory cortex, and from the arcuate premotor cortex (Alexander et al., 1986). Its afferences from primary motor cortex and ventral, dorsal, and mesial premotor areas are somatotopically organized. Somatosensory areas 3a, 1, 2 and 5 also send somatotopically organized projections that overlap motor areas. According to the somatotopy of the somatosensory cortico-putaminal projections, the leg is represented at dorsolateral level, the face at ventromedial level, and the arm in the intermediate zone between previous regions (Muakkassa & Strick d1979, Brinkman & Porter 1979). The putamen, in turn, sends topographically organized projections to the GPi and GPe (ventrolaterally) (DeVito et al. 1980, Johnson & Rosvold 1971, Parent et al.1984a) and to the caudolateral region of the SNr (Hedreen et al 1980, Nauta & Mehler 1966, Parent et a1 1984b, Szabo 1962, 1967). The motor portions of GPi and SNr project respectively to the oral part of ventrolateral nucleus to antirior ventral nuclei and to the medial part of the ventrolateral nucleusof the thalamus. The motor circuit is closed by projections from the oral part of ventrolateral, anterior ventral, and medial part of ventrolateralnuclei to the supplementary motor area, and to the premotor cortex. This circuit is of utmost importance in controlling the movement of skeletal muscles.

The models based solely on parallel processing, are not adequate to explain how information can be transformed across functional regions to implement learning and adaptability that is necessary in the development of goal-directed behaviors. Evidence from literature in primates and in rodents supports the idea that there are pathways by which information from separate cortico-basal-ganglia

loops can influence each other (Percheron and Filion, 1991; Francois et al., 1994; Joel and Weiner, 1994; Bevan et al., 1996; Bevan et al., 1997; Joel and Weiner, 1997; Groenewegen et al., 1999a; Groenewegen et al., 1999b; Haber et al., 2000; Bar-Gad and Bergman, 2001; McFarland and Haber, 2002). A possible mechanism of integration of information proposed, is the integration across BG regions. While projections from cortex terminate in a general topography in the BG structures, neurons located at the interface between functionally distinct, but topographically adjacent, projections could integrate diverse information, moreover dendrites and axons within each BG structure (for example dendritic arbors in the GP) often cross functional boundaries.(see Bevan et al.,1996; 1997). In this way, distal dendrites from one region invades an adjacent functional area. Another suggested mechanism is through a convergence of terminals from functionally areas onto smaller basal-ganglia regions.There is a dramatic decrease of cerebral tissue volume from the cerebral cortex to BG structure, this suggest a volumic convergence; also striatopallidal system anatomically is characterized by a volumic, a numeric, and a geometric convergence,indeed pallidal neurons are 100 times less numerous than spiny striatal neurons and disposed perpendicularly to striatal afferent (Percheron and Filion,1991; Yelnik et al., 1997; Yelnik, 2002; Haber et al., 2006; Draganski et al., 2008). A third mechanism is through complex non-reciprocal communication between structures (Joel and Weiner, 1997, Haber et al., 2000, McFarland and Haber, 2002); these pathways provide a directional flow of information between regions. For examples limbic striatum could influence motor output by striato-nigro-striatal pathway (Somogyi et al.,1981), was demonstrates indeed existence an interface between different striatal regions via the midbrain dopamine cells that forms an ascending spiral between regions. Another system that extend over connecting adjacent regions is thalamo-cortico-thalamic network. These networks provide a potential continuous feedforward mechanism of information flow; in this way, limbic pathways can interact with cognitive pathways, which, in turn, interact with to motor pathways.

1.4 Lateral grasping network and Input Channels

In the last thirty years, it has been amply demonstrated how the cortical control of motor behavior in primates is based on the integration of sensory and motor information, which is possible thanks to strong and reciprocal connections between the motor and premotor cortex and the posterior parietal areas (Caminiti et al, 2015; Rizzolatti et al 1998). In this context, functional and connection studies conducted in macaques have provided evidence for the existence of a cortical network

connecting specific temporal, parietal, prefrontal and premotor areas and involved in the selection and control of the finalized manual actions, and action recognition ("mirror system"). This cortical network has been defined "Lateral Grasping Network"(LGN; Borra et al., 2017). Information processing for control of motor behavior occurs not only through cortico-cortical connections, but also through the basal ganglia and cerebellar loops.

According to early models, different striatal territories are a target of specific cortical regions and in turn are at the origin of largely segregated basal ganglia-thalamo-cortical loops (Alexander et al., 1986). Subsequent studies confirmed this view and showed up a finer modular organization in which each main loop consists of several largely segregated closed subloops. In consequence, each subloop originates from, and projects to, individual cortical areas or limited sets of functionally related areas and involves distinct, relatively restricted, striatal zones or “input channels” (Strick et al. 1995; Middleton and Strick 2000). The subdivision of the motor putamen into different input channels provides the basis for parallel processing of different aspects of motor control. In studies using anterograde and retrograde neural tracers, it has been shown that several areas belonging to the same cortical network can send convergent projections to a single putaminal area. As shown by Nambu (2011) and Takada et al. (2013), projections from agranular frontal and cingulate motor areas overlap partially into a large putaminal sector located caudal to the level of the anterior commissure (AC). However, the overlap of the cortical terminal fields in the striatum cannot be provided simply based on cortical connectivity models. Based on a large number of injections of neuronal tracers in different prefrontal areas (orbitofrontal, ventromedial, and dorsolateral), rostral cingulate and dorsal premotor (PMd) (Haber et al.2006; Calzavara et al. 2007) a convergence of projections from areas of the same domain or even different domains (e.g. rostral PMd and area 9) has been observed, especially in the rostral caudate, that would provide an anatomical substrate for the integration of information from different cortical circuits (Haber 2010). Diffuse projections from one area may overlap with projections from another area, providing an anatomical substrate for modulation of signals transmitted to BG. From the different striatal zones, or input channels, would then originate a parallel output. These general principles also apply to the organization of corticostriatal projections from the frontal and cingulate motor areas to the motor putamen. Specifically, the striatal projection field from area M1 and the supplementary motor area (SMA), which are closely interconnected, are largely segregated, involving respectively the more lateral and more medial area of the motor putamen (Strick et al. 1995; Inase et al. 1996; Takada et al. 1998). The projections from PMv and PMd areas to the striatum, although separated, seem to overlap

partially with those of the SMA (Takada et al. 1998), while the projections from motor areas and caudal cingulus overlap those from area M1 (Takada et al. 2001). In the motor putamen therefore, there are several inputs channels specified by the convergence of motor area subsets. In the study by Gerbella et al. (2016), it was analyzed how the various areas of the lateral grasping network project to the striatum. After anterograde neural tracer injections, in the various prefrontal, premotor and parietal nodes of the network, this study showed that there is a partial overlap of the projections from all these areas, in two specific zones of the putamen, one localized 1.5 mm rostral to the anterior commissure, and the other about 6 mm caudal. These regions have been defined rostral and caudal hand-related input channel. These input channels are characterized by rather specific subsets of cortical input from hand-related VLPF, PMv, and IPL areas, and the rostral from the caudal are distinguished by input from F5p, which is the only node of the LG network connected to both the primary motor area and the spinal cord. In addition, it is possible that the caudal, but not the rostral input channel, is a target of projections from higher order ventral visual stream areas involved in object recognition (Tanaka 1996). As a result, it seems conceivable that these 2 input channels, related to the hand, are differentially involved in the processing of specific aspects, even high-order, for controlling the motor behaviour of the hand.

About the output channel, the internal globus pallidus (GPi) and the substantia nigra pars reticulata (SNr), the main output station of the Basal Ganglia, are organized in largely segregated output channels, each of them projecting via the thalamus to a specific cortical area (Middleton and Strick 2000; Kelly and Strick 2004). Striatal cells projecting to different output channels directed to closely related cortical areas can be intermixed (Saga et al. 2011). Moreover, different striatal zones, which are convergence sites of projections of individual body parts representations of M1 and S1, can in turn project on the same output channel (Flaherty and Graybiel 1994). It is therefore possible that the output from the various hand-related input channels could be conveyed back to all, or part, of the areas of the lateral grasping network in the framework of a closed loop organization. If this is the case, we could hypothesize a model of cortical-basal ganglia connectivity, in which signals from a definite area, are first sent to different striatal zones, where they are integrated with signals from other functionally related areas, and finally reconverge to the output channel projecting back to the same area (Gerbella et al., 2016).

1.5 Laminar organization of the corticostriatal projections

In the cerebral cortex laminar segregation of efferent neurons exists in relation to target structures. Neurons located in layer II and III, project to cortical regions of the same hemisphere or of contralateral hemisphere, while the neurons of the infragranular layers (V and VI) project mainly to sub-cortical structures but also to upper layers of higher level areas of the same hemisphere (Barbas 1986; Barbas & Rempel-Clower 1997).

In this context, one important aspect is the definition of the way in which cortical areas or sectors contribute to the projections to a specific striatal zone in terms of laminar origin of their projections. Based on studies conducted in different animal species, it is largely agreed that corticostriatal (CSt) neurons are typically located mostly in layer V and, in some cases, layer III of most cortical areas (see Gerfen and Bolam, 2010). In rodents, two main categories of corticostrial neurons have been distinguished: the intratelencephalic (IT) neurons, mainly located in layer III and upper layer V (Va), and the pyramidal tract (PT) neurons located in the lower layer V (Vb) (Levesque et al., 1996a; Levesque et al., 1996b; Reiner et al., 2003; Landry et al., 1984; Wilson, 1987; Levesque and Parent, 1998). IT neurons innervates the ipsilateral and contralateral cortex and striatum; PT neurons innervate the brainstem and spinal cord and present axon collaterals that innervate the striatum. This distinction in population of corticostriatal projection neurons was identified also in monkeys (Parent and Parent, 2006). In the macaque brain, based on retrograde tracer injections in the caudate, the contribution of layer III in the temporal cortex and PFC was found to be correlated with the density of CSt-labeled cells (Arikuni and Kubota, 1986; Saint-Cyr et al., 1990). Recently, this view has been seriously challenged by data of Griggs et al. (2017), based on retrograde tracer injections in the head or the tail of the macaque caudate showing that: (1) in the temporal cortex, laminar patterns of CSt projections from a given cortical sector markedly differ according to the striatal target; and (2) layer VI can heavily contribute to the projections to specific striatal targets**.**

In addition, the recent work of Bertero et al. 2022 shows in mouse auditory cortex a novel connection to the striatum, originating from layer 4, considered to be involved exclusively in intracortical circuits.

Accordingly, laminar patterns of CSt projections could be more complex than previously considered and could represent an important variable to evaluate in defining the possible contribution of cortical areas to the projections to a specific putaminal zone.

1.6 Crossed corticostriatal projections

The ipsilateral cerebral cortex is certainly the major source of afferents to the striatum. At the end of 19th century, the idea that the corpus callosum contained decussating axons directed to external and internal capsule has emerged. This view was rejected by the work of Lèvy Valensi (1910) in the monkey. Subsequently it was demonstrated that the striatum is also a target of crossed CSt projections originating from the contralateral (contra) hemisphere. The existence of these connections is well documented in rodents (Carman et al.1965; Wilson 1987; Alloway et al. 2009; Shepherd 2013), but although noted in the macaque brain since at least 50 years ago (Kemp and Powell, 1970), these projections have been so far somewhat neglected. Indeed, crossed CSt projections in the macaque brain have been reported in several studies after anterograde tracer injections in different cortical areas (Künzle, 1975, 1978; Liles and Updyke, 1985; Huerta and Kaas, 1990; Cavada and Goldman-Rakic, 1991; McGuire et al., 1991; Parthasarathy et al., 1992). However, these studies could not give a comprehensive qualitative and quantitative view of the regional origin of these projections to the various parts of the striatum. Jones et al. (1977) have been the only ones that described the origin of the crossed CSt projections based on retrograde tracer injections in the putamen in squirrel monkeys. However, this description was only qualitative and shown for only one subject. Accordingly, it is still largely unknown which is the effective size of the crossed CSt projections compared to the "direct" ones, whether crossed CSt projections originate from all the cortical areas that also project to the ipsilateral striatum, and whether the origin of crossed and direct CSt projections to a given striatal zone is symmetrical. Thus, it is still an open question whether crossed CSt projections could represent a potentially important variable to consider in defining the pattern of information convergence in the striatum.

The known data on BG suggest therefore complexity of these structures and of networks that involve them. In primate brain this system is more intricate than initially thought and several issues are still unclear.

This thesis aims to describe achieved results in our lab on topographical and laminar organization and neurochemical characterization of corticostriatal connectivity in non-human primates.
More precisely two studies were focused on two specific aspects of corticostriatal connectivity: laminar organization (study 1) and crossed projections (study2).

In the first study, based on retrograde tracer injections in different parts of the striatum, we have analyzed the laminar distribution of the labeled CSt neurons. Main aims were as follows: (1) to quantify the contribution of the different cortical layers to the projections to a given relatively restricted putaminal zone; (2) to see whether these contributions vary within the various labeled cortical regions; and (3) to assess whether possible differences in laminar distribution patterns are related to the labeled cells density, the cortical area, or the target putaminal zone.

In the second study, always by retrograde tracer injections in different parts of the striatum we have compared qualitatively and quantitatively the regional distribution of the labeled CSt cells in the contralateral versus the ipsilateral hemisphere.

2 MATERIALS AND METHODS

2.1 Subjects, surgical procedures, and selection of the injection sites

The experiments were conducted in five *Macaca mulatta* (Cases 61, 71 female; 75, 76, and 77 male) in which retrograde neural tracers were injected in different parts of the caudate and putamen. Animal handling as well as surgical and experimental procedures complied with the European law on the humane care and use of laboratory animals (Directives 86/609/EEC, 2003/65/CE, and 2010/63/EU), Italian laws in force regarding the care and use of laboratory animals (DL 116/92 and 26/2014), and were periodically approved by the Veterinarian Animal Care and Use Committee of the University of Parma and authorized by the Italian Ministry of Health.

Before the injection of neural tracers, we obtained scans of each brain using magnetic resonance imaging (MRI; Cases 71, 75, 76, 77: General Electric 7 T; Case 61: Paramed Medical System 0.22 T) to calculate the stereotaxic coordinates of the striatal target regions and the best trajectory of the needle to reach them. Under general anesthesia (Cases 61, 71, Zoletil, initial dose 20 mg/kg, i.m., supplemental 5–7 mg/kg/h, i.m.; Cases 75, 76, and 77, induction with Ketamine 10 mg/kg, i.m., followed by intubation, isoflurane 1.5–2%) and aseptic conditions, each animal was placed in a stereotaxic apparatus, and an incision was made in the scalp. The skull was trephined to remove the bone and the dura was opened to expose a small cortical region. After the tracer injections, the dural flap was sutured, the bone was replaced, and the superficial tissues were sutured in layers. During surgery, hydration was maintained with saline, and heart rate, blood pressure, respiratory depth, and body temperature were continuously monitored. On recovery from anesthesia, the animals were returned to their home cages and closely observed. Dexamethasone (0.5 mg/kg, i.m.) and prophylactic broad-spectrum antibiotics (e.g., Ceftriaxone 80 mg/kg, i.m.) were administered preoperatively and postoperatively, as were analgesics (e.g., Ketoprofen 5 mg/kg, i.m.).

2.2 Tracer injections and histologic procedures

Based on stereotaxic coordinates, the neural tracers Fast Blue (FB; 3% in distilled water, Dr. Illing Plastics), Diamidino Yellow (DY; 2% in 0.2 M phosphate buffer, pH 7.2, Dr. Illing Plastics), Wheat Germ Agglutinin (WGA; 4% in distilled water, Vector Laboratories), Dextran conjugated with Lucifer yellow (LYD; 10,000 MW, 10% 0.1 M phosphate buffer, pH 7.4, Invitrogen, Thermo Fisher Scientific),

and Cholera Toxin B (CTB) subunit, conjugated with Alexa Fluor 488 [CTB green (CTBg); 1% in 0.01 M phosphate-buffered saline, pH 7.4, Invitrogen, Thermo Fisher Scientific] were slowly pressure injected through a stainless steel 31 gauge beveled needle attached through a polyethylene tube to a Hamilton syringe. For all tracer injections, the needle was lowered to the striatum within a guiding tube to avoid tracer spillover in the white matter. Table 1 summarizes the locations of the injections, the injected tracers, and the amounts injected.

After appropriate survival periods following the injections (48 h for WGA, 21–28 d for the other tracers; Table 1), each animal was deeply anesthetized with an overdose of sodium thiopental and perfused through the left cardiac ventricle consecutively with saline (~2 L in 10 min), 3.5% formaldehyde (5 L in 30 min), and 5% glycerol (3 L in 20 min), all prepared in 0.1 m phosphate buffer, pH 7.4. Each brain was then blocked coronally on a stereotaxic apparatus, removed from the skull, photographed, and placed in 10% buffered glycerol for 3 d and 20% buffered glycerol for 4 d. In Case 75, the right inferotemporal cortex was removed for other experimental purposes. Finally, each brain was cut frozen into coronal sections of 60 μm (Cases 61and 75) or 50 μm (Cases 71, 76, and 77) thickness.

In all cases, sections spaced 300 μm apart, that is, one section in each repeating series of six in Cases 71, 76, and 77 and one in series of five in Cases 61 and 75, were mounted, air dried, and quickly coverslipped for fluorescence microscopy. Other series of sections spaced 300 μm apart were processed for visualizing CTBg (Cases 61, 71, 75, 76, and 77), LYD (Case 75), or WGA (Cases 76 and 77) with immunohistochemistry. Specifically, in all sections endogenous peroxidase activity was eliminated by incubation in a solution of 0.6% hydrogen peroxide and 80% methanol for 15 min at room temperature. For the visualization of CTBg, the sections were then incubated for 72 h at 4°C in a primary antibody solution of rabbit anti-Alexa Fluor 488 (1:15,000; Thermo Fisher Scientific) in 0.5% Triton and 5% normal goat serum in PBS and for 1 h in biotinylated secondary antibody (1:200; Vector Laboratories) in 0.3% Triton and 5% normal goat serum in PBS. For the visualization of LYD, the sections were then incubated for 96 h at 4°C in a primary antibody solution of or rabbit anti-LY (1:3000; Life Technologies, Thermo Fisher Scientific) in 0.5% Triton X-100 and 5% normal goat serum in phosphate buffer (PB) 0.1 m, and for 1 h in biotinylated secondary antibody (1:200; Vector Laboratories) in 0.3% Triton and 5% normal goat serum in PB. For the visualization of the WGA, the sections were incubated overnight at room temperature in a primary antibody solution of goat anti-WGA (1:2000; Vector Laboratories) in 0.3% Triton and 5% normal rabbit serum in PBS and for 1 h in

biotinylated secondary antibody (1:200; Vector Laboratories) in 0.3% Triton and 5% normal rabbit serum in PBS. Finally, in all sections the labeling was visualized using the Vectastain ABC Kit (Vector Laboratories) and then a solution of DAB (50 mg/100 ml; Sigma Millipore), 0.01% hydrogen peroxide, 0.02% cobalt chloride, and 0.03% nickel ammonium sulfate in 0.1 m PB.

In Case 75, a subset of sections spaced 1200 µm immunostained for CTBg were then incubated overnight at room temperature in a primary antibody solution of rabbit anti-NeuN (1:5000, Cell Signaling Technology; RRID: AB_2630395) in 0.3% Triton, 5% normal goat serum in PBS, and for 1 h in biotinylated secondary antibody (1:100, Vector Laboratories) in 0.3% Triton, 5% normal goat serum in PBS. Finally, NeuN-positive cells were visualized using the Vectastain ABC kit and DAB as a chromogen. With this protocol, in the same tissue sections, CTBg labeling was stained black and NeuN-positive cells were stained brown. In Case 75, an additional subset of sections spaced 1200 µm through the frontal lobe were incubated in a primary antibody solution of anti-Alexa-488 and in a biotinylated secondary antibody solution as described above, followed by incubation for 1 h in a solution of streptavidin Alexa-488-conjugated (1:500, Invitrogen) in PBS with 0.5% Triton. The same sections were then incubated overnight at room temperature in a primary antibody solution of mouse monoclonal SMI-32 (1:5000; Covance; RRID: AB_2315331), in PBS with 0.5% Triton and 2% normal goat serum, and for 1 h in a secondary antibody solution of goat anti-mouse conjugated with Alexa-568 (1:500, Invitrogen, Thermo Fisher Scientific), in PBS with 0.3% Triton and 2% normal goat serum.

In Case 77, selected sections were processed for revealing Alexa-488 with immunofluorescence as described above and then for in situ hybridization (ISH) using RNAscope Multiplex Fluorescent v2 Assay and RNA-Protein Co-detection Ancillary Kit (ACDBio-techne) and probes for Somatostatin (SOM) and glutamic acid decarbossilase (GAD). This approach allows a neurochemical identification of corticostriatal retrogradely labeled neurons.

In cases 61, 71, 76, and 77 one series of each sixth section (fifth section in Cases 61) was stained with the Nissl method (0.1% thionine in 0.1 M acetate buffer, pH 3.7).

Table 1. Animals used, location of injection site in the striatum, and type and amount of injected tracers

Case	Sex	Age	Weight	Hemisphere	Location	AP*	Tracer	Amount	Survival time
61	F		4.5	R	Putamen	1	CTBg 1%	1 x 2 µl	21 d
71	F	6.5	3.3	L	Putamen	−2	FB 3%	1 × 0.3 µl	28 d
				R	Putamen	−1	DY 2%	1 × 0.3 µl	21 d
75	M	6	3.5	L	Caudate	+6	LYD 10%	1 × 1 µl	28 d
				R	Putamen	0	CTBg 1%	1 × 1 µl	21 d
				R	Caudate	+1	DY 2%	1 × 0.25 µl	21 d
76	M	9	15	R	Caudate	+7	WGA 4%	1 × 0.3 µl	48 h
77	M	9	15	L	Putamen	−3	CTBg 1%	1 × 1 µl	21 d
				R	Putamen	+3	WGA 4%	1 × 0.2 µl	48 h

AP level according to the digital atlas of Reveley et al. (2017) in which AP = 0 is at the level of the AC.

2.3 Data analysis - Study 1

Injection sites, distribution of retrogradely labeled neurons, and areal attribution of the labeling

The criteria used for defining the injection site core and halo and identifying FB and CTBg labeling have been described previously (Luppino et al., 2003; Rozzi et al., 2006). The injection sites of Cases 71, 75, and 77 were completely restricted to the putamen, in case 76 the injection site was restricted to the caudate. In Case 61, the CTBg injection site had some involvement (<500 µm) of the white matter just above the putamen (Fig. 1. This white matter involvement, given its minimal extent and location in close contact with the putamen and considering that CTB is characterized by a limited uptake by axons of passage (Lanciego, 2015), should not have affected the results from this case, which were fully comparable with those of the other cases. The distribution of retrograde labeling in the cortex was analyzed in sections every 300 µm and plotted in sections every 1200 µm (Cases 61, 71r, and 75) or 600 µm (Cases 71l, 76, and 77) together with the outer and inner cortical borders, using a computer-based charting system. Data from individual sections were also imported into the 3D reconstruction software (Demelio et al., 2001) providing volumetric reconstructions of the monkey brain, including connectional and architectonic data.

The criteria and maps adopted for the areal attribution of the labeling were similar to those adopted in previous studies (see Borra et al., 2017). Specifically, the attribution of the labeling to the frontal

motor, cingulate, and opercular frontal areas was made according to architectonic criteria previously described (Matelli et al., 1985, 1991; Belmalih et al., 2009)

Figure 1 Location of the injection sites. Top, Drawings of coronal sections showing the location of the injection sites in the putamen depicted as a black zone corresponding to the core, surrounded by a gray zone corresponding to the halo. All sections are shown as from a right hemisphere. The AP level of the sections is indicated in relation to the digital atlas of Reveley et al. (2017), in which AP = 0 is at the level of the AC. Bottom, Fluorescence photomicrographs of the injection sites in the putamen. Scale bar in Case 75 applies to all. Dashed lines in the injection site of Case 61 indicate the deposit of the tracer in adjacent sections. C, Central sulcus; Cd, caudate nucleus; Cg, cingulate sulcus; GP, globus pallidus; ic, internal capsule; L, lateral fissure; OT, optic tract; Pt, putamen; RTh, reticularis thalami; S, spur of the arcuate sulcus; ST, superior temporal sulcus.

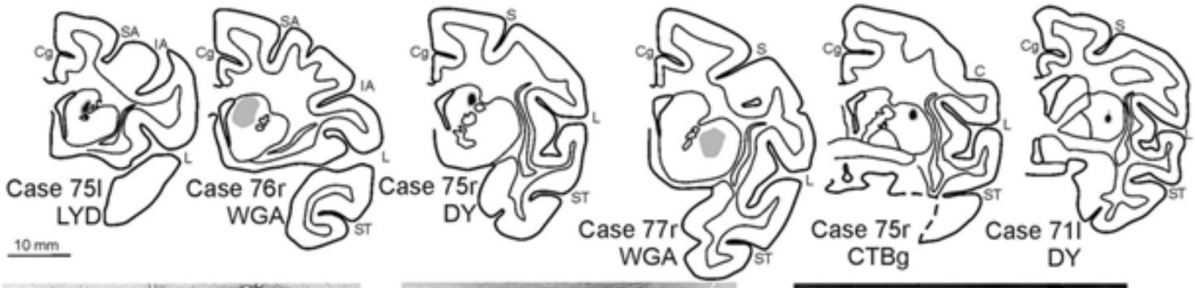
Case 75l LYD
Case 76r WGA
Case 75r DY
Case 77r WGA
Case 75r CTBg
Case 71l DY
10 mm

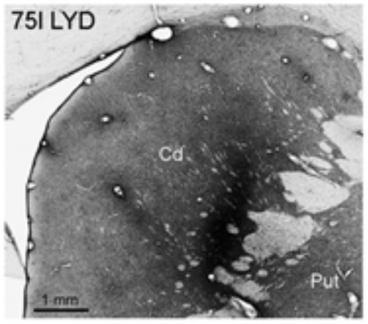
75l LYD
Cd
Put
1 mm

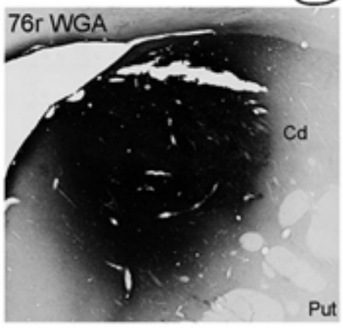
76r WGA
Cd
Put

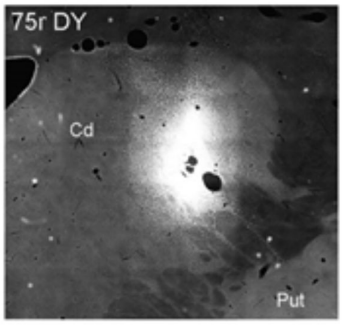
75r DY
Cd
Put

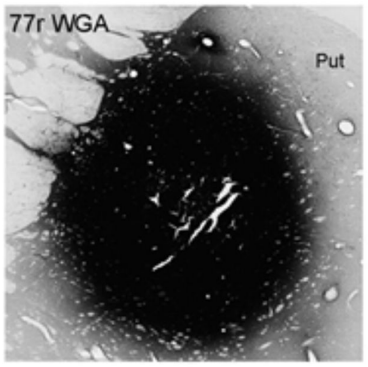
77r WGA
Put

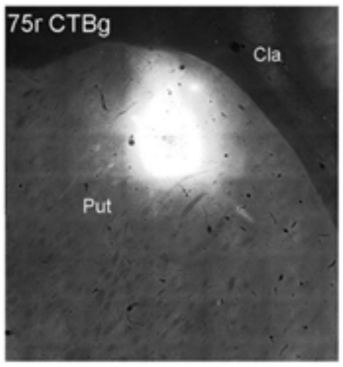
75r CTBg
Cla
Put

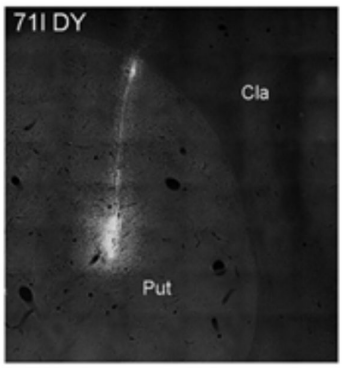
71l DY
Cla
Put

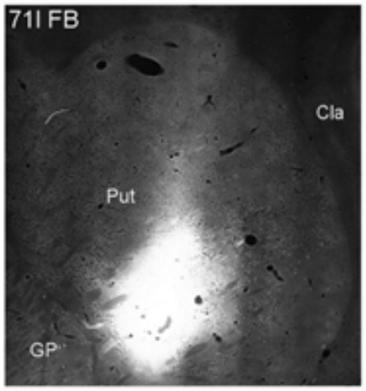
71l FB
Cla
Put
GP

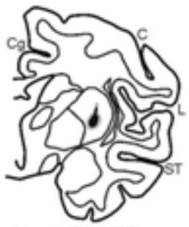
Case 71l FB


Case 77l CTBg

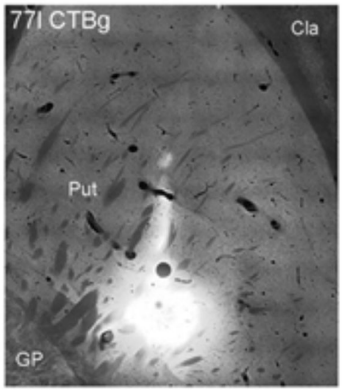
77l CTBg
Cla
Put
GP

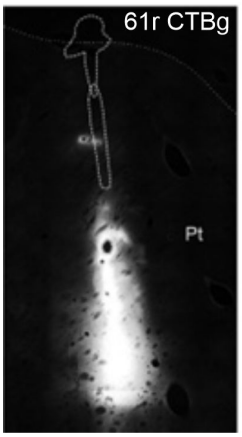
61r CTBg
Pt

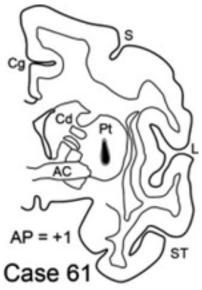
Cd
Pt
AC
AP = +1
Case 61

Quantitative analysis and laminar distribution of the labeling

In all cases, the number of labeled neurons plotted in the ipsilateral hemisphere was counted and the cortical input to the injected putaminal zone was then expressed in terms of the percentage of labeled neurons found in a given cortical subdivision, with respect to the overall cortical labeling found for each tracer injection.

In cases 61, 71, and 75, the laminar distribution of the labeled cells was analyzed quantitatively in pairs or triplets of close sections (spaced 300-600 µm), taken at different rostrocaudal levels through the frontal motor and cingulate cortex and the frontal opercular cortex (Fig. 2). Given that, in Cases 75 and 71r, the labeling distribution was quite similar, the same levels (two sections/level) were selected: the first level (A) was taken through F1, the second (B) through the caudal part of F3, the third (C) through the middle part of F3, and the fourth (D) through the rostral most part of F3. In Case 61, the labeling involved more rostral cortical territories than in Cases 75 and 71r; thus, the caudalmost analyzed level was level B, and it was possible to analyze a further rostral level (E) through areas F6 and F7. In Case 71l, the labeling was dense in relatively restricted cortical sectors; thus, the analysis was focused on these regions, at levels corresponding to B, C, and D, and was conducted in two (level D) or three (levels B and C) sections spaced 600 µm.

Quantitative analysis was also conducted in parietal, insular, and prefrontal sectors selected based on the distribution of the labeling in each case. For analyzing these regions, given that the laminar distribution of the labeling was apparently very constant, cortical sectors of 2 mm from two close sections (spaced 300-600 µm) were analyzed.

In case 76r WGA, the laminar distribution of the labeled cells was analyzed quantitatively in pairs of close sections, taken through the prefrontal cortex. Five different levels were selected: the first level (A) was taken through areas 32, 9, and 11, the second (B) through areas 24, 32, 9, and 14, the third (C) through areas 24 and 9/8B, the fourth (D) through area 45B, orbitofrontal and premotor cortex, the fifth (E) through 8 area. In Case 77r WGA, the laminar distribution of the labeled cells was analyzed only at level C.

The selected sections were photographed at 100× magnification through a digital camera incorporated into the microscope with an automatic acquisition system (NIS-Element; Nikon), and labeled neurons were plotted on the microphotographs. In the frontal sections of Cases 61, 71r, and 75 and in the prefrontal sections of Case 77r WGA, the entire extent of the prefrontal, cingulate,

frontal motor, and opercular frontal cortex was subdivided in 500-µm-wide cortical traverses perpendicular to the cortical surface and running through the entire cortical thickness, from the pial surface to the gray-white matter border. The width of the traverses was defined along a line running at the level of the layers III-V border. In the frontal sections of Case 71l and in the sections through the parietal, insular, and PFC (76r and 77r) in all cases, where the labeling was in general less rich, cortical traverses 1-mm-wide were defined in limited cortical sectors. Furthermore, microphotographs of immediately adjacent Nissl-stained sections were overlaid, and borders between different cortical layers were then transferred on the plots. Two types of analyses were conducted on the distribution of the labeled neurons. The first analysis aimed to obtain an estimate of the variations in overall richness of the labeling within and across the various labeled cortical sectors. To this purpose, we have first considered the total number of labeled cells observed in each traverse, in the entire cortical thickness. Then, to compensate for differences in the number of labeled cells because of variations of the cortical thickness between different areas or to oblique cutting of the cortical mantle, the total number of labeled cells was divided by the cortical thickness, measured from the pial surface to the gray-white matter border, expressed in millimeters. Thus, the richness of the labeling ("density") was expressed for each traverse in terms of number of labeled cells/mm cortical thickness. The second analysis aimed to quantify the proportion of CSt-labeled cells observed in the various layers. To this aim, for each traverse, the labeling was expressed in terms of percentage of labeled neurons localized in layers II-III, V, and VI.

The distribution of labeled neurons was also analyzed qualitatively across consecutive sections to exclude the possibility that the observed laminar distribution patterns of the labeling were only apparent because of an oblique cutting of the cortical mantle.

2.4 Data analysis - Study 2

Injection sites, distribution of retrogradely labeled neurons, and areal attribution of the labeling

All the injection sites used in this study shown in Figure 1.2 were completely restricted to the target striatal nucleus (caudate or putamen). The cortical distribution of retrograde labeling in the ipsilateral and contralateral hemisphere was plotted in sections every 600 µm (every 1200 µm in Case 75l LYD) together with the outer and inner cortical borders, using a computer-based charting system. Data from individual sections were then imported into three-dimensional (3D)

reconstruction software (Demelio et al., 2001) providing volumetric reconstructions of the monkey brain, including connectional and architectonic data.

The criteria and maps adopted for the areal attribution of the labeling were similar to those adopted in previous studies (Borra et al., 2017; Caminiti et al., 2017). Specifically, prefrontal, frontal, and cingulate motor and opercular frontal areas, where most of the labeling was located, were defined according to cytoarchitectonic and/or chemoarchitectonic criteria described in Matelli et al. (1985, 1991), Carmichael and Price (1994), Gerbella et al. (2007), Belmalih et al. (2009), and Saleem et al. (2014). Some prefrontal and cingulate areas have been considered together and are referred to as 9/8B, 24/32, 24a/b, 24c/d, 23a/b, 23/31, and 29/30. In the inferior parietal lobule, the gyral convexity areas were defined according to cytoarchitectonic and chemoarchitectonic criteria described in Gregoriou et al. (2006) and those of the lateral bank of the intraparietal sulcus based on connectional criteria described in Borra et al. (2008). The superior and medial parietal cortex were defined according to architectonic criteria described in Pandya and Seltzer (1982) and Luppino et al. (2005). For the caudal cingulate cortex, we adopted the cytoarchitectonic map proposed by Morecraft et al. (2004). Finally, the temporal labeling in the superior temporal sulcus was attributed based on the electrophysiological and architectonic map proposed by Boussaoud et al. (1990) and guided by the atlas of Saleem and Logothetis (2012), and the labeling in the superior temporal gyrus and auditory belt cortex was based on the architectonic, functional, and connectional map described by Kaas and Hackett (2000; Saleem et al. 2008). For the quantitative analysis, the temporal lobe was subdivided into four regions, the temporal pole (Tp), medial temporal (Tm), superior temporal (Ts), and inferior temporal (Ti)

Quantitative analysis and laminar distribution of the labeling

In all cases, the number of labeled neurons plotted in the ipsilateral and contralateral hemispheres was counted, and the cortical input to the injected striatal zone was then expressed in terms of the percentage of labeled neurons found in each cortical subdivision, with respect to the overall cortical labeling found for each tracer injection in the ipsilateral hemisphere or in both ipsilateral and contralateral hemispheres.

For the areas where the percentage of ipsi plus contra labeling was >1%, the number of labeled cells observed in the contralateral area was subdivided by the total number (ipsi plus contra) of labeled

cells to obtain a contralaterality index, which could range from one (all cells in the contralateral area) to zero (all cells in the ipsilateral area).

3 RESULTS

3.1 Study 1 - Location of the injection sites and general distribution of labeled CSt neurons in the ipsilateral hemisphere

All injections used for this study involved the putaminal region overlying the crossing of the anterior commissure (AC) at different dorso-ventral (DV) levels (Table 1; Fig. 1.1), except in case 76 where the injection involved the caudate head. In Cases 75 and 71r, the injection sites were located in a dorsal and a mid-dorsal part of the putamen, respectively, at about the antero-posterior (AP) level of the AC (Case 75), or slightly rostral (Case 71r). According to the putaminal motor somatotopy (e.g., Alexander and DeLong, 1985; Nambu, 2011), the injection site in Case 75 could correspond mostly to the trunk-leg motor representation and in Case 71r to the arm and trunk-leg motor representation. In Cases 71l and 61, the injection sites were located more ventrally in the putamen, 2 mm caudal and 1 mm rostral to the center of the AC, respectively. In Case 71l, the injection site could overlap with the hand and mouth motor representation. In Case 61, it extended for ∼4 mm in DV direction and the ventral part could at least partially overlap with the rostral "hand-related input channel" (Gerbella et al., 2016). In Case 76 the injection was located at about 7 mm rostral to the center of AC.

As expected, in all cases except Case 76, the majority of labeled cells was located in frontal motor areas (57%-75% of the labeled cells; Table 2) with additional, in several cases relatively robust, projections from other cortical regions, and their distribution in the ipsilateral hemisphere largely varied depending on the location of the injection site (Figs. 2 and 3). In Case 76 the majority of labeled cells was located in prefrontal and rostral cingulate areas.

In Cases 75 and 71r, the regional distribution of the labeling was quite similar: in both cases, ∼62% of the labeled cells were located within frontal motor areas, ∼19%-22% in the cingulate cortex, and ∼12%-17% in the parietal cortex. In both cases, the strongest input originated from F1 (primary motor cortex), mostly from the dorsal and medial part, and a very rich labeling involved the entire extent of F3 (supplementary motor area) and area 24c/d (cingulate motor areas) mostly in the caudal part, corresponding to area 24d (Table 3). Relatively strong projections originated also from F2 and, in Case 71r, in which the injection site extended more ventrally, also from F5. In the parietal cortex, in both cases, most of the labeling was in the dorsal part of the primary somatosensory area (SI) and of area PE and, in Case 71r, also in area PFG.

In Case 71l, the labeling was much weaker in the cingulate cortex and mostly confined to the frontal motor (76%) and parietal (19%) cortex (Table 2). In the frontal cortex, the labeling was very strong in the ventral premotor cortex, mostly in F5, also extending in the frontal operculum, and in the mid-ventral part of F1 (Table 3), as expected from the location of the injection site. Relatively robust labeling was observed in the rostral part of F3, likely involving the arm and face representation (Luppino et al., 1991). In the parietal cortex, labeled cells were mostly distributed in the ventral part of SI, and in secondary somatosensory area (SII), PF, PFG, and the anterior intraparietal area (AIP).

In Case 61, the cortical labeling was more extensive than in the other 3 cases, likely because of its more rostral location and relatively large DV extent. Specifically, the labeling very densely involved the ventral premotor, the ventrolateral PFC, and the IPL areas PFG, PG, and AIP, which likely reflects involvement of the rostral "hand-related input channel." The labeling densely involved also F3 (mostly the mid-rostral part), F2, and 24c/d and, less densely, areas F6, 24a/b and the insula (Tables 2 and 3).

In Case 76, cortical labeling was densest in prefrontal areas 9 and 8B (21%) and in cingulate areas rostral 24 and 32 (40% ca). Less dense labeling involved other lateral prefrontal areas (46, 45, and 8; 15%), area 14, and orbitofrontal areas 11, 13, and 12o**.**

Table 2. Regional distribution (%) and total number (n) of labeled neurons observed following tracer injections in the motor putamen

Case	Prefrontal	Cingulate	AFC*	Parietal	Insula	Temporal	n. cells
75	0,7	19,4	61,7	16,7	1,6	-	59653
71r	1,6	21,9	61,6	11,9	3	-	60757
71l	0,5	3,4	75,5	18,6	1,2	0,8	36628
61	8,4	18,3	57	7,5	6,1	2,7	105724

*AFC = Agranular Frontal Cortex

Table 3. Distribution (%) in the agranular frontal and cingulate cortex and in the frontal operculum (FrOp) of labeled neurons observed following tracer injections in the motor putamen

Case	24c/d	F6	F7	F3	F2	FrOp	F5	F4	F1
75	14,4	0,8	0,3	12,7	7,1	2,2	2,5	2,0	34,1
71r	14,4	0,8	0,5	13,2	6,5	2,4	7,9	3,3	26,9
71l	2,5	0,1	-	6,9	0,7	7,6	33,4	8,2	18,6
61	12,3	3,7	1,2	10,6	9,3	16,5	10	3,0	2,7

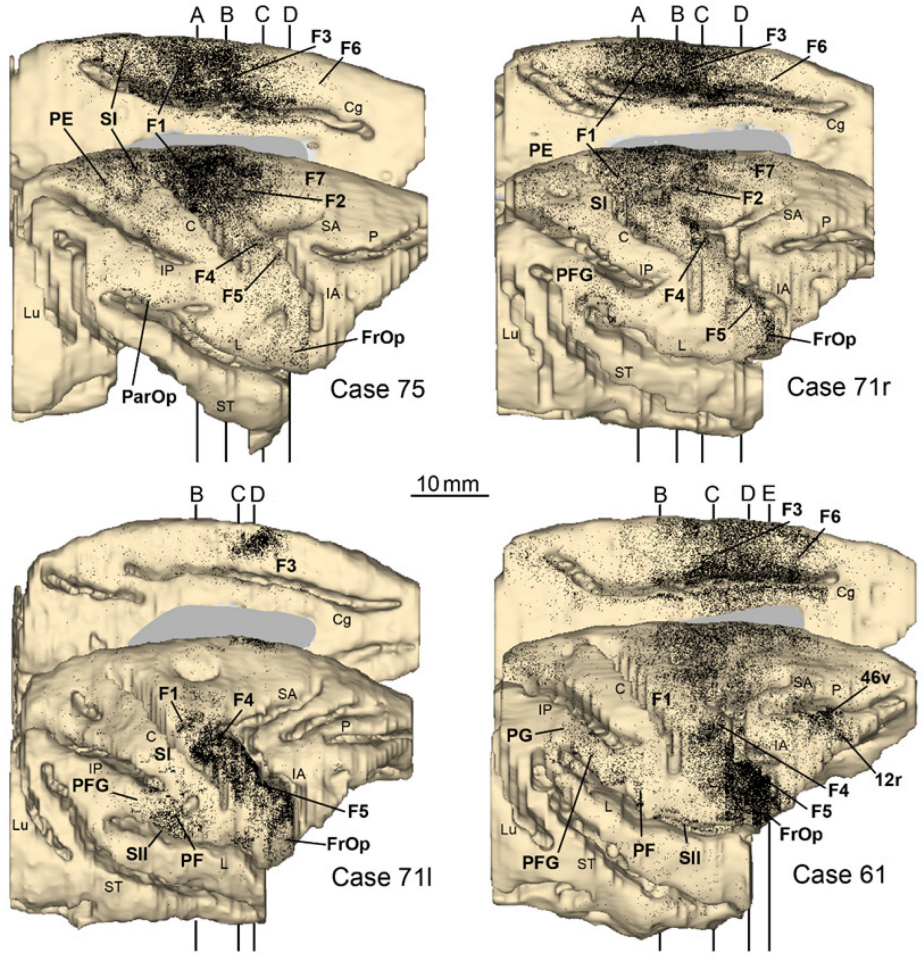

Figure 2. Distribution of the cortical labeling observed after injections in the putamen. The distribution of the retrograde labeling is shown in dorsolateral and medial views of the 3D reconstructions of the injected hemispheres in which each dot corresponds to one labeled neuron. In each reconstruction, solid lines indicate the levels (A-E) of the sections selected for the quantitative analysis. For the sake of comparison, also Case 71l is shown as right. FrOp, Frontal operculum; IA, inferior arcuate sulcus; IP, intraparietal sulcus; Lu, lunate sulcus; P, principal sulcus; ParOp, parietal operculum; SA, superior arcuate sulcus. Other abbreviations as in Figure 1.

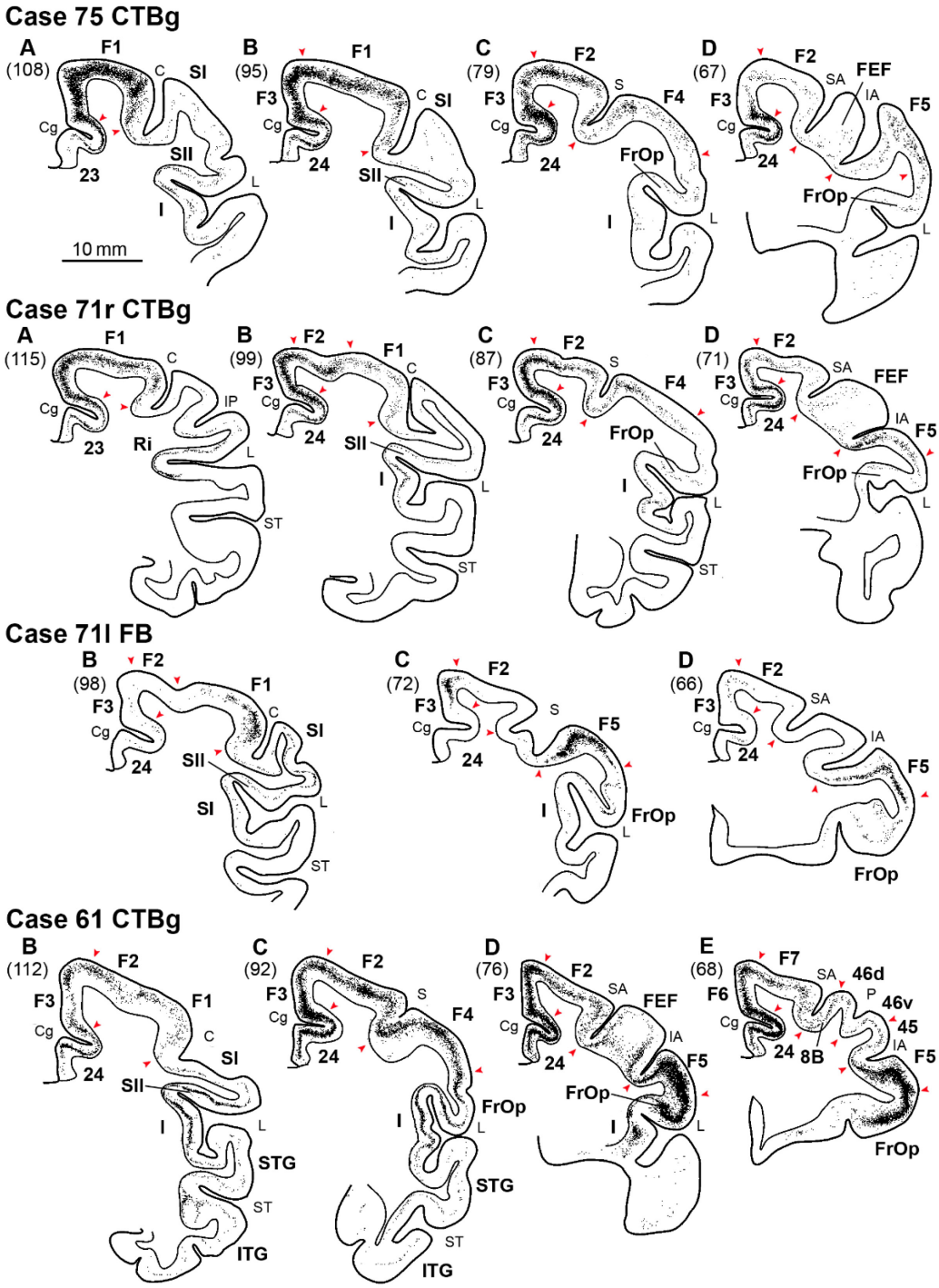

Figure 3. Distribution of the cortical labeling in one representative section from each level selected for the quantitative analysis. Section drawings are in a caudal to rostral order (A-E) and were taken at the levels shown in Figure 2. Section number is indicated in brackets. Arrowheads indicate borders of frontal motor areas. Subcortical labeling is not shown. A, Amygdala; FEF, frontal eye field; I, insula; ITG, inferior temporal gyrus; LG, lateral geniculate nucleus; Ri, retro-insular cortex; STG, superior temporal gyrus; STh, subthalamic nucleus; Th, thalamus. Other abbreviations as in Figures 1 and 2.

Laminar distribution of CSt-labeled cells in the frontal motor, cingulate, and frontal opercular cortex

As shown in detail below, in general, the laminar distribution pattern of the labeled CSt cells in the frontal motor and opercular cortex markedly differed across the various labeled zones and very rarely showed the pattern commonly described for the primate brain, characterized by CSt cells almost completely confined to layer V. For example, in the frontal motor cortex, in only 8% of the 1009 cortical bins (500-µm-wide) analyzed in 36 sections from all cases, labeled cells in layer V were >66% and in 58% of the bins they were <50%. Indeed, labeled cells almost everywhere in these regions tended to distribute over almost the entire cortical depth, involving, at a variable extent, layers III, V, and VI. Noteworthy, there were also labeled CSt neurons in the underlying white matter, which have been described in a previous study (Borra et al., 2020).

Figure 4 shows the results of the quantitative analysis conducted in sections through F1, which was very richly labeled in Cases 75, 71r, and 71l. In sections sampled from Cases 75 and 71r, taken caudally in F1 (Figs. 2 and 3, level A), in the granular cingulate area 23 the labeling by far predominantly involved layer V, as in most of the sampled bins labeled cells in this layer were >80% in Case 75 and >90% in Case 71r (Fig. 5*A*, *B*). In Case 75, at the transition of area 23 with F1, the laminar distribution pattern radically changed, as the proportion of labeled cells in layers III and VI increased considerably (Fig. 5*C*). For example, in section 108, there were ∼12-13 mm (bins 16-41) in which the proportion of layer V labeled cells was ∼40% and that of either layer III or layer VI was ∼30%, whereas in section 109, the proportion of layer VI labeled cells tended to be ∼20%. Interestingly, this pattern remained unchanged despite clear changes in labeling density, even when it abruptly halved in the range of very few bins (e.g., bins 28-31 in section 108). In Case 71r, the laminar distribution pattern in a sector of F1, similar to that sampled in Case 75, was somewhat different: the proportion of labeled cells in layer V tended to be higher than that in layers III and VI, though remaining for the whole extent of F1 in both the sampled sections at ∼50%. In Case 71l, F1 was sampled in a triplet of close sections in a more lateral part (Figs. 2 and 3, level B), mostly in the bank of the central sulcus, where the labeling in this area was richest. In all three samples, the proportion of labeled cells in layer VI tended to be quite low, but that in layer III was as high or, in several bins, even higher than in layer V, being >50% in 8 mm of 13 mm sampled (Fig. 5*E*). A similar pattern was also observed in bins located in the bank of the central sulcus in Case 75.

In all cases, layer V labeled cells in F1 were all relatively small and tended to be densely packed mainly in the upper part of the layer, corresponding to sublayer Va. In Case 75, SMI-32

immunofluorescence, which reveals neurofilament proteins expressed in subpopulations of layer III and V pyramids (Hof and Morrison, 1995), including the larger ones in layer Vb in the frontal motor cortex (Geyer et al., 2000; Belmalih et al., 2009), showed that CTBg labeled neurons, though invading layer Vb, were considerably smaller than larger SMI-32-immunopositive pyramids (compare Fig. 5*C*, *D*). The analysis of these double-labeled sections also clearly showed that a high proportion of CTBg-labeled cells was located well below the large layer Vb pyramids, in layer VI.

Rostral to F1, the cingulate area 24c/d and the medial premotor cortex corresponding to F3 were sampled at different AP levels together with the adjacent sectors of F1 or F2 (levels B, C, and D; Figs. 6–8). Figure 7 shows the results of the analysis conducted in pairs of sections taken in all cases at about the middle of F3, possibly corresponding to the arm representation of this area (level C). In area 24c/d, labeled cells were mainly located in layer V, although, especially in Case 61, in several bins, the proportion of cells located in layers III and VI was ~40%. In Cases 75 and 71r, the laminar distribution pattern of labeled cells in F3 (Fig. 5*F*) was substantially similar to that observed in F1. In Case 61, the percentage of layer V-labeled cells was in most of the bins ~40%, in layer III tended to match that of layer V, whereas in layer VI it was lower and quite variable. In Case 71l, relatively dense labeling was observed in a restricted zone in the mid-rostral part of F3. Here, in two of three sampled sections, labeled cells tended to be located mainly in layer V (~60%), whereas in one section the proportion of labeled cells in layer VI matched that in layer V. In F2, the density of labeled cells tended to be lower than in F3 and their laminar distribution tended to be similar to that observed in F3, though more variable across bins. Similar laminar distribution patterns were observed in Cases 75, 71r, and 61 in the caudal part of areas 24c/d and F3 (level B; Fig. 6).

At level D (Figs. 2 and 3), through the rostralmost part of F3, at the border with F6, a different laminar distribution pattern was observed in Cases 75 and 71r, characterized by a clear increase in the percentage of labeled cells in layer V, compared with the more caudal levels (Fig. 8). In Case 61, ~40%-50% of the labeled cells were located in layer V, and the remaining were almost equally subdivided in layers III and VI.

An additional more rostral level (level E) was sampled in Case 61 through areas 24c/d and F6, where rich labeling was located (Fig. 9). The laminar distribution of the labeling was similar to that observed more caudally in area 24c/d and rostral F3.

Accordingly, as observed for F1, there were differences in the laminar origin of CSt projections from medial and dorsal premotor areas, which were not correlated with the density of the labeling, but likely with the target putaminal zone.

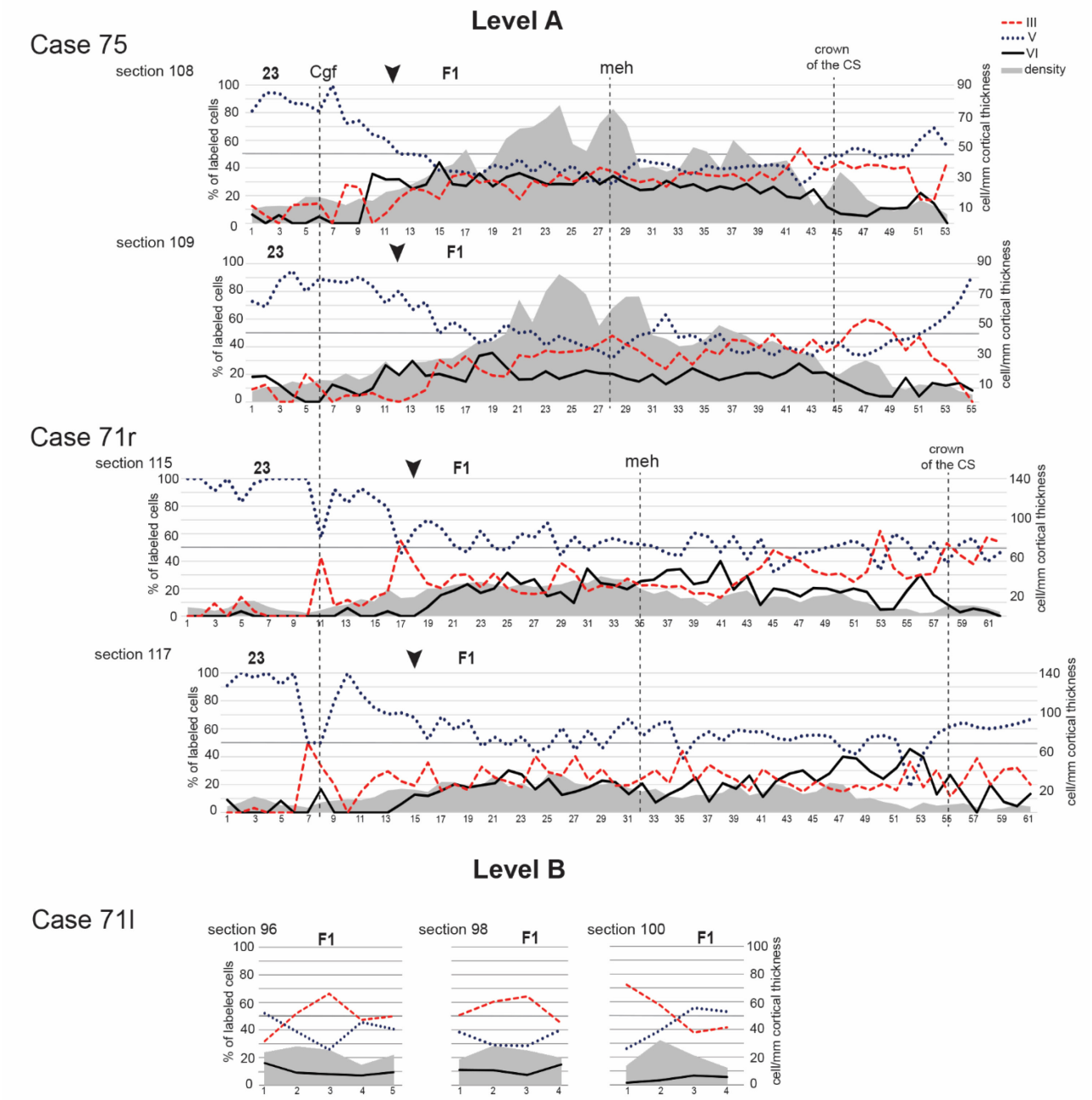

Figure 4. Percent laminar distribution and density of the retrograde labeling in F1. Graphs represent data from Cases 75, 71r (level A, 2 sections each), and 71l (level B, 3 sections). For each case, on the left, one section drawing shows the analyzed cortical sector and layer V shaded in light blue. Graphs from Cases 75 and 71r are aligned at the level of the fundus of the cingulate sulcus (a), indicated by a vertical dashed line. The other vertical dashed lines indicate the level of the medial edge of the hemisphere (b) and the shoulder of the central sulcus (c). Graphs from Case 75 and 71r represent data from 500-mm-wide bins from the region in which the labeled cell density was constantly higher than 10 labeled cells/bin/mm. In graphs from Case 71l, the bins are 1-mm-wide and located in the lateral part of F1, in the bank of the central sulcus. Arrowheads indicate the location of areal borders.

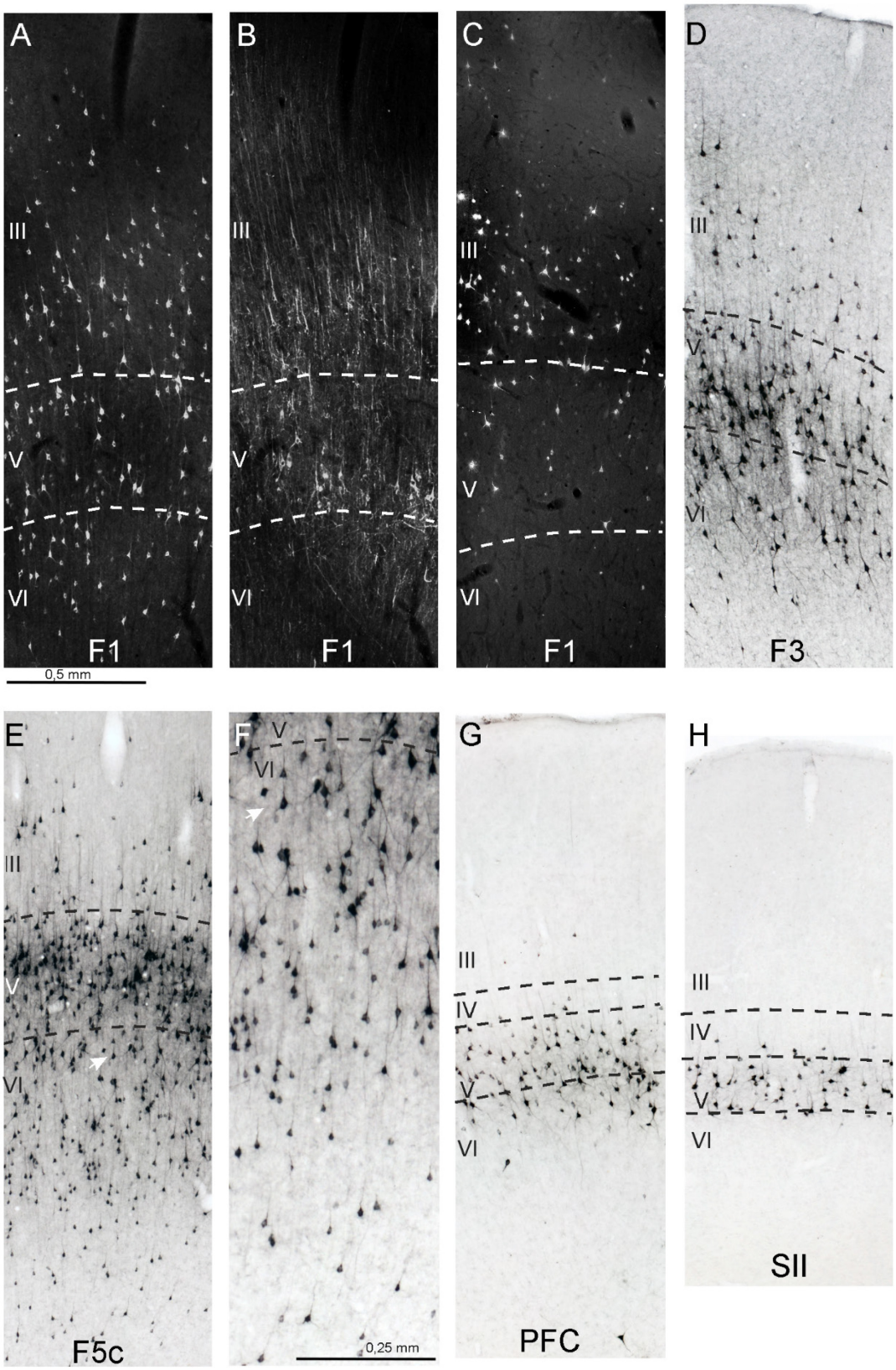

Figure 5. Examples of laminar distribution of the labeling. A, B (section 110), C, D (section 106), and F (section 93) are from Case 75. B, D, SMI-32 immunofluorescence in A and C, respectively. E (section 98) is from Case 71l. G (section 76, enlarged in H), I, Case 61. J, Case 7

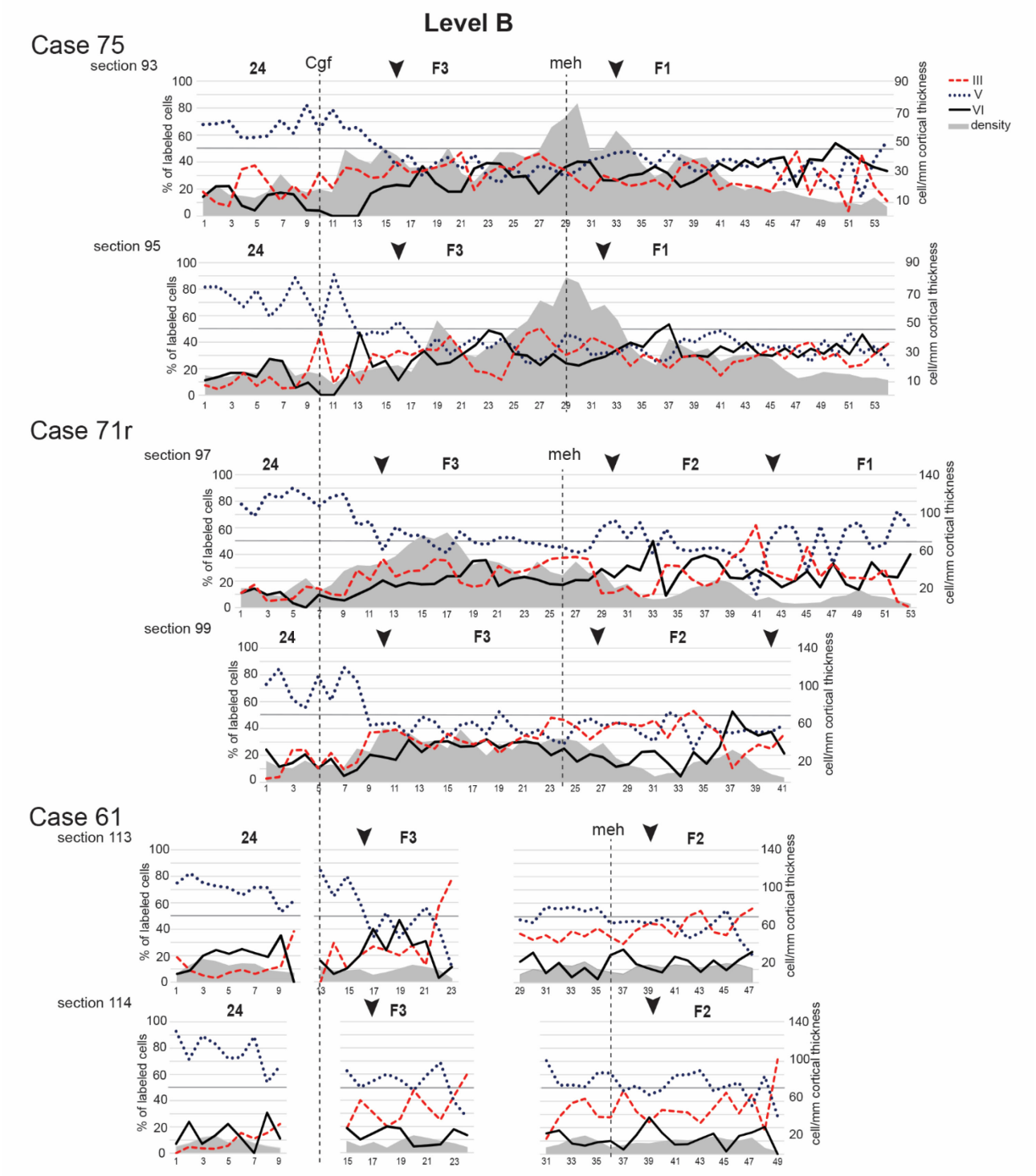

Figure 6. Percent laminar distribution and density of the retrograde labeling in the cingulate and frontal motor cortex at level B in Cases 75, 71r, and 61. Conventions as in Figure 4.

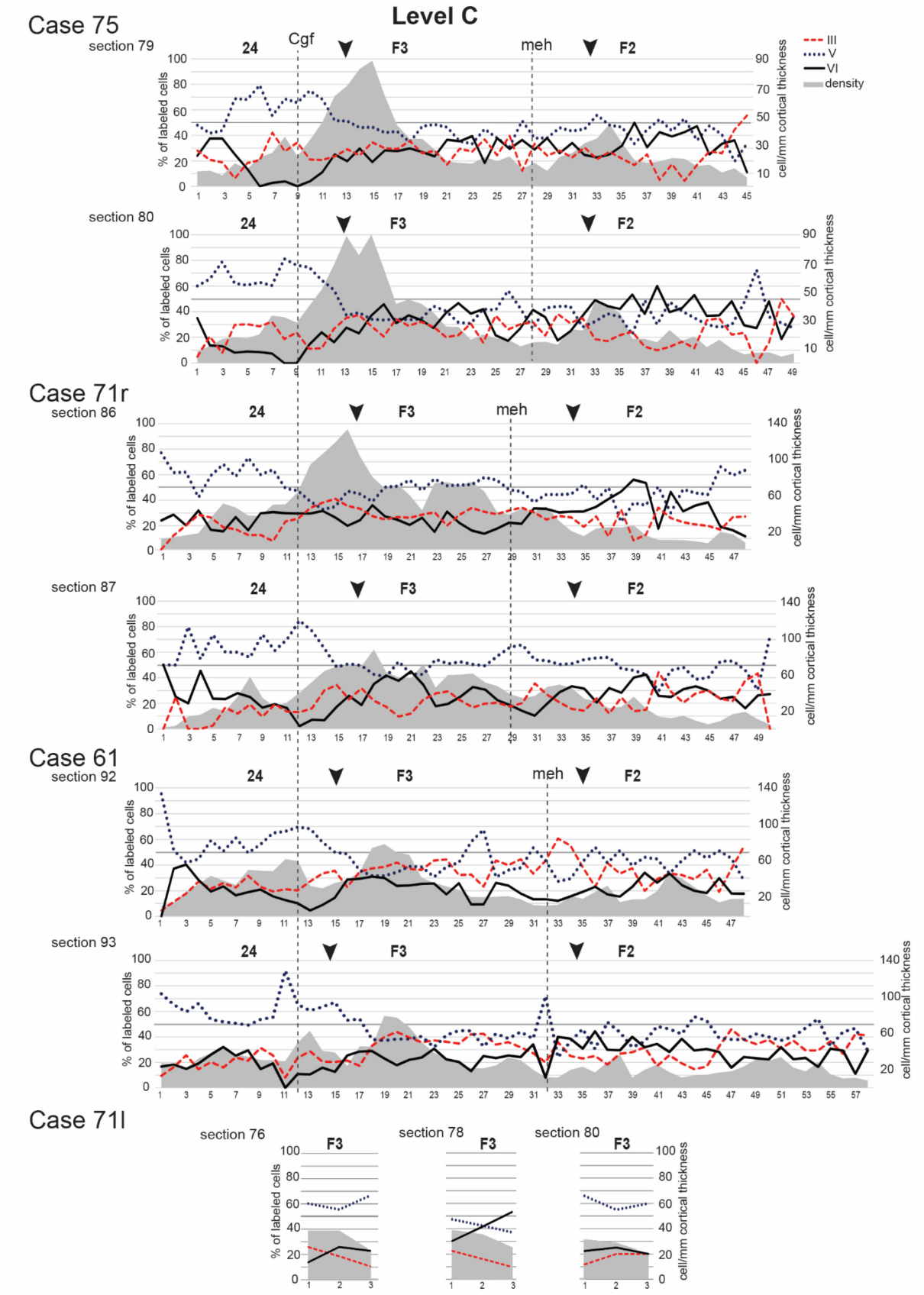

Figure 7. Percent laminar distribution and density of the retrograde labeling in the cingulate and frontal motor cortex at level C in all cases. Conventions as in Figure 4.

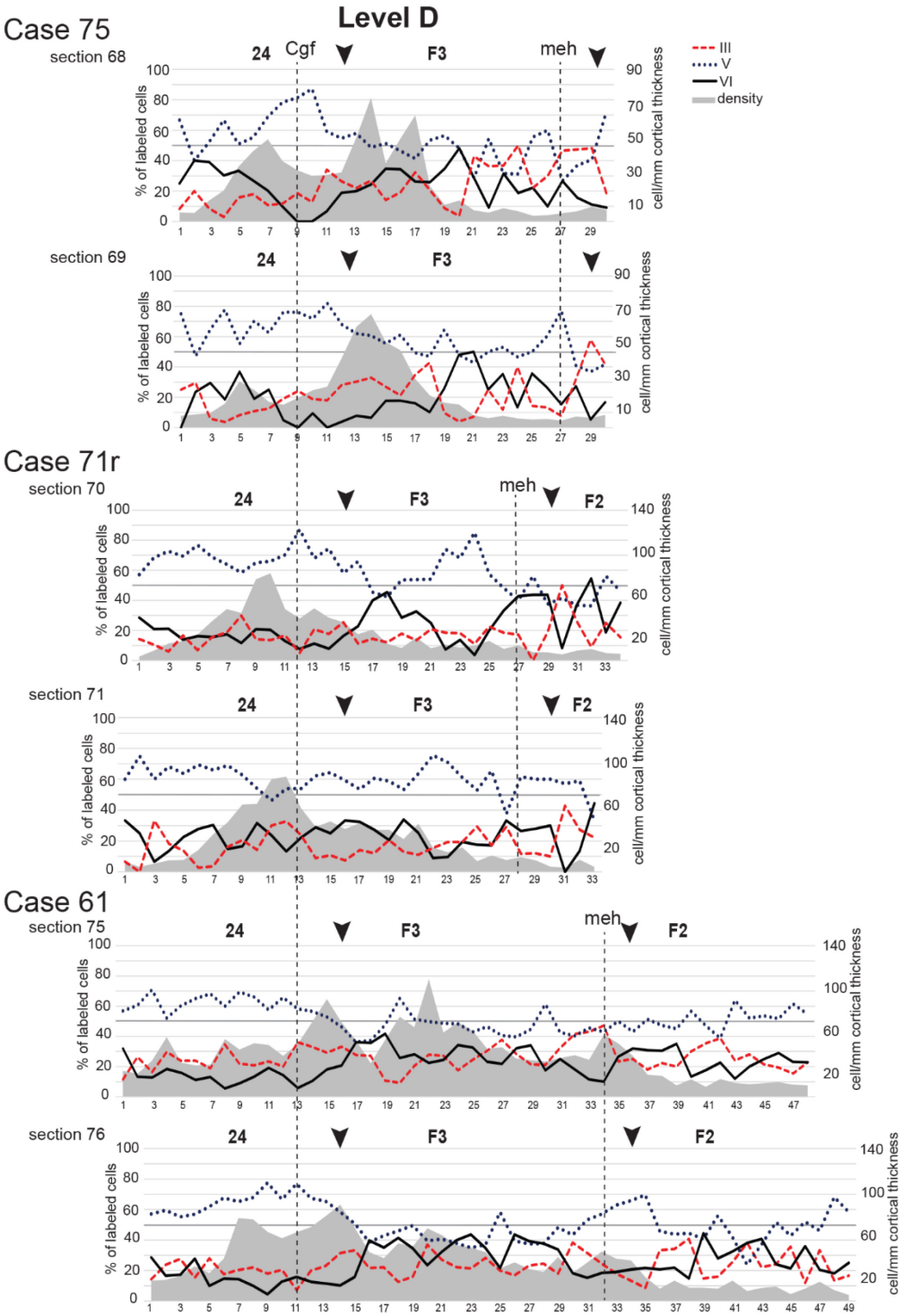

Figure 8. Percent laminar distribution and density of the retrograde labeling in the cingulate and frontal motor cortex at level D in Cases 75, 71r, and 61. Conventions as in Figure 4.

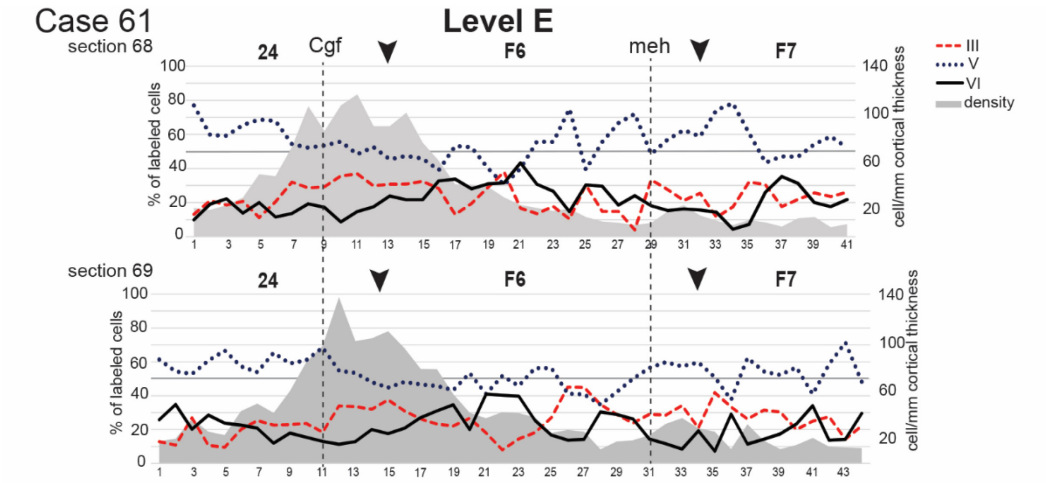

Figure 9. Percent laminar distribution and density of the retrograde labeling in the cingulate and frontal motor cortex at level E in Case 61. Conventions as in Figure 4..

In three cases (61, 71r, and 71l), there was rich labeling also in the ventral premotor cortex (Fig. 10). In Case 61, the laminar distribution of the labeled cells in this region was examined through F5 and the frontal operculum (levels D and E) and more caudally through F4 (level C). In Cases 71l and 71r, the labeling was rich in restricted zones of F5 and F4, which were sampled at levels D and C, respectively. In Case 61, in the F5 sector buried within the postarcuate bank (subdivision F5a), labeled cells were by far predominantly located in layer V. This pattern markedly changed in the F5 sector extending on the convexity cortex (subdivision F5c), where the percentage of labeled cells located in layer VI considerably increased, matching in several bins that of layer V (~40%; Fig. 5*G*). More ventrally, in the frontal operculum, at level E, the contribution of layer VI further increased, reaching in most of the bins percent values of at least 60%, whereas more caudally (level D) tended to be similar to that observed for F5c. In F5c and in the frontal operculum, as well as in all the other frontal motor areas, labeled cells in layer VI tended to be more concentrated in the upper part of the layer and included pyramidal and nonpyramidal neurons (Fig. 5*H*). Finally, in F4 (level C), ~50% of the labeled cells was in layer V.

In Cases 71l and 71r, the laminar distribution pattern observed in F5a (both cases) and in F4 (Case 71r) was very similar to that described for Case 61. In contrast, the laminar distribution pattern observed in F5c in Case 71l was markedly different from that observed in Case 61: the percentage of labeled cells in layer V was by far predominant and that of layer VI was ~10%. This observation was a further clear example that a given premotor area can project to different parts of the motor putamen with a differential contribution of the various cortical layers.

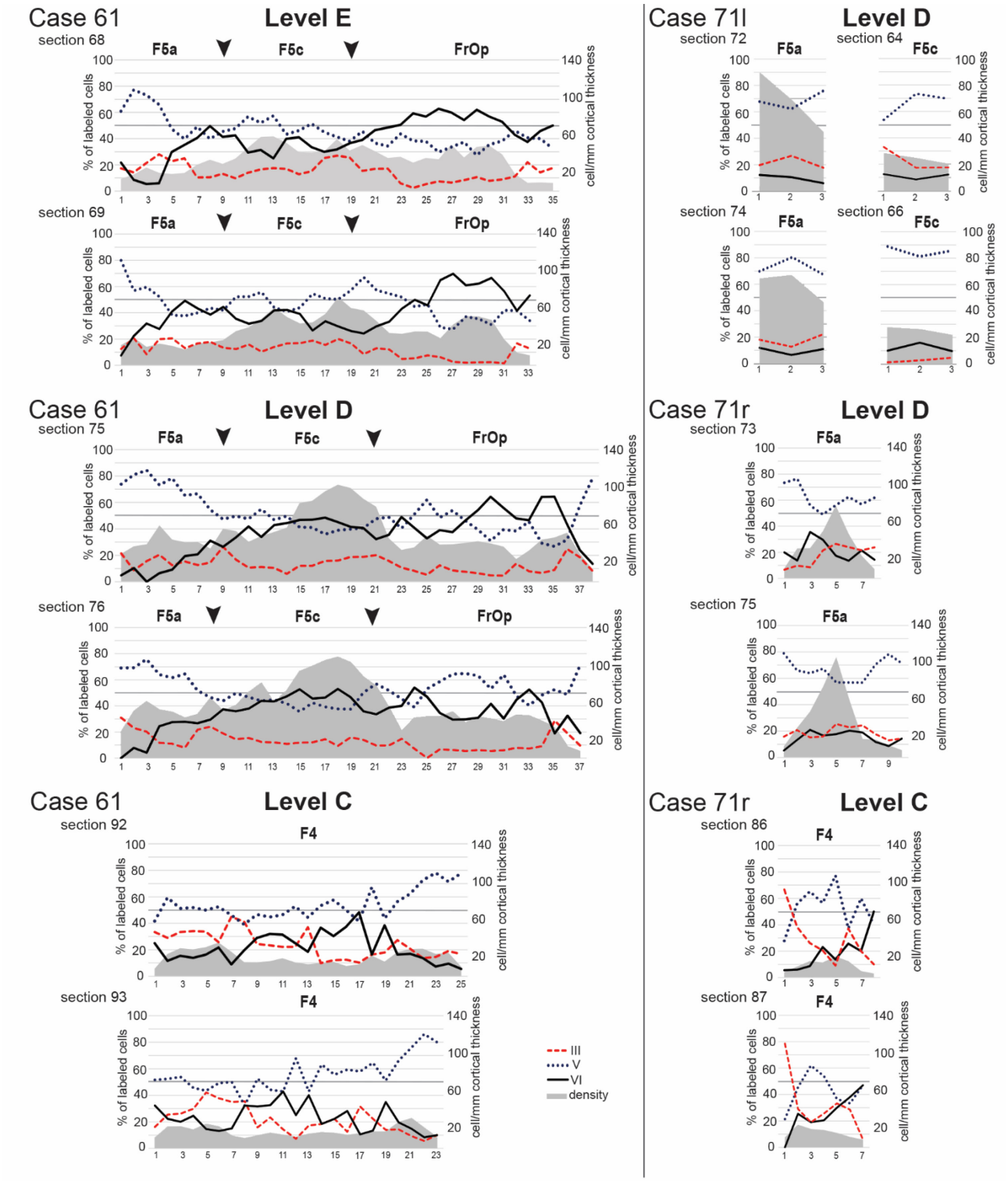

Figure 10. Percent laminar distribution and density of the retrograde labeling in the ventral premotor and opercular frontal cortex. Graphs from Case 61 show data from a cortical region of sections at levels E and D running from the fundus of the arcuate sulcus (left) through F5a, F5c, and the frontal operculum and at level C through F4 on the convexity cortex. Graphs from Case 71l show data from cortical sectors 3-mm-wide of sections taken at level D within the arcuate bank (F5a) or on the convexity cortex (F5c). Graphs from Case 71r show data from cortical sectors taken at level D (in F5a) and level C (in F4) in which the density of labeled cells was .10 cells/bin/mm. Conventions as in Figure 4.

Laminar distribution of CSt-labeled cells in the PFC

As shown for the frontal areas, also in prefrontal cortex laminar distribution pattern of the labeled CSt cells was different across the various labeled zones. In case 76, rostrally (level A), in area 9 and 32, more than 50% of the labeled CSt cells were located in layer V, but in some regions (of about 3 mm) layer III and VI hosted about 20-40% of the labeled cells. In orbitofrontal area 11, labeled CSt cells were in layers III and V. More caudally (level B), in area 32 labeled CSt cells were again mainly in layer V, while in the medial area 9 and in area 24 were almost equally distributed in layer III and V. In area 14, more than 50% of the labeled CSt cells were in layer V (Fig 11). At level D, in area 45B labeled CSt cells were mainly located in layer V and III, in the orbitofrontal cortex tended to be more equally distributed across layer III, V, and VI. In premotor area F6 labeled CSt cells tended to be equally distributed in layer III, V, and VI.Area 8 in level E showed labeled CSt cells mainly located in layer III (about 70%). At level C, area 8B after injection in the caudate (Case 76), labeled CSt cells were in layer V and III; after injection in the precommissural putamen (Case 77) labeled CSt cells were mainly in layer V and VI, while layer III hosted very few labeled neurons (Fig 12).

In Case 61, after injection in the putamen at the level of the anterior commissure, relatively rich labeling was observed in the ventrolateral PFC, more densely involving areas 46v and 12r. In this region, the majority of the labeled cells was located in layer V; but as observed in the insular cortex, there was a relatively robust contribution (up to 40% of the labeled cells) of layer VI (Fig. 5I).

Figure 11 3D reconstructions of C76 injected hemispheres ; each dot corresponds to one labeled neuron, showing the distribution of the cortical labeling observed after injections in the caudate. The distribution of the retrograde labeling is shown in dorsolateral and medial views. On the 3D recostructions are indicated the levels at which the analyzed sections were taken. Graphs show percent laminar distribution and density of the retrograde labeling in PFC. (levels A,B,D,E). For each levels, on the left, one section drawing shows the analyzed cortical sector and layer V shaded in light blue. Graphs from Case 76 represent data from 500-mm-wide bins from the region in which the labeled cell density was constantly higher than 10 labeled cells/bin/mm.

Case 76 WGA in the Caudate

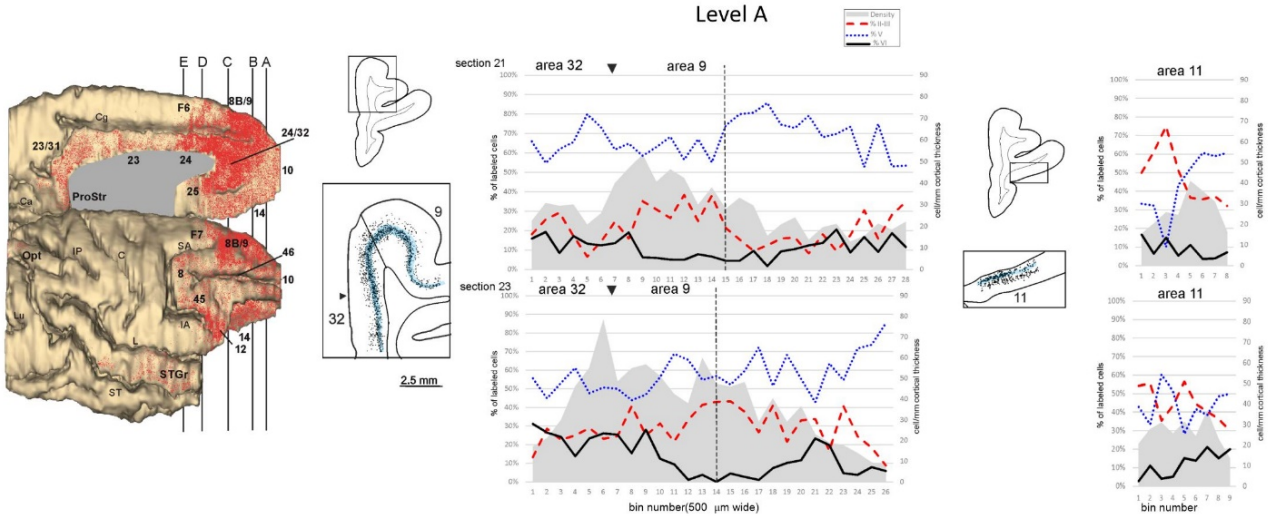

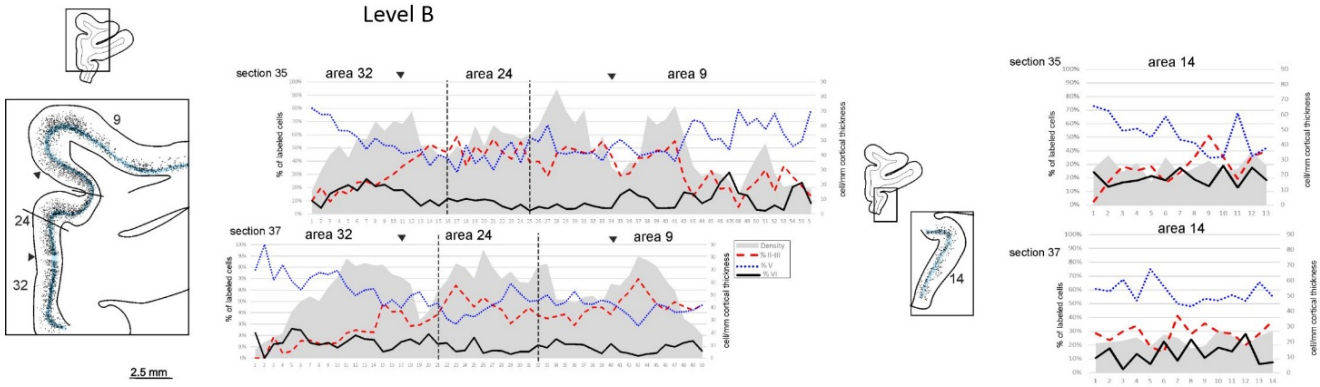

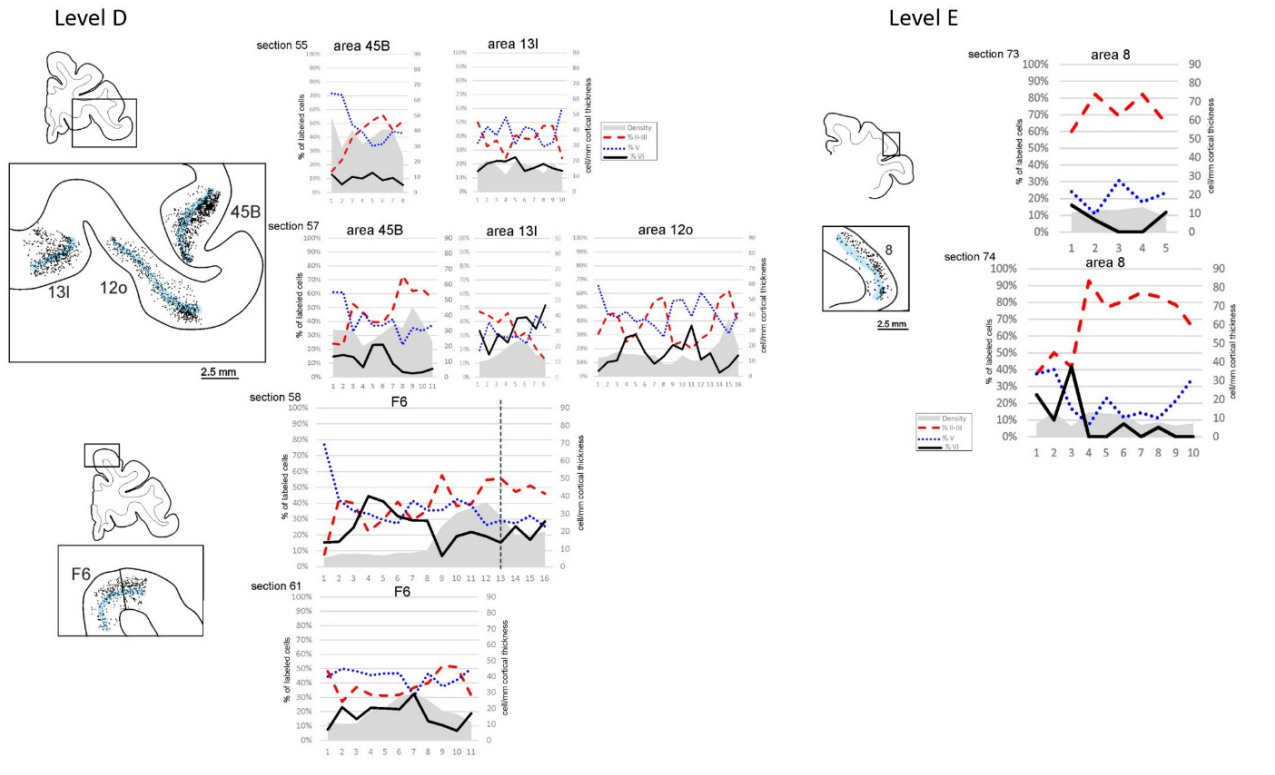

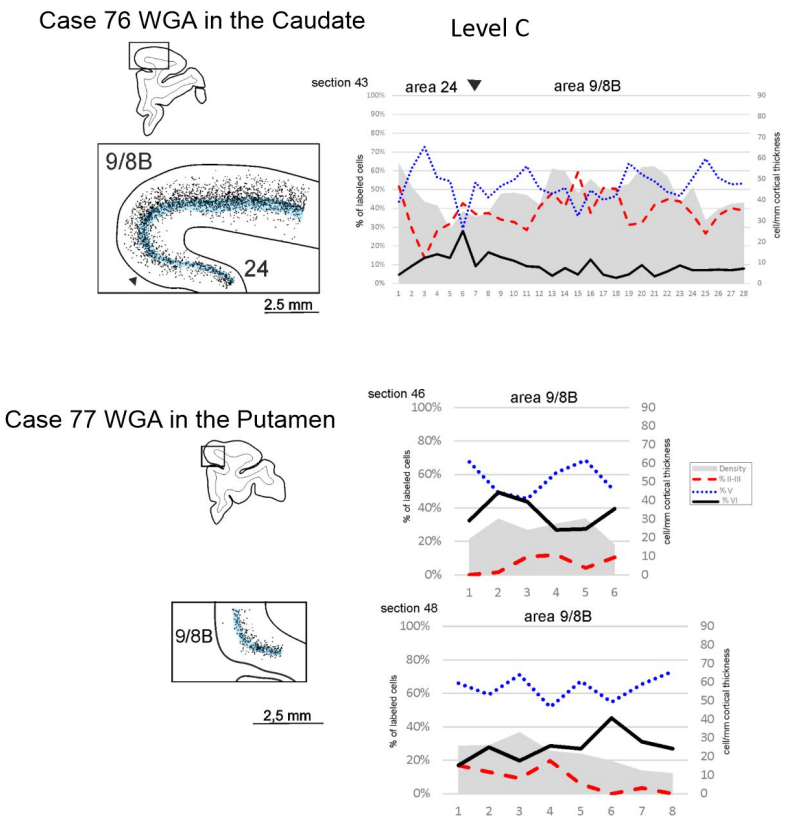

Figure 12 Percent laminar distribution and density of the retrograde labeling at level C in C76 and C77

Laminar distribution of CSt-labeled cells in the parietal and insular cortex.

Differently from what was observed in the frontal motor and cingulate cortex and in the frontal opercular cortex, in the parietal and insular cortex, the laminar distribution of the CSt-labeled cells was substantially uniform and characterized by pyramidal cells predominantly confined to layer V, with some of them in the position of layer IV. Specifically, in the parietal cortex, independently from the labeled area and from the richness of the labeling, labeled cells in layer V (plus layer IV) tended to be almost everywhere >80%, with the remaining mostly localized in layer VI (Fig. 5*J*). In the insular cortex, labeled cells were by far predominantly located in layer V in Cases 75, 71r, and 71l in which the labeling was relatively poor. In Case 61, in which labeling in the insula was considerably richer, most of the labeled cells was located in layer V; and a variable, but robust, proportion was located in layer VI.

Figure 13 show in case 77, cortical regions in which some CSt cells in layer VI that seems potentially inhibitory . These sections, sampled from ventral premotor, primary motor, parietal, and cingulate

motor cortex were processed with both immunohistochemistry and RNAscope (ISH), using probes for gabaergic markers.

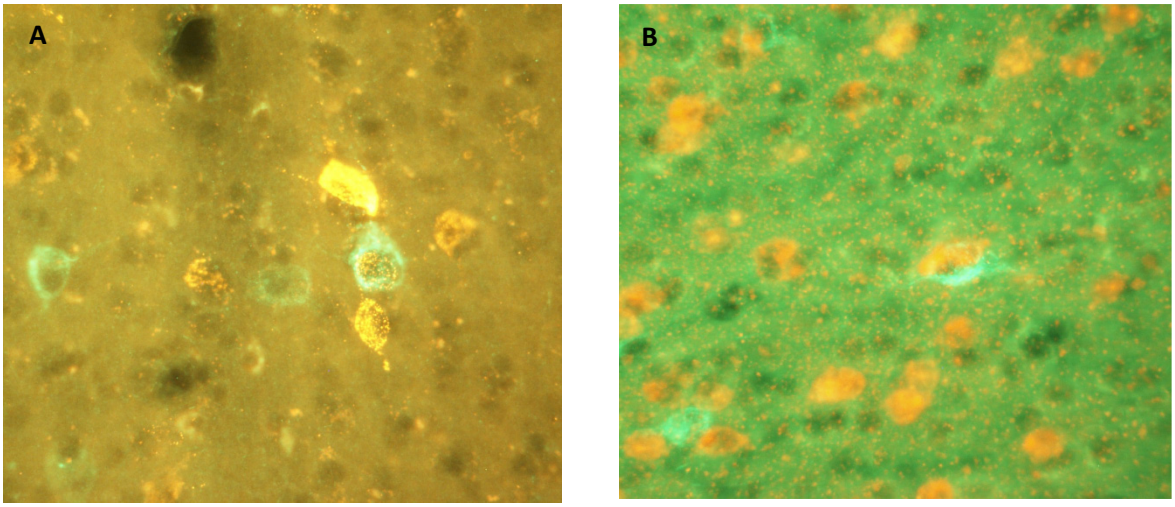

Figure 13 Examples of double labelled Cst cells : **A** CTB + and SOM+ **B** CTB + and GAD+ in region F1.

3.2 Study 2 - Crossed CSt projections

Crossed CSt projections have been observed in all the cases used for this study. The proportion of labeled cells in the contralateral versus ipsilateral hemisphere largely varied according to the location of the injection site, showing a gradient in which crossed CSt projections were strongest to the caudate head and body, less strong to the rostral putamen and dorsal motor putamen, and lowest to the middle or midventral motor putamen, where the hand is represented (Alexander and DeLong, 1985). In general, the distribution of the labeled CSt cells in the contralateral hemisphere differed for several aspects from that observed in the ipsilateral hemisphere (Fig.14). Indeed, contralateral areas with CSt projections were always a subset of the ipsilateral areas with CSt projections. Specifically, in all the cases, the areas in the posterior parietal, temporal, and insular cortex that exhibited even relatively robust labeling in the ipsilateral hemisphere had virtually no labeling in the contralateral hemisphere (Fig. 14). Nevertheless, there were areas in the contralateral hemisphere whose relative contribution to the crossed CSt projections was much higher than that of the homolog ipsilateral areas to the direct CSt projections. The frequency distributions of the labeled CSt cells per area in the ipsilateral and the contralateral hemisphere were compared by the Pearson's chi-square test and likelihood ratio chi-square test (Fig. 14). Both test showed a statistically significant difference ($p < 0.001$) among the distributions in all the cases.

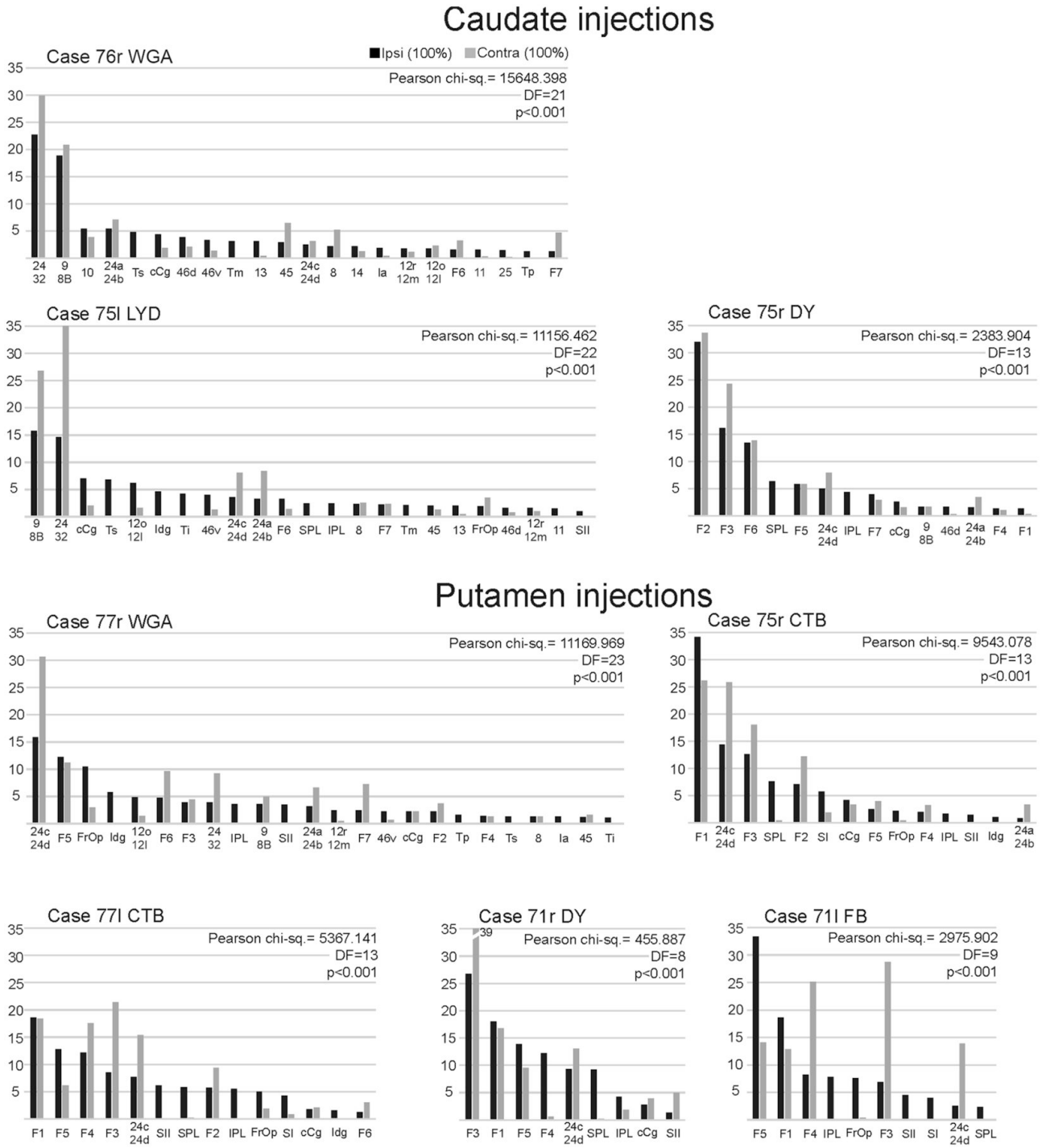

Figure 14. Percentage of areal distribution of the total retrograde labeling observed in the ipsilateral hemisphere (black) compared with that of the total retrograde labeling observed in the contralateral hemisphere (gray) in all the cases of the present study. In each graph, areas are ordered based on the amount of ipsilateral labeling (only areas with ipsilateral labeling .1%).Superior parietal (SPL) areas and inferior parietal (IPL) areas are grouped. The results of the statistical analysis are reported in which the frequency distributions of the labeled CSt cells per area in the ipsilateral and the contralateral hemisphere were compared (Pearson chi-square test for independence). cCg Caudal cingulate cortex (areas 23, 31, 29, 30); DF, degree of freedom; Ia, agranular insula; Idg, disgranular insula.

Crossed CSt projections to the caudate nucleus

Two tracer injections were placed in the caudate head. In Case 76 right (76r) the WGA injection site was slightly more rostral and medial than the LYD injection site of Case 75 left (75l; Fig. 1). As largely expected, in the ipsilateral hemisphere the highest proportion of labeled cells was located in the prefrontal cortex (Figs. 15, 16, Table 2), mostly involving areas 9/8B, followed by the rostral cingulate cortex, mostly involving the rostral area 24/32 and the rostral cingulate gyrus (area 24a/b). Relatively robust labeling was also observed in the temporal cortex involving in both cases belt/parabelt auditory areas, the superior temporal polysensory area, and the medial temporal cortex and in Case 75l LYD, the rostral inferotemporal cortex. Much weaker was the labeling observed in rostral premotor, insular, and caudal cingulate cortex and in Case 75l LYD, in the parietal cortex. In both cases, the percentage of labeled CSt cells observed in the contralateral hemisphere was robust, i.e., ∼30% of the total number of ipsilateral plus contralateral CSt cells (Figs. 15, 16, Table 3).

In the contralateral hemisphere virtually all the labeling was located in frontal and cingulate areas, whereas the parietal, temporal, and insular cortex were virtually devoid of labeling (Table 3). In both cases the labeling in the contralateral hemisphere was mostly concentrated in the rostral cingulate areas 24/32 and in prefrontal areas 9/8B, which were the most densely labeled areas in the ipsilateral hemisphere (Fig. 17). In both cases these two contralateral areas were among the five most labeled ones. However, in contralateral area 10 in Case 76r WGA and in the orbital (12o) and lateral (12l) part of area 12 in Case 75l LYD the labeling was relatively much weaker compared with the ipsilateral hemisphere. Weaker labeling also involved rostral premotor areas and the caudal cingulate cortex.

In Case 75r DY, the injection site was located in the caudate body at about the level of the anterior commissure (AC; Fig. 1). The distribution of the labeling in the ipsilateral hemisphere (Fig. 18, Table 2) was markedly different from that observed in the two cases previously described, involving mostly dorsal and medial premotor areas, primarily areas F3, F2, and F6 and to a lesser extent area F7. In area F3, the labeling mostly involved its rostral half. Less dense labeling was located in the ventral premotor cortex, motor cingulate (24c/d), inferior parietal (anterior intraparietal, PFG, PG) and caudal superior parietal (caudal PE (Pec), cingulate PE (Peci), medial PG (PGm), V6A) areas. This labeling distribution suggests that the injection site involved a striatal sector related to visuomotor and somatomotor control of arm movements. Also in this case, the labeling in the contralateral hemisphere was quite robust (∼30% of the ipsilateral plus contralateral CSt labeled cells) and was

virtually all located in frontal and cingulate areas (Table 3). Specifically, the areal distribution of the labeled CSt cells (Fig. 17) in all the various premotor and cingulate areas was quite similar in the two hemispheres, and contralateral areas F2 and F3 were among the five most labeled areas, considering both the ipsilateral and contralateral hemispheres.

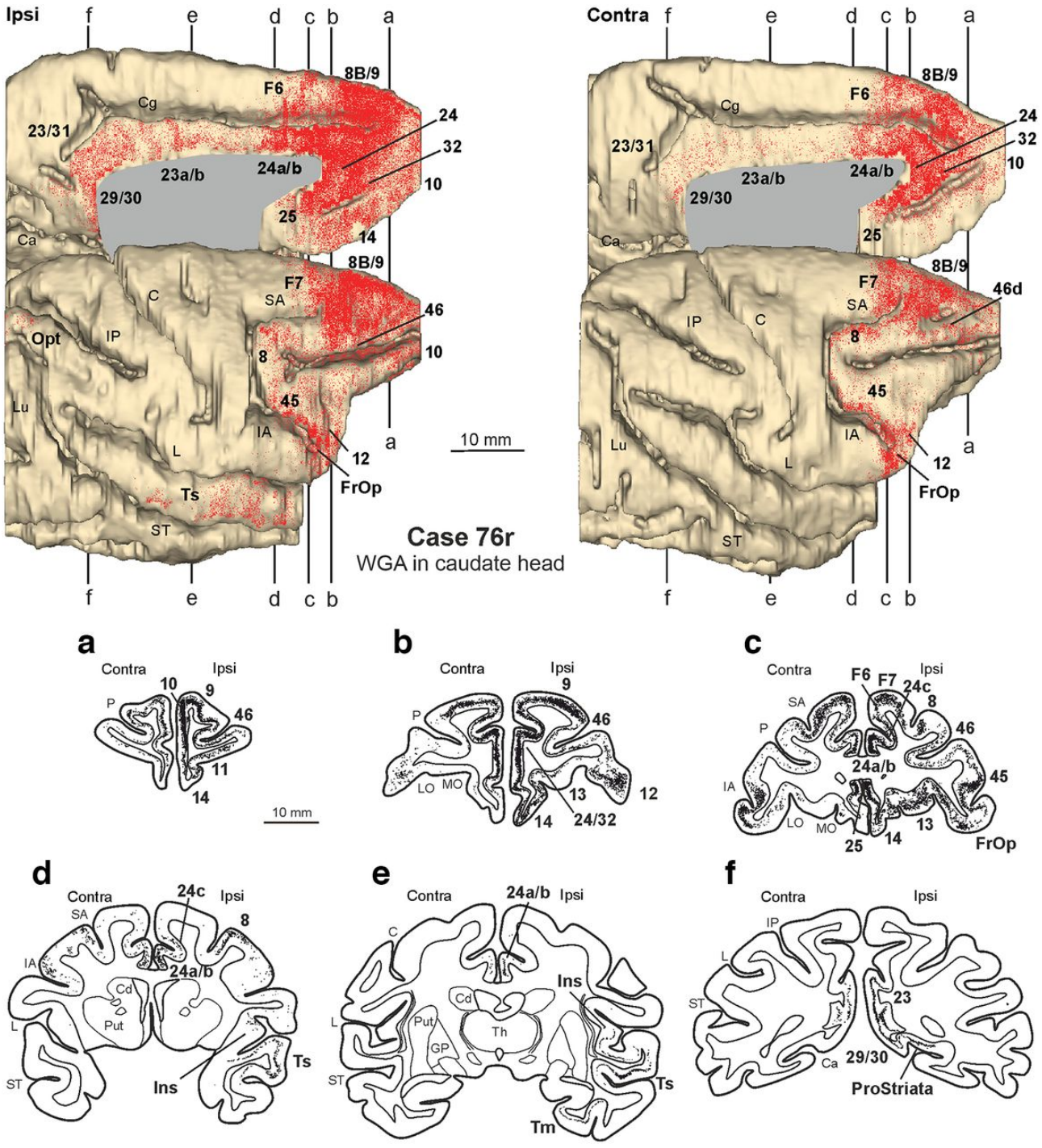

Figure 15. Distribution of the retrograde labeling observed after injection of WGA in the head of the caudate in Case 76r. The labeling is shown in dorsolateral and medial views of the 3D reconstructions of the injected (ipsilateral) and the contralateral hemisphere and in drawings of coronal sections. For the sake of comparison, in this and in the subsequent figures, all the 3D reconstructions are shown as a right hemisphere with the injected hemisphere on the left and all drawings with the injected hemisphere on the right. a–f, Sections are shown in a rostral to caudal order. The levels at which the sections were taken are shown on the 3D reconstructions of both hemispheres. Each dot corresponds to one labeled neuron. C, Central sulcus; Ca, calcarine fissure; Cd, caudate nucleus; Cg, cingulate sulcus; GP, globus pallidus; IA, inferior arcuate sulcus; Ins, insula; IP, intraparietal sulcus; L, lateral sulcus; LO, lateral orbital sulcus; Lu, lunate sulcus; MO, medial orbital sulcus; Opt, occipito-temporo-parietal area; P, principal sulcus; Put, putamen; SA, superior arcuate sulcus; ST, superior temporal sulcus; Th, thalamus.

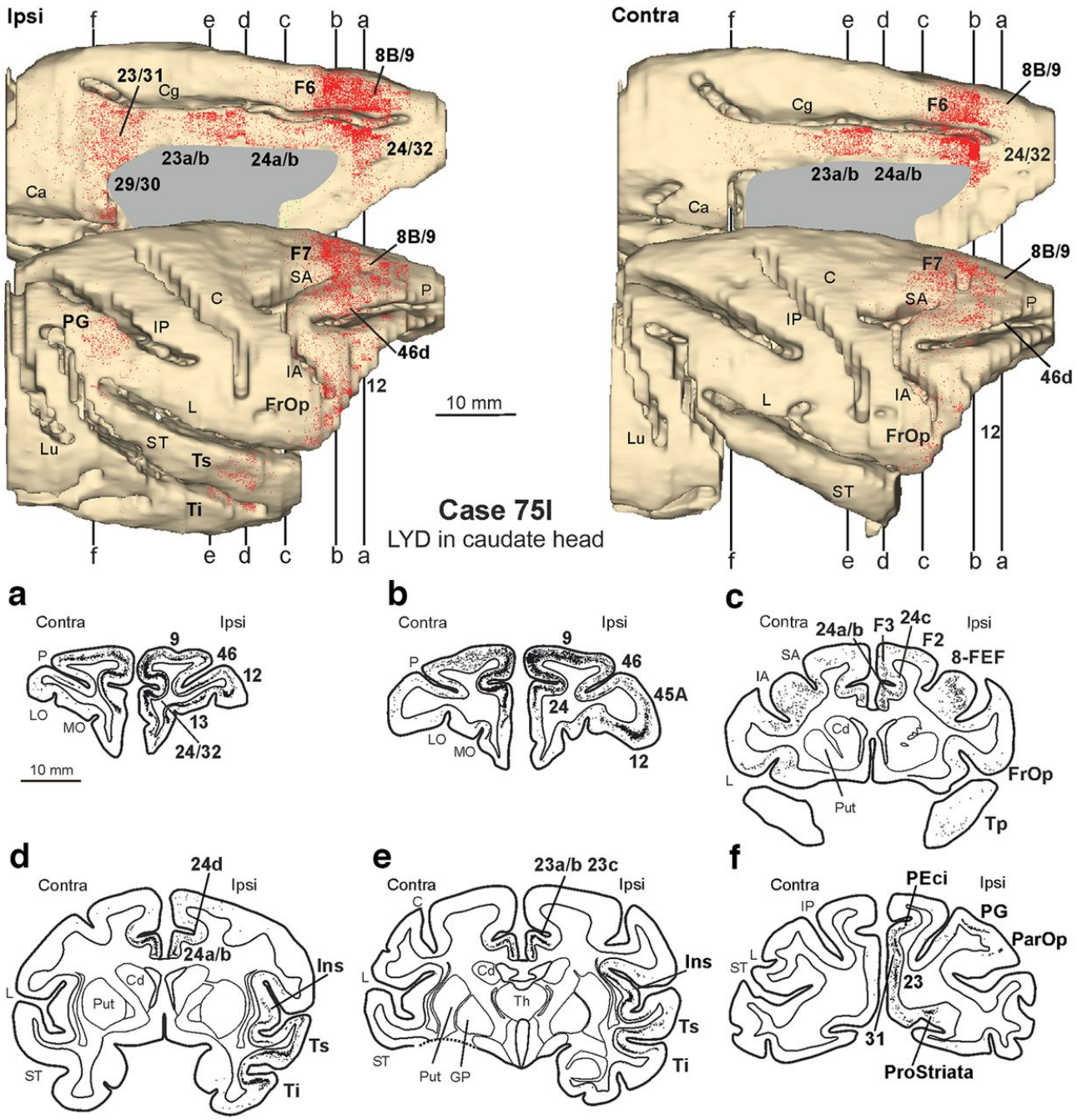

Figure 16. Distribution of the retrograde labeling observed after injection of LYD in the head of the caudate in Case 75l. The labeling is shown in dorsolateral and medial views of the 3D reconstructions of the injected (ipsilateral) and contralateral hemispheres and in drawings of coronal sections. C, Central sulcus; Ca, calcarine fissure; Cd, caudate nucleus; Cg, cingulate sulcus; GP, globus pallidus; IA, inferior arcuate sulcus; Ins, insula; IP, intraparietal sulcus; L, lateral sulcus; LO, lateral orbital sulcus; Lu, lunate sulcus; MO, medial orbital sulcus; P, principal sulcus; ParOp, parietal operculum; Put, putamen; SA, superior arcuate sulcus; ST, superior temporal sulcus; Th, thalamus. Conventions are defined in the legend to Figure 3

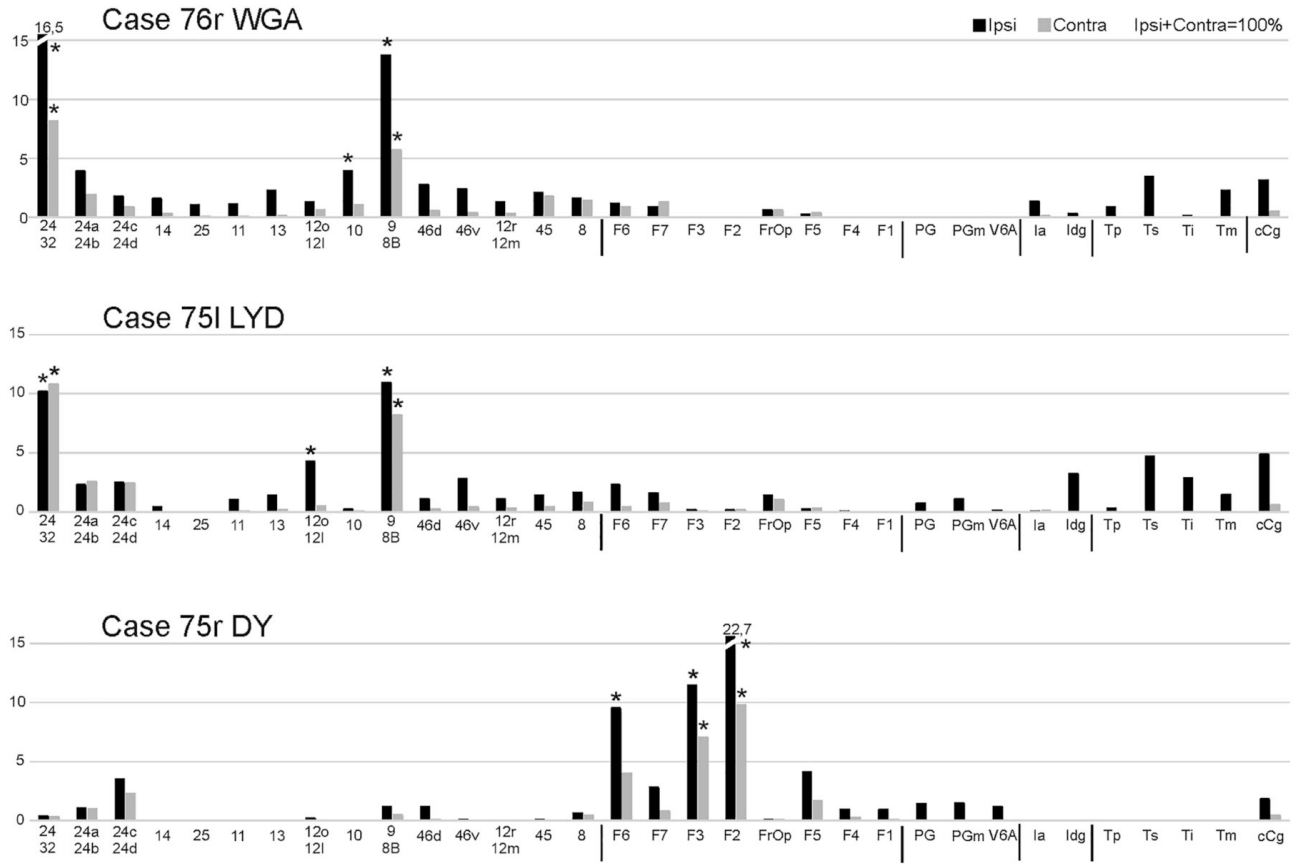

Figure 17 Percentage distribution of the total (ipsi plus contra) retrograde labeling in ipsilateral (black) and contralateral (gray) areas observed after the tracer injections in the caudate. The asterisks indicate the five most labeled areas. cCg, Caudal cingulate cortex (areas 23, 31, 29, 30); Ia, agranular insula; Idg, disgranular insula

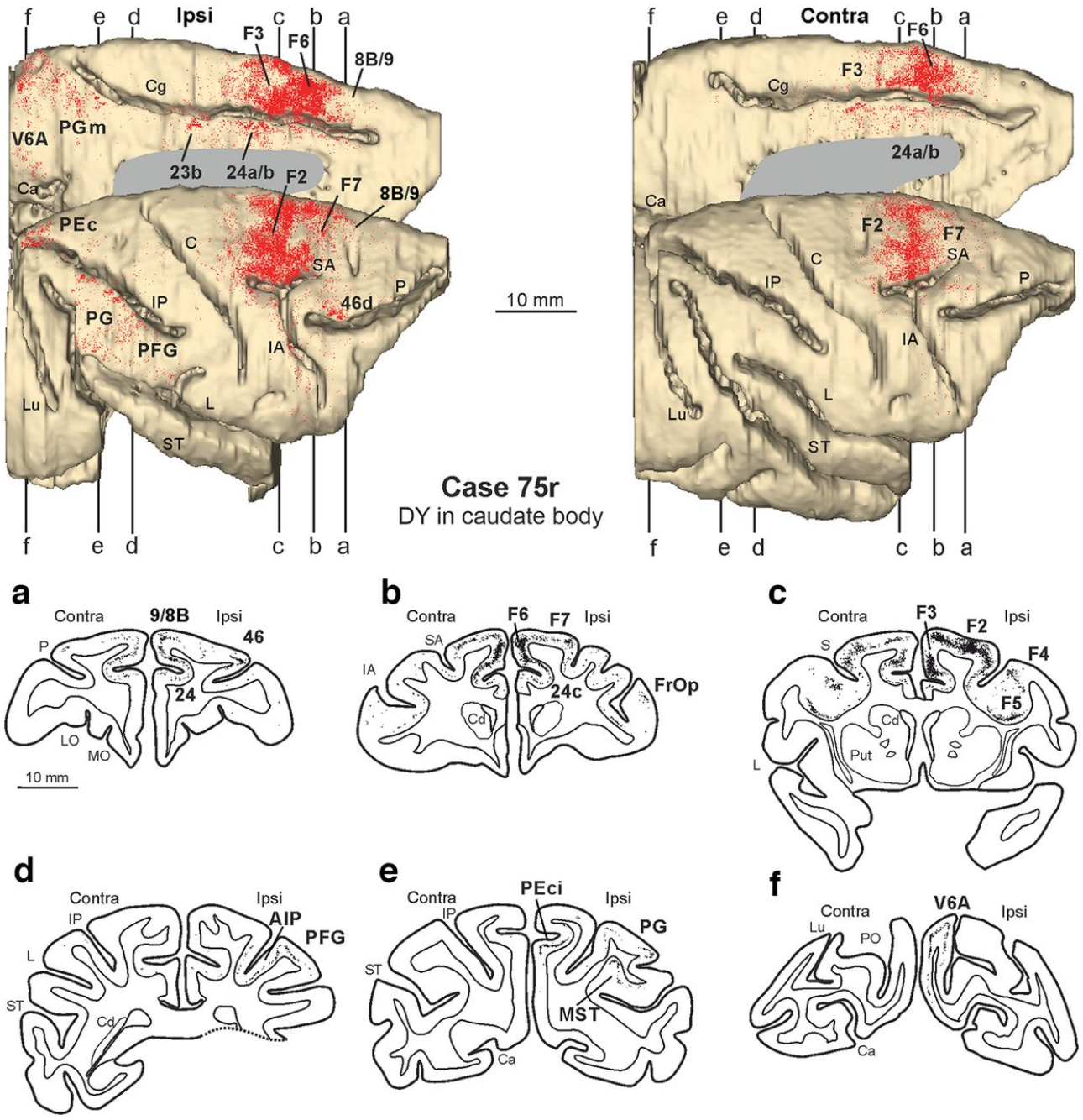

Figure 18. Distribution of the retrograde labeling observed after injection of DY in the caudate body in Case 75r. The labeling is shown in dorsolateral and medial views of the 3D reconstructions of the injected (ipsilateral) and contralateral hemisphere and in drawings of coronal sections. AIP, anterior intraparietal area; C, Central sulcus; Ca, calcarine fissure; Cd, caudate nucleus; Cg, cingulate sulcus; IA, inferior arcuate sulcus; IP, intraparietal sulcus; L, lateral sulcus; LO, lateral orbital sulcus; Lu, lunate sulcus; MST, medial superior temporal area; MO, medial orbital sulcus; P, principal sulcus; PO, parieto occipital sulcus; Put, putamen; S, spur of the arcuate sulcus; SA, superior arcuate sulcus; ST, superior temporal sulcus. Conventions as in Figure 3.

Table 2. Regional distribution (%) and total number (n) of labeled cortical neurons observed in the ipsilateral hemisphere, following tracer injections in the caudate and in the putamen

	Case	Rostral cingulate	Pref	Motor	Parietal	Insula	Temp	Caudal cingulate	Other	Total	n. cells
Caudate	75l LYD Lateral head AC + 6	21,5	37,8	8,4	6,1	4,8	13,5	7	0,9	100	42183
	76r WGA Medial head AC + 7	30,6	48,5	4,1	0,1	2,3	9,4	4,4	0,6	100	140790
	75r DY Body AC – 0,5	7	4,8	74,1	11,5	0	0	2,6	0	100	33082
Putamen	77r WGA Rostral AC + 3	23	17,5	37,8	8,1	7	4,3	2,3	0	100	99341
	75r CTBg Dorsal Motor	15,3	0,7	61,9	16,6	1,4	0	4,1	0	100	119306
	77l CTBg Middle Motor	8,3	1	64,5	21,6	2	0,8	1,8	0	100	75292
	71r DY Middle Motor	9,4	0	72,1	15,1	0,5	0,1	2,8	0	100	8360
	71l FB Mid-ventral Motor	2,6	0,5	75,5	18,6	1,2	0,8	0,8	0	100	36628

Table 3. Regional distribution (%) and total number (n) of labeled cortical neurons observed in both ipsilateral and contralateral hemisphere.

	Case		rostral cingulate	Pref	Motor	Parietal	Insula	Temp	caudal cingulate	Other	Total
Caudate	**75l LYD** Lateral head n = 60609	Ipsi	15	26,3	5,9	5	3,3	9,3	4,9	0.6	69,6
		Contra	15,8	11,1	2,8	0,1	0,1	0	0,6	0	30,4
	76l WGA Medial head n = 193668	Ipsi	22,2	35,3	3	0,1	1,7	6,8	3,2	0,4	72,7
		Contra	11	12,5	3,2	0	0,1	0	0,5	0	27,3
	75r DY Body n = 46626	Ipsi	5	3,4	52,6	8,1	0	0	1,8	0	70,9
		Contra	3,6	1,1	23,9	0	0	0	0,5	0	29,1
Putamen	**77l WGA** Rostral n =119738	Ipsi	19	14,5	31,3	6,7	5,8	3,5	1,9	0	82,7
		Contra	7,9	1,9	7	0	0,1	0	0,4	0	17,3
	75r CTBg dorsal motor n = 154075	Ipsi	11,8	0,5	47,8	13	1,2	0	3,2	0	77,5
		Contra	6,6	0,1	14,6	0,5	0	0	0,7	0	22,5
	77l CTBg Middle Motor n = 85579	Ipsi	7,2	1	56,6	19,1	1,8	0,7	1,6	0	88
		Contra	2,1	0	9,6	0,1	0	0	0,2	0	12
	71r DY Middle Motor n = 9603	Ipsi	8,2	0	62,9	13,1	0,4	0,1	2,4	0	87,1
		Contra	1,7	0	9,7	1	0	0	0,5	0	12,9
	71l FB Mid-ventral motor n = 38407	Ipsi	2,4	0,5	72	17,8	1,1	0,8	0,8	0	95,4
		Contra	0,7	0	3,8	0	0	0	0,1	0	4,6

Crossed CSt projections to the putamen

Five tracer injections involved the putamen, one more rostrally (Case 77r WGA) and the others at the same level of or caudal to the AC, at different dorsoventral levels (Fig. 1).

The injection site in Case 77r WGA was located relatively ventrally in the precommissural putamen. In the ipsilateral hemisphere (Fig. 19), the labeling was densest in the premotor cortex, especially area F5, frontal operculum, and rostral cingulate cortex, especially area 24c/d. Less dense labeling involved prefrontal, parietal, and insular cortex and, more weakly, temporal and caudal cingulate cortex. The very weak labeling in area F1 suggests that the injection site involved a putaminal sector rostral to the motor putamen as usually defined. The distribution of the labeling involving the ventral premotor area F5, frontal operculum, rostral F3, ventrolateral prefrontal sectors including area 12 and ventral area 46, and inferior parietal and opercular parietal sectors suggests that the injection site involved a striatal sector related to hand and mouth motor control, at least in part corresponding to the rostral striatal target of the lateral grasping network projections (Gerbella et al., 2016). In the contralateral hemisphere, the amount of CSt labeled neurons was relatively robust, although lower than that observed for the caudate tracer injections (Table 3). Specifically, labeled CSt cells were mostly equally distributed between the rostral cingulate and premotor cortex and only marginally involved prefrontal and caudal cingulate cortex. Again, parietal and temporal cortex, but also the insula, were virtually devoid of labeling. The areal distribution of the labeling (Fig. 20) shows that the ratio of labeled CSt cells in the contralateral versus ipsilateral cortical areas was quite low for F5 and frontal operculum and relatively high for the rostral cingulate areas and premotor areas F6 and F7. Contralateral area 24c/d was among the five most labeled areas, considering ipsilateral and contralateral areas.

In Case 75r CTBg, the injection site was placed in the dorsal part of the putamen at about the level of the AC (Fig. 1). In the ipsilateral hemisphere (Fig. 21), labeled CSt cells were mostly concentrated in the frontal and cingulate motor cortex. As expected from the somatotopy of the motor putamen (Alexander and DeLong, 1985), in the frontal motor cortex labeled cells were densest in the medial part of F1 and in the caudal half of F3 suggesting that the injection site involved the leg/trunk representation. Additional weaker labeling was observed in dorsomedial primary somatosensory area (SI), in the superior parietal area PE, and in the caudal cingulate cortex. In the contralateral hemisphere, labeled CSt cells were ~22% of the total ipsilateral plus contralateral labeling and were observed almost completely in the frontal motor cortex, mainly in F1, F3, and F2, and in area 24c/d, except for some weak labeling in the parietal cortex (mostly in SI) and in the caudal cingulate cortex.

As observed in other cases, of the five most labeled cortical areas, two were in the contralateral hemisphere (Fig. 20). Furthermore, based on the number of labeled cells, about one-third of the overall input to the injected striatal zone from areas 24c/d, F3, and F2 originated from the contralateral hemisphere (nearly one-fifth from contralateral F1).

Three tracer injections were placed more ventrally in the motor putamen at different rostrocaudal levels (Fig. 1). In Case 71r DY the injection site was located in the middle of the motor putamen and was much smaller than expected, likely because the volume of tracer injected was smaller than planned. In Cases 77l CTBg and 71l FB, the injections were located slightly more caudal and ventral. In all these cases, the labeling in the ipsilateral hemisphere was mostly located in the frontal and cingulate motor cortex, but ~15–20% of the labeled cells were in the parietal cortex (Table 2). As expected from the somatotopy of the motor putamen (Alexander and DeLong, 1985), the labeling involved in all cases the middle part of F1 and F3 and ventral premotor areas F5 and F4, suggesting involvement by the injection sites of the arm/hand representation (Figs. 20, 22, 23). In Cases 77l CTBg and 71l FB the labeling extended also more ventrally in F1 and in F5, more rostrally in F3 and in the frontal operculum, suggesting an involvement also of the face/mouth representation. In the parietal cortex the most labeled areas were SI, secondary somatosensory area (SII), and PE and rostral inferior parietal areas. In the contralateral hemisphere, the number of labeled cells (5–12%) was considerably lower than that observed after the other putaminal and the caudate injections (Table 3). However, this labeling involved a limited number of contralateral areas (Fig. 14), so the relative contribution of the crossed projections to the whole input from areas 24c/d, F3, and F1 was ~10–20%. Interestingly, in Cases 71l FB and 77l CTBg the contralateral labeling tended to be densest in rostral F3 and in Case 71l FB in the lateral part of the ventral premotor cortex, likely involving preferentially face/mouth fields. Furthermore, except for some sparse labeling located in SI (also SII in Case 71r DY), the contralateral parietal labeling was negligible, even if in these three cases the ipsilateral parietal cortex hosted 13–19% of the overall labeled cells.

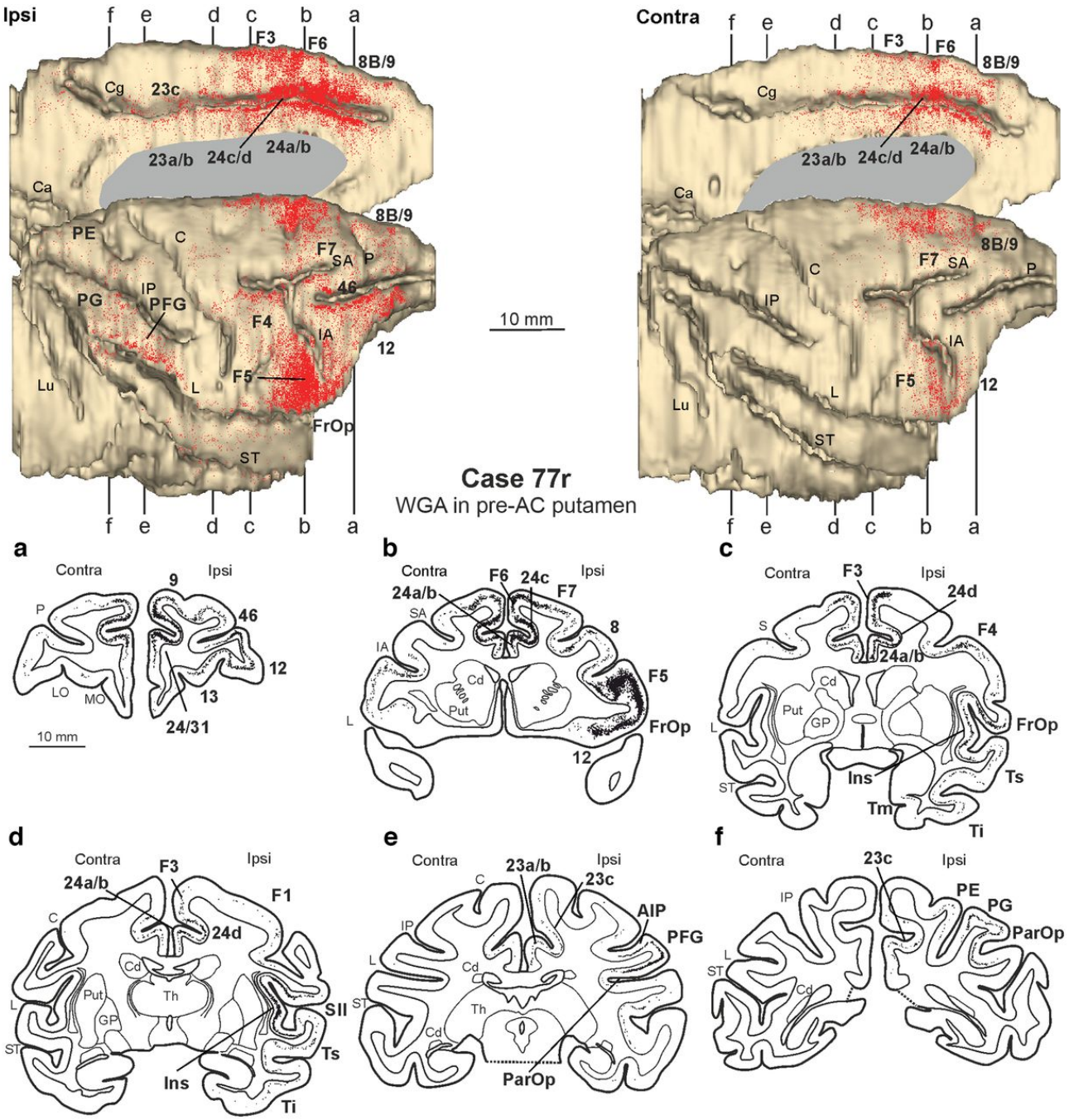

Figure 19. Distribution of the retrograde labeling observed after injection of WGA in the precommissural putamen in Case 77r. The labeling is shown in dorsolateral and medial views of the 3D reconstructions of the injected (ipsilateral) and contralateral hemisphere and in drawings of coronal sections. AIP, anterior intraparietal area; C, central sulcus; Ca, calcarine fissure; Cd, caudate nucleus; Cg, cingulate sulcus; GP, globus pallidus; IA, inferior arcuate sulcus; Ins, insula; IP, intraparietal sulcus; L, lateral sulcus; LO, lateral orbital sulcus; Lu, lunate sulcus; MO, medial or-bital sulcus; P, principal sulcus; ParOp, parietal operculum; Put, putamen; SA, superior arcuate sulcus; S, spur of the arcuate sulcus; ST, superior temporal sulcus; Th, thalamus. Conventions as in Figure 3.

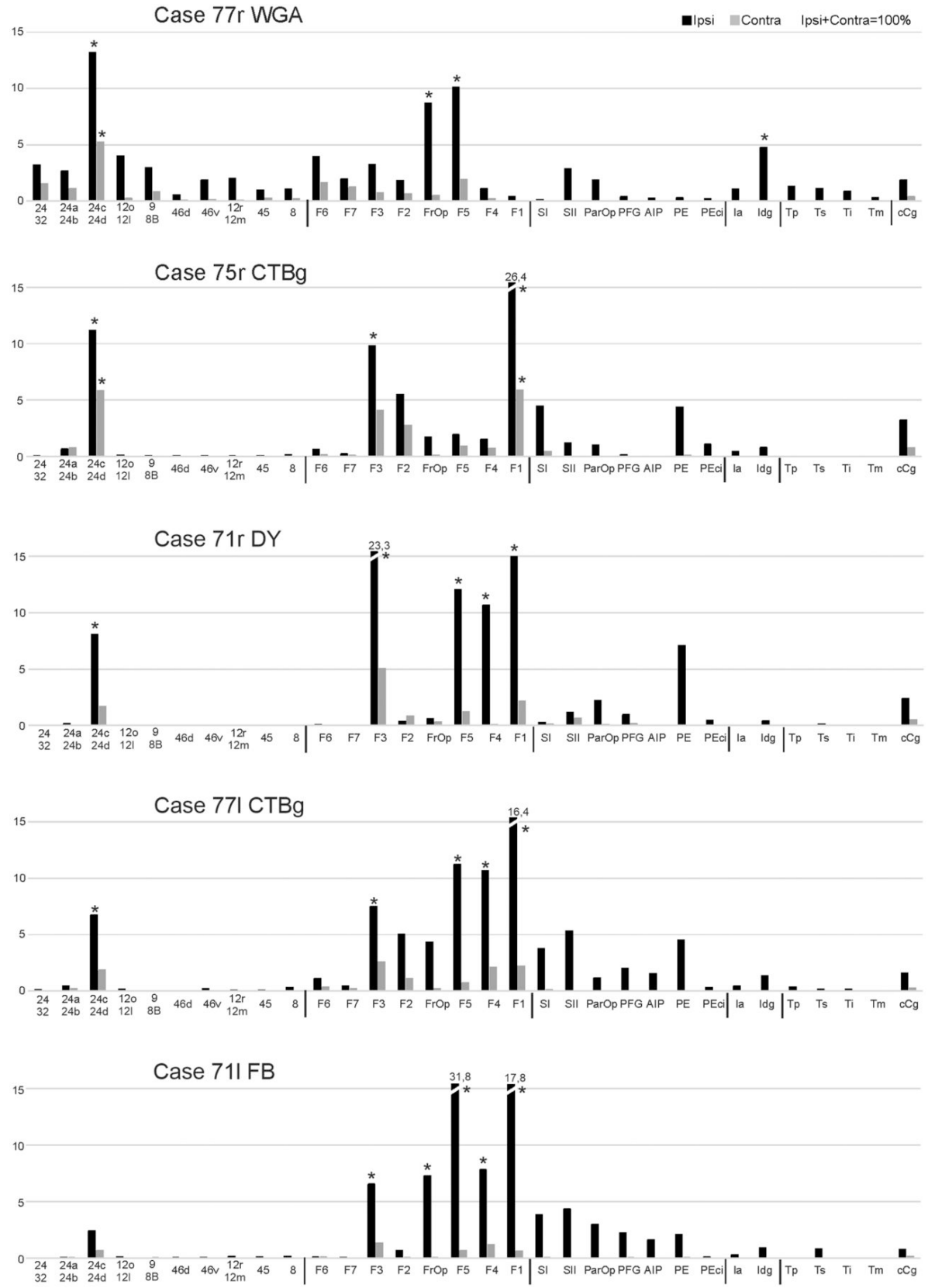

Figure 20. Percentage distribution of the total (ipsi plus contra) retrograde labeling in the ipsilateral (black) and contralateral (gray) areas observed after the tracer injections in the putamen. The asterisks indicate the five most labeled areas. AIP, anterior intraparietal area; cCg, caudal cingulate cortex (areas 23, 31, 29, 30); Ia, agranular insula; Idg, disgranular insula; ParOp, parietal operculum.

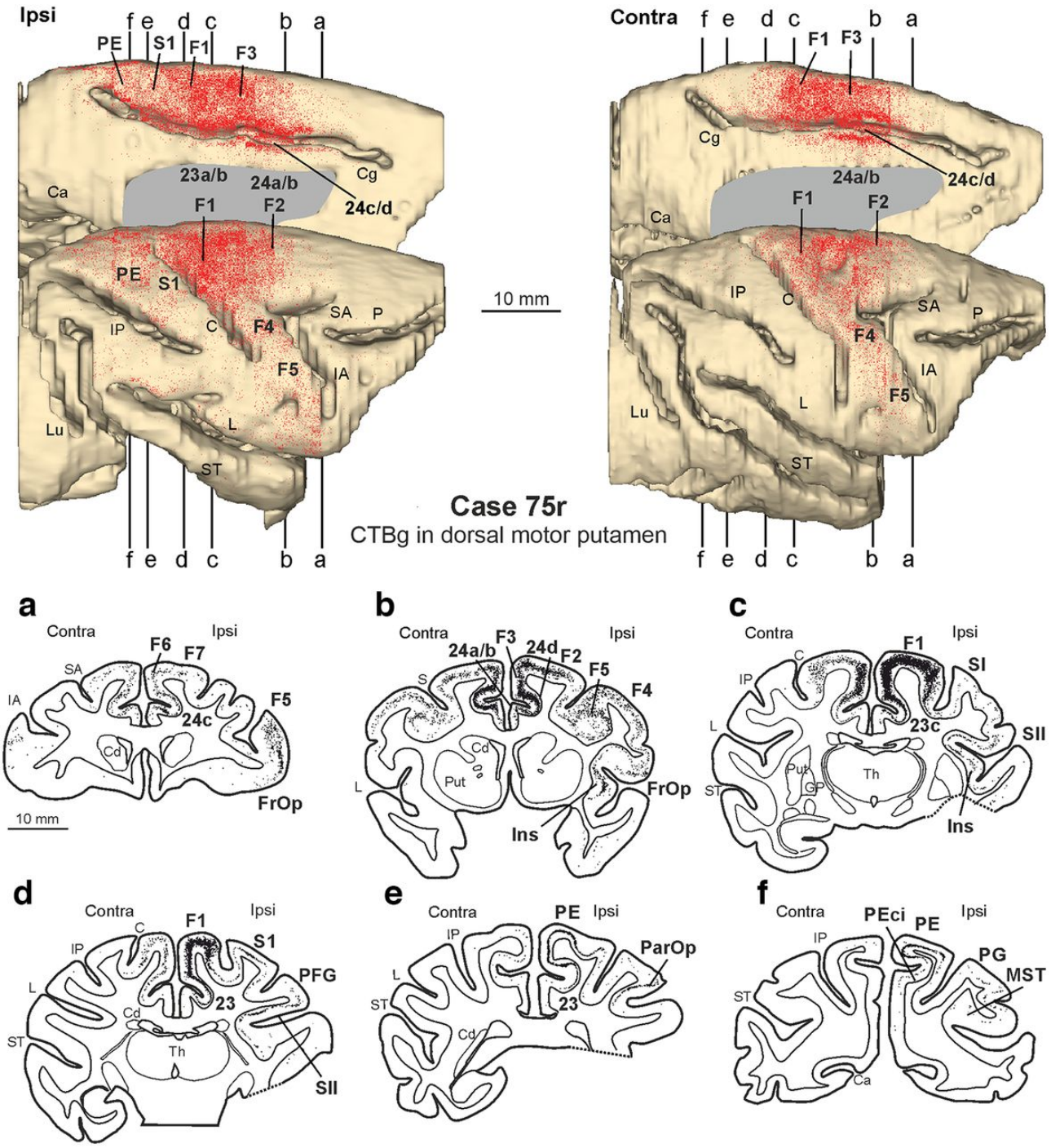

Figure 21. Distribution of the retrograde labeling observed after injection of CTBg in the dorsal part of the motor putamen in Case 75r. The labeling is shown in dorsolateral and medial views of the 3D reconstructions of the injected (ipsilateral) and contralateral hemisphere and in drawings of coronal sections. C, central sulcus; Ca, calcarine fissure; Cd, caudate nucleus; Cg, cingulate sulcus; GP, globus pallidus; IA, inferior arcuate sulcus; Ins, insula; IP, intraparietal sulcus; L, lateral sulcus; LO, lateral orbital sulcus; Lu, lunate sulcus; MO, medial orbital sulcus; MST, medial superior temporal area; P, principal sulcus; ParOp, parietal operculum; PO, parieto occipital sulcus; Put, putamen; S, spur of the arcuate sulcus; SA, superior arcuate sulcus; ST, superior temporal sulcus; Th, thalamus. Conventions as in Figure 3.

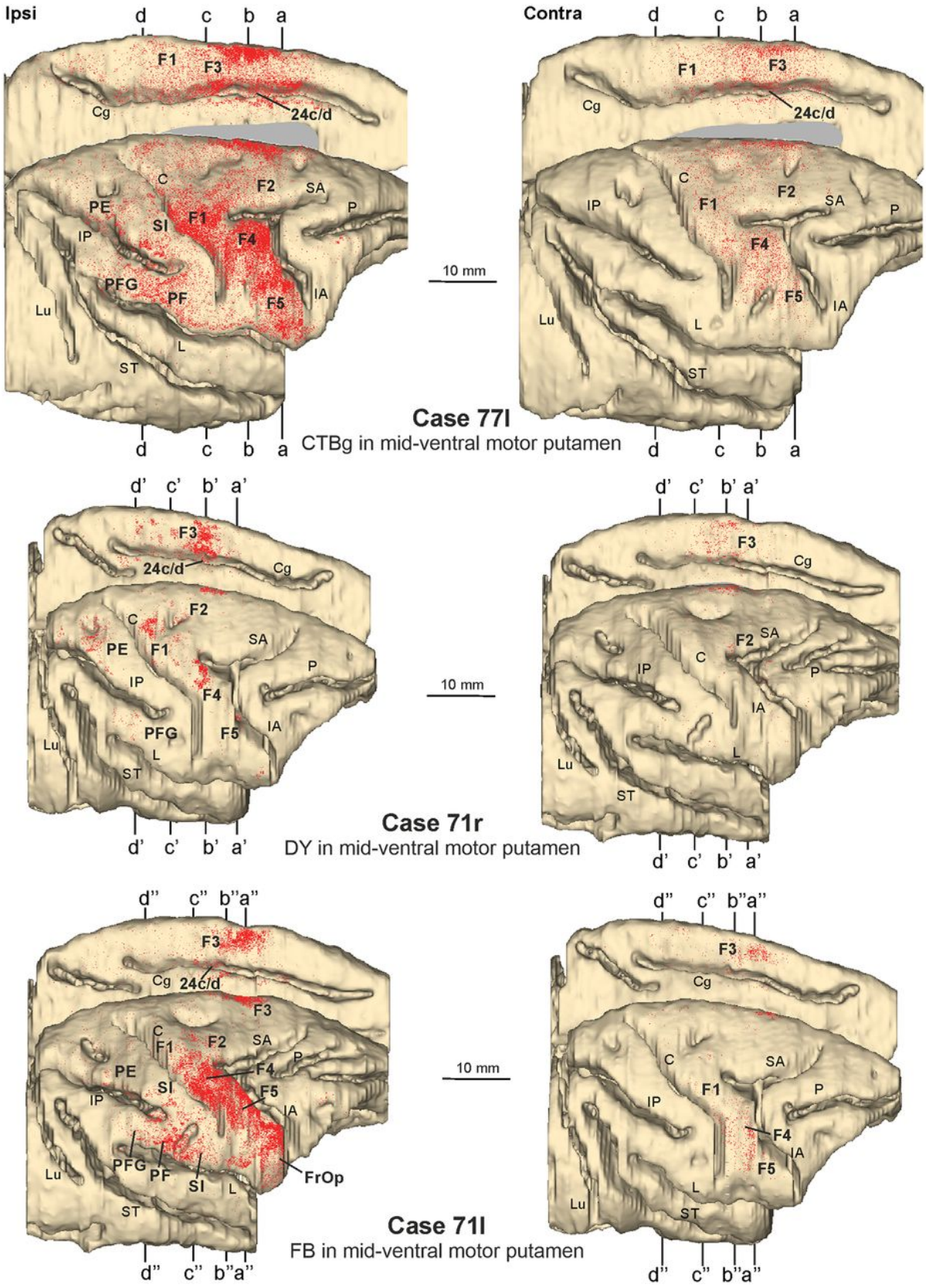

Figure 22. Distribution of the retrograde labeling observed after injection of CTBg in Case 77l, DY in Case 71r, and FB in 71l in the midventral motor putamen, shown in dorsolateral and medial views of the 3D reconstructions of the injected (ipsilateral) and contralateral hemispheres. On the 3D reconstructions of both hemispheres of all cases are indicated the levels at which the sections, shown in Figure 11, were taken. C, Central sulcus; Cg, cingulate sulcus; IA, inferior arcuate sulcus; IP, intraparietal sulcus; L, lateral sulcus; Lu, lunate sulcus; P, principal sulcus; SA,superior arcuate sulcus; ST, superior temporal sulcus. Conventions as in Figure 3.

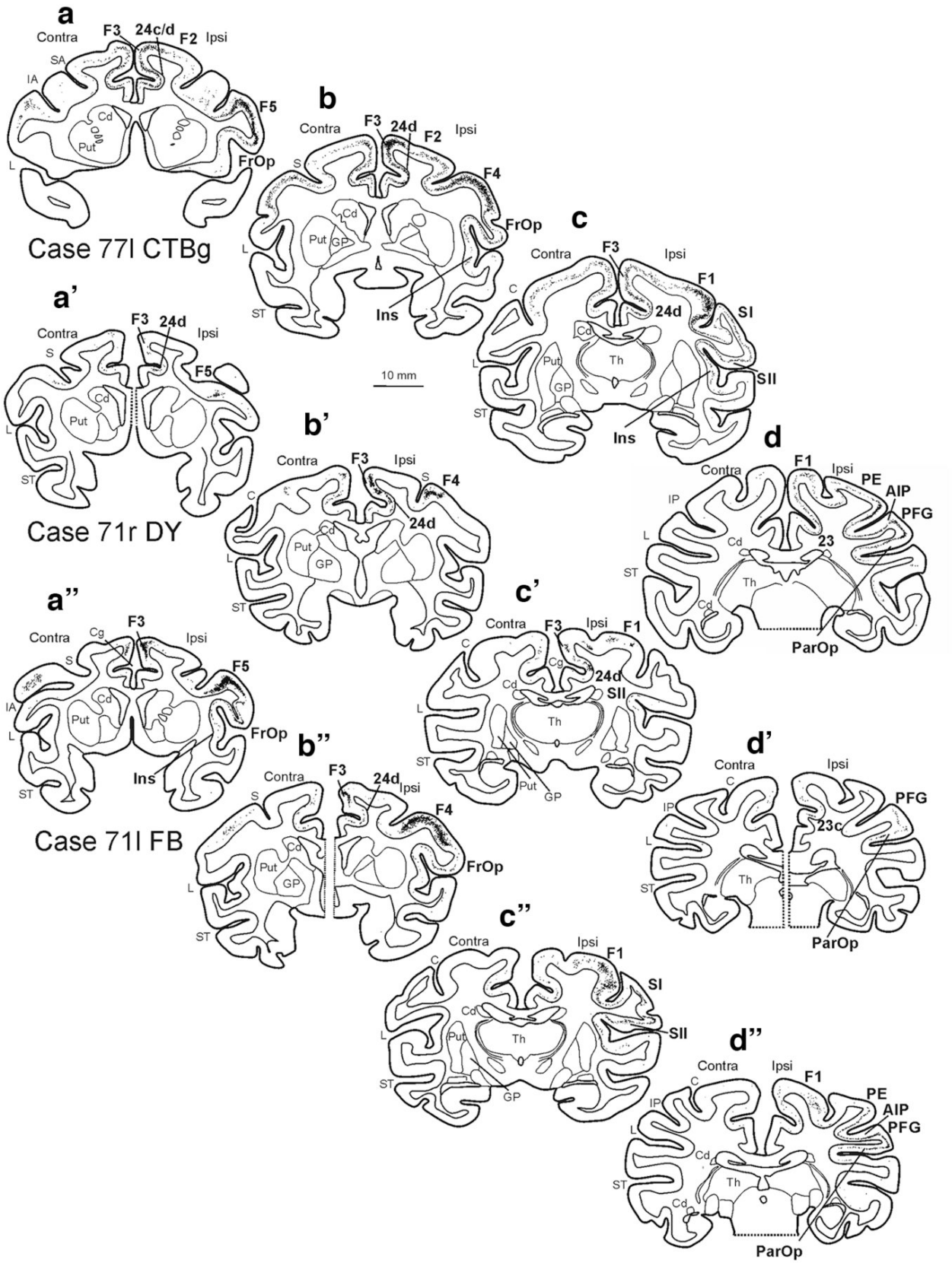

Figure 23. Distribution of the retrograde labeling observed after injection of CTBg in Case 77l, DY in Case 71r, and FB in 71l in the midventral motor putamen, shown in drawings of coronal sections taken at levels indicated in Figure 10. AIP, anterior intraparietal area; C, central sulcus; Cd, caudate nucleus; Cg, cingulate sulcus; GP, globus pallidus; IA, inferior arcuate sulcus; Ins,insula; IP, intraparietal sulcus; L, lateral sulcus; ParOp, parietal operculum; Put, putamen; S, spur of the arcuate sulcus; SA, superior arcuate sulcus; ST, superior temporal sulcus; Th, thalamus.Conventions as in Figure 3.

Laterality of CSt projections

Our data showed that the relative balance of ipsilateral and contralateral projections from frontal and cingulate areas widely varied. Accordingly, we examined whether the proportion of contralateral CSt projections (i.e., contralaterality index equals contralateral cells in area X/ipsi plus contra cells in area X) in each cortical area was related to the total amount of ipsi plus contralateral labeling in that area (Fig. 24). This analysis did not show a correlation between the contralaterality index and total labeling across cortical areas ($r = 0.27$). Rather, the cortical areas with the largest projections to a striatal injection site could have either high (>0.3, area 24/32 after caudate head injections) or low contralaterality indexes (F5 and F1 after midventral motor putamen injections). Similarly, other areas [F6, F7, and frontal operculum (FrOp)] with moderate projections (<5%) also exhibited a relatively high contralaterality index in some cases and a low contralaterality index in other cases. Furthermore, in several cases, the contralaterality index of the CSt projections appears to vary according to the target striatal zone. For example, area 24c/d exhibited a relatively high contralaterality index for the projections to the caudate and a lower one for the projections to the putamen, independently from the strength of its projections. Among the frontal motor areas, F3 showed a relatively high contralaterality index for the projections to the caudate body and dorsal motor putamen and a lower one for the projections to the midventral motor putamen, again independently from the strength of its projections. Finally, F1 had a higher contralaterality index for its projections to the leg/trunk-related motor putamen and a quite low one for the projections to the hand-related motor putamen.

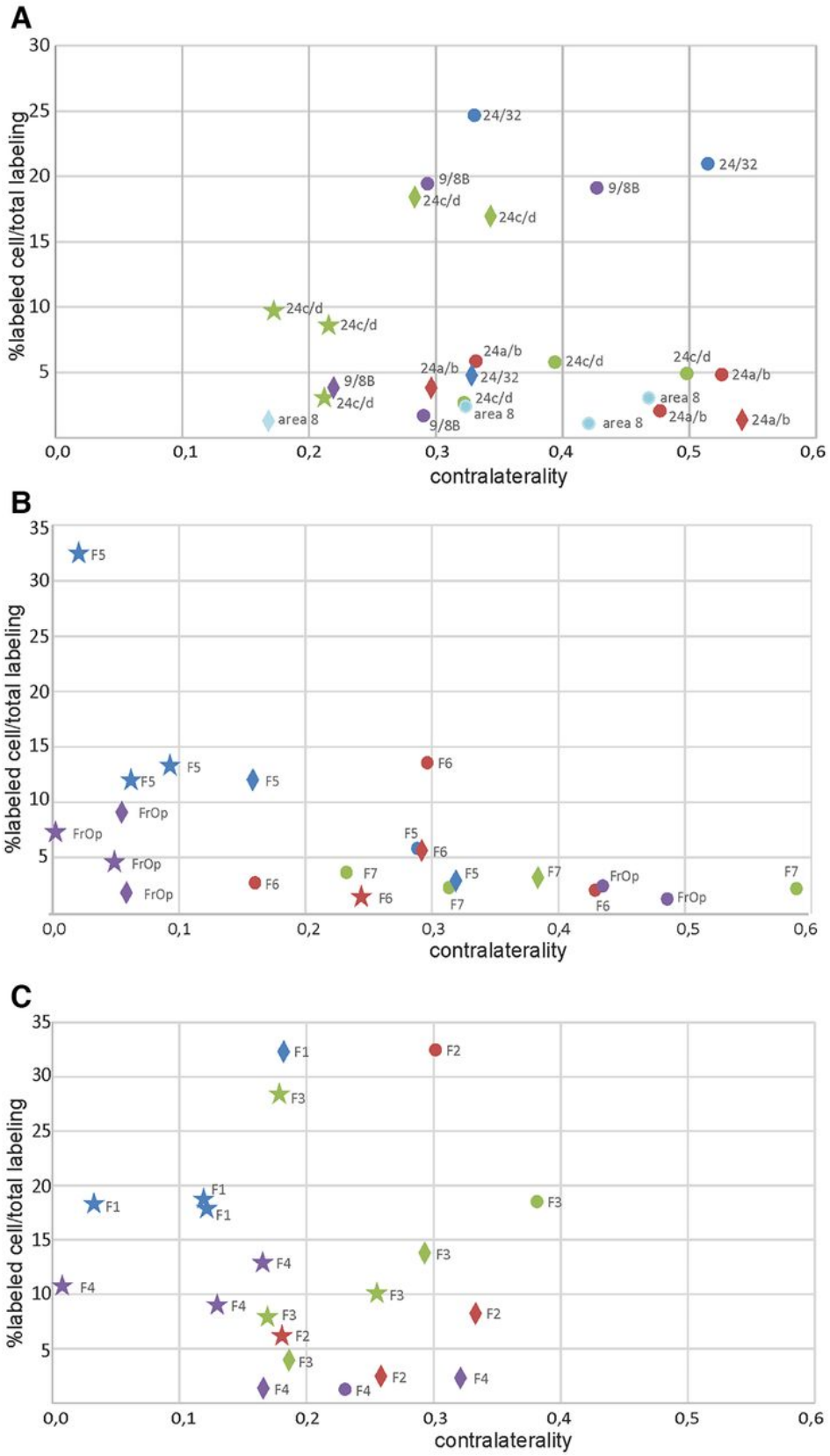

Figure 24 Contralaterality [contralateral cells in area X/(ipsi 1 contra cells in area X)] of CSt projections from rostral cingulate and prefrontal (A), rostral premotor (B), and caudal premotor and primary motor (C) areas shown in relation to the richness (percentage of ipsilateral plus contralateral CSt cells) of the labeling. Only areas in which the total (ipsi plus contra) labeling was.1% are considered in the graphs. Values from injections in the caudate are shown with dots, those from injections in rostral and dorsal motor putamen with diamonds, and those from injections in midventral motor putamen with stars. Different colors identify different areas.

4 Discussion

The present studies provide new data on two aspects of the corticostriatal connectivity organization in the macaque brain.

The study 1 shows that CSt projections from frontal motor areas and frontal operculum do not originate almost exclusively from layer V, as commonly assumed in primate models of CSt interactions, as almost everywhere in these regions the contribution of layers III and VI to these projections is comparable or even stronger than that of layer V. Furthermore, laminar distribution patterns of the CSt projections can largely vary within these regions independently from the richness of the projections and from the projecting area/field, but likely according to the target striatal zones. Thus, cortical areas appear to project in different ways to different zones of the striatum, so that different striatal zones are targets of characteristically weighted laminar projections from the various input areas.

The study 2 provides a detailed description of the origin and strength of striatal input from the contralateral (crossed CSt projections) hemisphere in the non-human primate. As has been noted over the last 50 years, striatal input is dominated by the ipsilateral cortex, but the results of the present study now demonstrate that a substantial input originates also from the contralateral cortex. Whereas ipsilateral projections originate from cingulate, frontal, parietal, insular, and temporal cortex, crossed CSt projections originate almost exclusively from cingulate, prefrontal, and frontal motor areas. In some cases, the contribution of contralateral cingulate and frontal areas is quite high and even equal to that from the same area of the ipsilateral hemisphere. The crossed CSt projections from the primary motor cortex tend to be relatively robust for the leg/trunk representation and weak for the hand representation. Overall, the distribution of crossed CSt projections suggests that they may provide a substrate for bilateral integration of motor, motivational, and cognitive signals during behavior.

These observations extend current models of CSt interactions, provide an even more complex picture of the possible mode of information processing in the basal ganglia for motor and non motor functions, and highlight that crossed CSt projections could be an important variable to consider in defining the pattern of information convergence in the striatum.

4.1 Study 1 - Laminar origin of CSt projections

The laminar origin of CSt projections has been described in several studies, showing differences across species. In cats, CSt neurons were observed mostly in layer III (Kitai et al., 1976; Oka, 1980;

Royce, 1982); whereas in dogs, mostly in layer V or III in PFC and motor cortex, respectively (Tanaka, 1987). In rats, CSt neurons have been observed mostly in layer V, and at a variable extent across studies in layer III (e.g., Veening et al., 1980; McGeorge and Faull, 1989; Akintunde and Buxton, 1992; Wall et al., 2013). In macaques, after putaminal injections, CSt neurons in the motor cortex were described almost exclusively in layer Va (Jones et al., 1977), or primarily in layer Va, but also in layers III and Vb (McFarland and Haber, 2000; Kaneda et al., 2002). After caudate injections, the labeling in PFC was observed primarily in layer V, with a minor contribution from layer III, correlated with labeling density (Arikuni and Kubota, 1986; Goldman-Rakic and Selemon, 1986; Saint-Cyr et al., 1990; Yeterian and Pandya, 1994; Ferry et al., 2000). It is worth noting that, in all these studies, the laminar distribution of CSt-labeled cells has been evaluated only qualitatively, which could be at the basis of an underestimation of the involvement of layers III and VI. Furthermore, the lack of quantitative analysis in virtually all studies of CSt projections prevents comparisons of the contribution of the various layers across different areas, tracer injections, and studies. The commonly assumed notion that CSt neurons in the macaque brain are primarily located in layer V (Gerfen and Bolam 2010; Shepherd, 2013) has been challenged by Griggs et al. (2017). This study showed that projections from specific temporal areas to the caudate head originated mostly from layer V and occasionally from layer III, whereas projections from the same areas to the caudate tail originated from layers III and VI. Accordingly, this study first showed that laminar distribution patterns of CSt projections from a given cortical area can markedly differ according to the target striatal zone and that, in macaques, layer VI can be a relevant source of CSt projections. Present data, based on quantitative analysis of the laminar distribution of CSt neurons, confirm and extend these observations showing that, also in the frontal motor, in the frontal opercular, and prefrontal cortex, CSt neurons are not located primarily in layer V and that layer VI can be a major source of CSt projections (e.g., area F5c in Case 61). Labeled CSt neurons in layer VI in ventral premotor cortex were noticed also by McFarland and Haber (2000). Finally, the present data also show that after tracer injections in different parts of the putamen, different laminar distribution patterns can be observed in a given cortical area. For example, after the injections in Case 61 and in Case 71l, the laminar distribution patterns of the labeled neurons in area F5 were markedly different. Laminar distribution patterns can differ also across different fields of the same area, as observed in F1 and F3. Noteworthy, these patterns did not change depending on the richness of the labeling. Thus, similarly to the temporal cortex, in the motor cortex laminar distribution patterns of CSt projections appear to vary according to the target striatal zone. Present data, as well as those of Griggs et al.

(2017), raise the question of whether this new model of laminar architecture of CSt projections applies also to other cortical regions. In parietal and cingulate cortex, CSt-labeled cells involved almost exclusively or predominantly layer V. Although the putamen is a major target of CSt parietal projections (Cavada and Goldman-Rakic, 1991; Yeterian and Pandya, 1993), we cannot rule out the possibility that projections to the caudate originate also from other layers. In the insular cortex, we observed labeled CSt neurons in layers V, or V-VI; and Chikama et al. (1997), after injections in the ventral striatum, observed labeling in the agranular insula involving layer III. In the PFC, Griggs et al. (2017) observed differences in CSt projections from layer III to the caudate tail and head; and in the present study, we observed CSt neurons mainly in layers V and VI, after injection in Putamen, and mainly in layers III and V, after injection in the caudate. Accordingly, also in the prefrontal and insular cortex, laminar distribution patterns of CSt projections vary according to the target striatal zone.

Functional considerations

Previous data suggested that specific striatal zones are targets of converging input from interconnected cortical areas, thus are integral part of specific large-scale functionally specialized networks (Gerbella et al., 2016; Choi et al., 2017a, b). Present data show that cortical areas may project in different ways to different striatal zones, suggesting that they are targets of specific combinations of signals originating from the various cortical layers of the areas of a given network. These observations extend current models of CSt interactions, suggesting much more complex modes of information processing in the basal ganglia for different motor and non-motor functions, and opening new questions on the architecture of the CSt circuitry. Rodent studies provided evidence for different populations of neurons located in different cortical layers and differentially involved in the CSt circuitry: intrathelencephalic neurons, located in layers III and Va, which also project to other cortical areas, and pyramidal-tract neurons located in layer Vb, which also project to brainstem and spinal cord (Reiner et al., 2010). However, the presence of pyramidal-tract neurons in macaques, suggested by Parent and Parent (2006), is not supported by electrophysiological data (Bauswein et al., 1989). Furthermore, Jones et al. (1977) showed that CSt neurons are smaller than corticospinal neurons and in the present study we have not observed large layer Vb labeled pyramids. Rodent studies have also provided evidence for inhibitory somatostatin or parvalbumin-positive GABAergic CSt neurons located in layers III, V, and VI (Jinno and Kosaka, 2004; Lee et al., 2014; Rock et al., 2016), which may differentially modulate striatal output and motor activity (Melzer et al., 2017). Although long range projecting GABAergic cortical neurons have been described in macaques by Tomioka and Rockland (2007), no evidence has been provided so far for

inhibitory CSt neurons. Double-labeling experiments will be necessary to verify whether also in the macaque there are inhibitory CSt neurons as observed in rodents. Current models of cortical circuitry suggest that the various cortical layers display distinct responses and dynamics (see Douglas and Martin, 2004). Specifically, in the premotor cortex, activity generated by thalamic or cortical input first involves the middle layers and then superficial and deep layers (Godlove et al., 2014): in superficial layers, neural activity is predominantly related to choices, whereas in deeper layers to the motor output (Chandrasekaran et al., 2017). Finally, in frontal areas, deep layers appear to modulate the activity of the superficial layers related to maintaining contents in working memory (Bastos et al., 2018). Thus, different putaminal zones would collect signals originating from similar sets of hand-related cortical areas, for example, the "lateral grasping network," but differing in term of coding and timing, even when originating from the same area. Furthermore, layers III, V, and VI broadcast signals in different directions (e.g., feed-forward, or feed-back) to other cortical areas of the network. Accordingly, each striatal zone would be involved in a very specific way in the flow of information within the cortico-subcortical network. In this context, noteworthy is the observation that layer VI can be a robust source of CSt projections. Layer VI hosts pyramidal neurons projecting to the thalamus (corticothalamic, CT) or to other cortical areas (corticocortical, CC; see Thomson, 2010). It is thus an open question whether pyramidal layer VI CSt neurons observed in the present study represent a new class of layer VI pyramids or they belong to the CT and/or the CC types. After tracer injections in the thalamus and in the caudate, Yeterian and Pandya (1994) did not find double-labeled neurons in the PFC, where CSt-labeled cells were observed almost exclusively in layer V. Thus, this study does not rule out the possibility that there are indeed layer VI CSt neurons, which also project to the thalamus. Accordingly, it is possible that striatal zones receive from layer VI neurons signals, which are sent also as feed-back signals either to cortical areas of the network and/or to thalamic nuclei, possibly to the basal ganglia recipient ones. Further studies are necessary to characterize connectionally and neurochemically layer VI CSt neurons and to define the possible role of this projection in the basal ganglia circuitry.

4.2 Study 2- Crossed CSt projections

Crossed CSt projections have been first noted in the rabbit, cat, and rat (Carman et al., 1965) and then in the macaque (Kemp and Powell, 1970; Fallon and Ziegler, 1979) based on degenerative changes in the striatum after cortical lesions. Crossed CSt projections have been then described in the macaque after neural tracer injections in the primary motor and premotor (Künzle, 1975, 1978;

Liles and Updyke, 1985; Huerta and Kaas, 1990; Parthasarathy et al., 1992), prefrontal (McGuire et al., 1991), and parietal (Cavada and Goldman-Rakic, 1991) cortex. These studies, based on anterograde tracer injections at the cortical level, could not give a comprehensive picture of the origin of the crossed CSt projections to a given striatal sector and an estimate of the weight of these projections compared with the direct ones. To our knowledge, only Jones et al. (1977) provided a qualitative description of crossed CSt projections based on injections of a retrograde tracer in the motor putamen in the squirrel monkey. As in Jones et al. (1977), after injections in the motor putamen we found an almost symmetrical distribution of labeled CSt cells in the ipsilateral versus contralateral frontal cortex and a virtual absence of labeled CSt cells in the contralateral parietal cortex. The very poor or even absent labeling observed in the contralateral parietal cortex in all the cases of the present study, including those in which labeling in the ipsilateral parietal cortex was quite robust, is in apparent discrepancy with the observations of Cavada and Goldman Rakic (1991) after very large tracer injections in different parietal areas. It is possible that CSt parietal cells are relatively few and sparsely project to the striatum, so they are very difficult to be labeled after restricted injections of retrograde tracers in the striatum. On the other hand, as in the present study, Griggs et al. (2017) showed contralateral labeling in the frontal and cingulate, but not in the parietal, temporal, and insular cortex after tracer injections in the caudate head or tail. The present observations that the crossed CSt projections in the macaque originate predominantly from frontal and cingulate areas are in good agreement with the results of McGuire et al. (1991) and Innocenti et al. (2017), based on tracer injections at the cortical level. Specifically, McGuire et al. (1991) noted that some areas (e.g., area 46) display relatively weak crossed projections, whereas other areas (e.g., F3-supplementary motor area proper) appear to project almost equally to both ipsilateral and contralateral striatum. In this context, it could be worth noting that in the present data there were some areas that were always sources of relatively weak additional projections, in most cases showing a relatively high contralaterality index. It is possible that in our cases the target striatal zones of these areas have been only marginally involved. However, it could be also that some areas tend to have sparse and diffuse bilateral CSt projections. Crossed CSt projections may also be present in the human brain. Based on tractographic data, Innocenti et al. (2017) found that as in macaques, crossed CSt projections in humans originate predominantly from frontal areas but also from parietal regions of the superior and inferior parietal lobule and from the superior temporal gyrus. The presence in humans of crossed CSt projections from specific posterior parietal regions is supported by functional connectivity data (Jarbo and Verstynen, 2015). Neurodevelopmental

studies showed that in mice soon after birth, crossed CSt projections originate from almost the entire hemisphere, whereas after 2 weeks they originate mainly from frontal and cingulate areas possibly because of either retraction of initial collaterals to the contralateral striatum or death of an early developmental population of CSt neurons (Sohur et al., 2014). Accordingly, the presence of crossed CSt projections from parietal and temporal areas in humans, but not in macaques, could be accounted for by a differential maturation of these projections across different species.

Functional considerations

As discussed above in this thesis, early models of CSt projections in nonhuman primates have favored a modular organization of the striatum in which different striatal zones are targets of specific cortical regions (Alexander et al., 1986) and, in turn, are at the origin of largely segregated basal ganglia-thalamo-cortical loops (Middleton and Strick, 2000; Kelly and Strick, 2004). Subsequent studies have revealed a higher level of complexity of the corticostriatal projections topography. First, the cortical input to a specific striatal zone originates not only from a limited set of closely related neighbor areas, as initially described (Takada et al., 1998; Nambu, 2011; Averbeck et al., 2014) but also from distant, interconnected areas jointly involved in large-scale functionally specialized cortical networks (Gerbella et al., 2016; Choi et al., 2017). Second, as shown in our data in the Study 1, and in Griggs et al.2017, the different striatal zones are targets of characteristically weighted laminar projections from multiple input areas. Finally, the present data suggest that information processing in the striatum can also rely on substantial input from the contralateral hemisphere. As crossed CSt projections in the macaque brain have been so far poorly considered, their possible contribution to information processing in the striatum still remains to be defined. These projections could indeed provide a substrate for interhemispheric transfer of signals in parallel to the callosal connectivity. Based on conduction delay estimations, it has been suggested that crossed CSt projections mediate a transfer of information considerably faster than through the callosal connectivity (Innocenti et al., 2017). Furthermore, whereas callosal projections connect almost entirely the two hemispheres (Innocenti et al., 2022), crossed CSt projections originates mostly from frontal and cingulate areas, suggesting a role more focused on motor control and/or executive functions. In this context, crossed CSt projections could provide the substrate for bilateral diffusion of motor, motivational, and cognitive signals necessary for reinforcement learning and selection of those actions or action sequences that are most appropriate for achieving a behavioral goal (Averbeck and O'Doherty, 2022) and for inhibitory control of impulsive motor behavior (Oguchi et al., 2021). Furthermore, in the motor putamen, crossed CSt projections could have a role in

controlling actions or action sequences involving both sides of the body. Indeed, brain imaging evidence in humans showed bilateral activation in the motor putamen during the execution of unilateral simple foot, hand, and mouth movements (Gerardin et al., 2003). Interestingly, in the left putamen the activation foci for the right- or left-hand movements appeared largely segregated (Gerardin et al., 2003), resembling the segregation between the terminal fields of direct and crossed CSt projections to the striatal hand representation in the squirrel monkey (Flaherty and Graybiel, 1993). Furthermore, bilateral activation of the striatum has been observed during the execution of right-hand finger-tapping tasks with increasing degrees of complexity (Lehéricy et al., 2006; Bednark et al., 2015). The observed striatal activation foci tended to shift progressively more rostrally with the increase in complexity or frequency of the task execution (Lehéricy et al., 2006). Finally, bilateral striatal activation has been observed during early phases of visuomotor adaptation of arm movements (Seidler et al., 2006) and especially in the anterior striatum during the encoding of novel working memory items (Geiger et al., 2018). According to Wymbs et al. (2012) bilateral putamen activity is necessary for the strengthening of motor–motor associations at the basis of action chunking processes. Chunking in motor sequencing is considered a key function of the basal ganglia and allows groups of individual movements to be prepared and executed as a single motor program facilitating learning and performance of complex sequences (Halford et al., 1998). Crossed CSt projections could play a potentially important role in behavioral compensation after brain lesions. Specifically, these projections could have a role in compensatory relearning of motor strategies in the context of the reorganization mechanisms of the motor system occurring after cortical stroke (Balbinot and Schuch, 2019). In support of this proposal, there is evidence in rodents for axonal sprouting of crossed CSt projections and neurochemical signs of increased cell activity in the denervated striatum after sensorimotor cortex lesions (Napieralski et al., 1996; Cheng et al., 1998; Uryu et al., 2001). The presence in macaques of crossed CSt projections that appear even stronger than in rodents is an incentive for experimental studies in nonhuman primates and clinical studies in neurologic patients focused on the role of these projections in compensatory mechanisms after stroke.

REFERENCES

Akintunde A, Buxton DF (1992) Origins and collateralization of corticospinal, corticopontine, corticorubral and corticostriatal tracts: a multiple retrograde fluorescent tracing study. Brain Res. 586:208–218.

Albin R. L., Young A. B., Penney J. B. (1989). The functional anatomy of basal ganglia disorders. *Trends Neurosci.* 12, 366–375. 10.1016

Alexander GE, DeLong MR (1985) Microstimulation of the primate neostriatum. II. Somatotopic organization of striatal microexcitable zones and their relation to neuronal response properties. J Neurophysiol. 53:1417–1430.

Alexander GE, DeLong MR, Strick PL (1986) Parallel organization of functionally segregated circuits linking basal ganglia and cortex. Annu Rev Neurosci. 9:357–381.

Arikuni T, Kubota K. (1986) The organization of prefrontocaudate projections and their laminar origin in the macaque monkey: a retrograde study using HRP-gel. J Comp Neurol. 244:492–510.

Assous M,. Tepper J.M (2019) Cortical and thalamic inputs exert cell type-specific feedforward inhibition on striatal GABAergic interneurons J. Neurosci. Res., pp. 1491-1502, 10.1002

Averbeck BB, Lehman J, Jacobson M, Haber SN (2014) Estimates of projection overlap and zones of convergence within frontal-striatal circuits. J Neurosci 34:9497–9505.

Averbeck B, O'Doherty JP. (2022). Reinforcement-learning in fronto-striatal circuits. Neuropsychopharmacology. 47:147-162.

Balbinot G, Schuch CP. (2019). Compensatory relearning following stroke: cellular and plasticity mechanisms in rodents. Front Neurosci. 12:1023.

Barbas, H., Mesulam, M. M. 1981. Organization of afferent input to subdivisions of area 8 in the rhesus monkey. 1. Compo Neural. 200 : 407-3 1

Barbas H (1986) Pattern in the laminar origin of corticocortical connections. J Comp Neurol 252:415–422.

Barbas H, Rempel-Clower N (1997) Cortical structure predicts the pattern of corticocortical connections., Cerebral Cortex, Volume 7, Issue 7, Pages 635–646

Bar-Gad I., Bergman H. (2001) Stepping out of the box: information processing in the neural networks of the basal ganglia Curr. Opin. Neurobiol., 11, pp. 689-695

Bastos AM, Loonis R, Kornblith S, Lundqvist M, Miller EK (2018) Laminar recordings in frontal cortex suggest distinct layers for maintenance and control of working memory. Proc Natl Acad Sci U S A.115:1117–1122.

Bauswein E, Fromm C, Preuss A (1989) Corticostriatal cells in comparison with pyramidal tract neurons: contrasting properties in the behaving monkey. Brain Res. 493:198–203.

Bednark JG, Campbell ME, Cunnington R. (2015). Basal ganglia and cortical networks for sequential ordering and rhythm of complex movements. Front Hum Neurosci. 9:421.

Belmalih A, Borra E, Contini M, Gerbella M, Rozzi S, Luppino G (2009) Multimodal architectonic subdivision of the rostral part (area F5) of the macaque ventral premotor cortex. J Comp Neurol 512:183–217.

Bertero, A., Verrillo, L., Apicella, A.J.,(2022) A novel layer 4 corticofugal cell type/projection involved in thalamo-cortico-striatal sensory processing. J. Neurosci. 42 (8), 1383–140

Bevan M.D., Smith A.D., Bolam J.P. (1996) The substantia nigra as a site of synaptic integration of functionally diverse information arising from the ventral pallidum and the globus pallidus in the rat Neuroscience, 75, pp. 5-12

Bevan M.D., Clarke N.P., Bolam J.P. (1997) Synaptic integration of functionally diverse pallidal information in the entopeduncular nucleus and subthalamic nucleus in the rat J. Neurosci., 17, pp. 308-324

Bolam JP, Izzo PN, Graybiel AM (1988) Cellular substrates of the histochemically defined striosome/matrix system of the caudate nucleus: A combined Golgi and immunocytochemical study in cat and ferret. *Neuroscience* 24: 853–875

Borra, E., Gerbella, M., Rozzi, S., & Luppino, G. (2015). Projections from caudal ventrolateral prefrontal areas to brainstem preoculomotor structures and to Basal Ganglia and cerebellar oculomotor loops in the macaque. *Cerebral cortex (New York, N.Y. : 1991)*, *25*(3), 748–764.

Borra E, Gerbella M, Rozzi S, Luppino G (2017) The macaque lateral grasping network: A neural substrate for generating purposeful hand actions. Neurosci Biobehav Rev. 75:65–90.

Borra E, Luppino G, Gerbella M, Rozzi S, Rockland KS (2020) Projections to the putamen from neurons located in the white matter and the claustrum in the macaque. J Comp Neurol 528, 453–467

Bostan A. C., Dum R. P., Strick P. L. (2010). The basal ganglia communicate with the cerebellum. *Proc. Natl. Acad. Sci. U S A* 107, 8452–8456. 10.1073/pnas.1000496107

Boussaoud D, Ungerleider LG, Desimone R. 1990. Pathway for motion analysis: cortical connections of the medial superior temporal and fundus of the superior temporal visual areas in the macaque. J Comp Neurol. 296:462–495.

Brinkman, C., Porter, R. 1979. Supplementary motor area in the monkey: Activity of neurons during performance of a learned motor task. 1. Neurophysiol. 42: 681-709

Cacciola A., Milardi D., Anastasi G. P., Basile G. A., Ciolli P., Irrera M., et al.. (2016a). A direct cortico-nigral pathway as revealed by constrained spherical deconvolution tractography in humans. *Front. Hum. Neurosci.* 10:374. 10.3389/fnhum.2016.00374

Cacciola A., Calamuneri A., Milardi D., Mormina E., Chillemi G., Marino S., et al.. (2017b). A connectomic analysis of the human basal ganglia network. *Front. Neuroanat.* 11:85. 10.3389/fnana.2017.00085

Cacciola A., Milardi D., Bertino S., Basile G. A., Calamuneri A., Chillemi G., et al.. (2019). Structural connectivity-based topography of the human globus pallidus: implications for therapeutic targeting in movement disorders. *Mov. Disord.* 34, 987–996. 10.1002/mds.27712

Calzavara R, Mailly P, Haber SN. (2007) Relationship between the corticostriatal terminals from areas 9 and 46, and those from area 8A, dorsal and rostral premotor cortex and area 24c: an anatomical substrate for cognition to action. Eur J Neurosci. 26:2005–2024.

Caminiti R, Borra E, Visco-Comandini F, Battaglia-Mayer A, Averbeck BB, Luppino G (2017) Computational architecture of the parieto-frontal network underlying cognitive-motor control in monkeys. eNeuro 4: ENEURO.0306-16.2017.

Carman JB, Cowan WM, Powell TP, Webster KE. (1965). A bilateral cortico-striate projection. J Neurol Neurosurg Psychiatry. 28:71-7.

Carmichael ST, Price JL. (1994). Architectonic subdivision of the orbital and medial prefrontal cortex in the macaque monkey. J Comp Neurol. 346:366–402.

Carpenter, M. B., Nakano, K., Kim, R. (1976) Nigrothalamic projections in the monkey demonstrated by autoradiographic technics. J. Camp. Neural. 165 : 401-16

Cavada C, Goldman-Rakic PS (1991) Topographic segregation of corticostriatal projections from posterior parietal subdivisions in the macaque monkey. Neuroscience. 42:683–696.

Chandrasekaran C, Peixoto D, Newsome WT, Shenoy KV (2017) Laminar differences in decision-related neural activity in dorsal premotor cortex. Nat Commun. 8:614. Published 2017 Sep 20. doi:10.1038/s41467-017-00715-0

Chikama M, McFarland NR, Amaral DG, Haber SN (1997) Insular Cortical Projections to Functional Regions of the Striatum Correlate with Cortical Cytoarchitectonic Organization in the Primate J Neurosci. 17: 9686–9705.

Cheng HW, Tong J, McNeill TH. (1998). Lesion-induced axon sprouting in the deafferented striatum of adult rat. Neurosci Lett. 242:69-72.

Choi EY, Ding SL, Haber SN (2017a) Combinatorial inputs to the ventral striatum from the temporal cortex, frontal cortex, and amygdala: implications for segmenting the striatum. eNeuro. 4:ENEURO.0392-17.2017.

Choi EY, Tanimura Y, Vage PR, Yates EH, Haber SN (2017b) Convergence of prefrontal and parietal anatomical projections in a connectional hub in the striatum. Neuroimage. 146:821–832.

da Silva N. M., Ahmadi S. A., Tafula S. N., Cunha J. P. S., Bötzel K., Vollmar C., et al.. (2017). A diffusion-based connectivity map of the GPi for optimised stereotactic targeting in DBS. *Neuroimage* 144, 83–91. 10.1016/j.neuroimage.2016.06.018

Demelio S, Bettio F, Gobbetti E, Luppino G. (2001) Three-dimensional reconstruction and visualization of the cerebral cortex in primates. In: Data visualization 2001 (Ebert D, Favre J, Peikert R, eds) pp 147–156. New York, NY, USA: Springer Verlag.

Desban M, Gauchy C, Glowinski J, Kemel ML (1995) Heterogeneous topographical distribution of the striatonigral and striatopallidal neurons in the matrix compartment of the cat caudate nucleus. *J Comp Neurol* 352: 117–133

DeVito, J. L., Anderson, M. E., Walsh, K. E. (1980) A horseradish peroxidase study of afferent connections of the globus pallid us in Macaca mulatta. Exp. Brain Res. 38 : 65- 73

Divac, 1, Rosvold, H. E., Szwarcbart, M. K. (1967) Behavioral effects of selective ablation of the caudate nucleus. J. Compo Physiol. Psychol. 63: 184-90

Donoghue JP, Herkenham M 1986. Neostriatal projections from individual cortical fields conform to histochemically distinct striatal compartments in the rat. *Brain Res* 365: 397–403

Douglas RJ, Martin KA (2004) Neuronal circuits of the neocortex. Annu Rev Neurosci. 27:419–451.

Draganski B, Kherif F, Kloppel S, Cook PA, Alexander DC, Parker GJ . *et al* (2008). Evidence for segregated and integrative connectivity patterns in the human basal ganglia. *J Neurosci* 28: 7143–7152.

Dum R. P., Li C., Strick P. L. (2002). Motor and nonmotor domains in the monkey dentate. *Ann. N Y Acad. Sci.* 978, 289–301. 10.1111/j.1749-6632.2002.tb07575.

Fallon JH, Ziegler BT. (1979) The crossed cortico-caudate projection in the rhesus monkey. Neurosci Lett 29-32. doi: 10.1016/0304-3940(79)91524-6.

Flaherty AW, Graybiel AM. (1993). Two input systems for body representations in the primate striatal matrix: experimental evidence in the squirrel monkey. J Neurosci. 13:1120-37.

Flaherty AW, Graybiel AM. (1994) Input-output organization of the sensorimotor striatum in the squirrel monkey. J Neurosci. 14:599–610.

Ferry AT, Ongür D, An X, Price JL (2000) Prefrontal cortical projections to the striatum in macaque monkeys: evidence for an organization related to prefrontal networks. J Comp Neurol. 425:447–470.

Francois C. , Yelnik J. , Percheron G., Fenelon G. (1994) Topographic distribution of the axonal endings from the sensorimotor and associative striatum in the macaque pallidum and substantia nigra Exp. Brain Res., 102 , pp. 305-318

Frankle W. G., Laruelle M., Haber S. N. (2006). Prefrontal cortical projections to the midbrain in primates: evidence for a sparse connection. *Neuropsychopharmacology* 31, 1627–1636. 10.1038/sj.npp.1300990

Fujiyama F, Sohn J, Nakano T, Furuta T, Nakamura KC, Matsuda W, Kaneko T (2011) Exclusive and common targets of neostriatofugal projections of rat striosome neurons: A single neuron-tracing study using a viral vector. *Eur J Neurosci* 33: 668–677

Geiger LS, Moessnang C, Schäfer A, Zang Z, Zangl M, Cao H, van Raalten TR, Meyer-Lindenberg A, Tost H. (2018). Novelty modulates human striatal activation and prefrontal-striatal effective connectivity during working memory encoding. Brain Struct Funct. 223:3121-3132.

Gerardin E, Lehéricy S, Pochon JB, Tézenas du Montcel S, Mangin JF, Poupon F, Agid Y, Le Bihan D, Marsault C. 2003. Foot, hand, face and eye representation in the human striatum. Cereb Cortex. 13:162-9. doi: 10.1093/cercor/13.2.162.

Gerbella M, Belmalih A, Borra E, Rozzi S, Luppino G. 2007. Multimodal architectonic subdivision of the caudal ventrolateral prefrontal cortex of the macaque monkey. Brain Struct Funct. 212:269–301.

Gerbella M, Borra E, Mangiaracina C, Rozzi S, Luppino G (2016) Corticostriate Projections from Areas of the "Lateral Grasping Network": Evidence for Multiple Hand-Related Input Channels. Cereb. Cortex 221:59–78.

Gerfen CR 1984. The neostriatal mosaic: Compartmentalization of corticostriatal input and striatonigral output systems. *Nature* 311: 461–464

Gerfen CR (1992) The neostriatal mosaic: Multiple levels of compartmental organization. *Trends Neurosci* 15: 133–139

Gerfen CR, Bolam P (2010) The neuroanatomical organization of the basal ganglia. In: Handbook of basal ganglia structure and function (Steiner H, Tseng KY, eds.), pp 3–32. London: Academic Press.

Geyer S, Matelli M, Luppino G, Zilles K (2000) Functional neuroanatomy of the primate isocortical motor system. Anat Embryol 202:443–474.

Giménez-Amaya JM, Graybiel AM (1990) Compartmental origins of the striatopallidal projections in the primate. *Neuroscience* 34: 111–126

Godlove DC, Maier A, Woodman GF, Schall JD (2014) Microcircuitry of agranular frontal cortex: testing the generality of the canonical cortical microcircuit. J Neurosci. 34:5355–5369.

Goldman-Rakic PS, Selemon LD (1986) Topography of Corticostriatal Projections in Nonhuman Primates and Implications for Functional Parcellation of the Neostriatum. In Sensory-Motor Areas and Aspects of Cortical Connectivity (Jones EG et al, eds), pp447–466. Plenum Press, New York.

Graybiel AM, Ragsdale CW (1978) Histochemically distinct compartments in the striatum of human, monkey and cat demonstrated by acetylcholinesterase staining. *Proc Natl Acad Sci* 75: 5723–5726

Graybiel AM (1984) Correspondance between the dopamine islands and striosomes of the mammalian striatum. *Neuroscience* 13: 1157–1187

Graybiel AM (1990) Neurotransmitters and neuromodulators in the basal ganglia. *Trends Neurosci* 13: 244–254

Gregoriou GG, Borra E, Matelli M, Luppino G. 2006. Architectonic organization of the inferior parietal convexity of the macaque monkey. J Comp Neurol. 496:422–451.

Griggs WS, Kim HF, Ghazizadeh A, Costello MG, Wall KM, Hikosaka O (2017) Flexible and Stable Value Coding Areas in Caudate Head and Tail Receive Anatomically Distinct Cortical and Subcortical Inputs. Front Neuroanat. 11:106.

Groenewegen H.J., Galis-de Graaf Y., Smeets W.J. (1999)a Integration and segregation of limbic cortico-striatal loops at the thalamic level: an experimental tracing study in rats J. Chem. Neuroanat., 16, pp. 167-185

Groenewegen H.J. , Wright C.I. , Beijer A.V. , Voorn P. (1999)b Convergence and segregation of ventral striatal inputs and outputs Ann. N.Y. Acad. Sci., 877 , pp. 49-63

Haber S.N. , Fudge J.L., McFarland N.R. (2000) Striatonigrostriatal pathways in primates form an ascending spiral from the shell to the dorsolateral striatum J. Neurosci., 20 , pp. 2369-2382

Haber SN, Kim KS, Mailly P, Calzavara R (2006). Reward-related cortical inputs define a large striatal region in primates that interface with associative cortical inputs, providing a substrate for incentive-based learning. *J Neurosci* 26: 8368–8376.

Haber S. (2010) Integrative networks across basal ganglia circuits. In: Steiner H, Tseng KY, editors. Handbook of basal ganglia structure and function. Oxford: Elsevier. p. 409–427.

Halford GS, Wilson WH, Phillips S. (1998) Processing capacity defined by relational complexity: implications for comparative, developmental, and cognitive psychology. Behav. Brain Sci.21, 803–831, discussion 831–864.

Hedreen, J., DeLong, M. R., Holm, G. (1980) Striatonigral relationship in macaques. Soc. N eurosci. Abstr. 6: 272

He, J., Kleyman, M., Chen, J., Alikaya, A., Rothenhoefer, K.M., Ozturk, B.E., Wirthlin, M., Bostan, A.C., Fish, K., Byrne, L.C., Pfenning, A.R., Stauffer, W.R., (2021) Transcriptional and anatomical diversity of medium spiny neurons in the primate striatum. Curr. Biol. 31 (24), 5473–5486 e5476

Hikosaka, O., Takikawa, Y., & Kawagoe, R. (2000). Role of the basal ganglia in the control of purposive saccadic eye movements. *Physiological reviews*, *80*(3), 953–978.

Hof PR, Morrison JH (1995) Neurofilament protein defines regional patterns of cortical organization in the macaque monkey visual system: a quantitative immunohistochemical analysis. J Comp Neurol 352:161–186.

Hoshi E., Tremblay L., Féger J., Carras P. L., Strick P. L. (2005). The cerebellum communicates with the basal ganglia. *Nat. Neurosci.* 8, 1491–1493. 10.1038/nn1544

Huerta MF, Kaas. JH. 1990. Supplementary eye field as defined by intracortical microstimulation: connections in macaques. J Comp Neurol 293:299-330.

Ilinsky, I. A., Jouandet, M. L., Goldman Rakic, P. S. 1985. Organization of the nigrothalamocortical system in the rhesus monkey. J. Comp. Neurol. 236 : 3 15-30

Inase M, Sakai ST, Tanji J. (1996) Overlapping corticostriatal projections from the supplementary motor area and the primary motor cortex in the macaque monkey: an anterograde double labeling study. J Comp Neurol. 373:283–296.

Innocenti GM, Dyrby TB, Andersen KW, Rouiller EM, Caminiti R. (2017). The crossed projection to the striatum in two species of monkey and in humans: behavioral and evolutionary significance. Cereb Cortex. 27:3217-3230.

Innocenti GM, Schmidt K, Milleret C, Fabri M, Knyazeva MG, Battaglia-Mayer A, Aboitiz F, Ptito M, Caleo M, Marzi CA, Barakovic M, Lepore F, Caminiti R. (2022). The functional characterization of callosal connections. Prog Neurobiol. 208:102186.

Jarbo K, Verstynen TD. (2015) Converging structural and functional connectivity of orbitofrontal, dorsolateral prefrontal, and posterior parietal cortex in the human striatum. J Neurosci. 35:3865-78.

Jinno S, Kosaka T (2004) Parvalbumin is expressed in glutamatergic and GABAergic corticostriatal pathway in mice. J Comp Neurol. 477:188–201.

Joel D., Weiner I. (1994) The organization of the basal ganglia-thalamocortical circuits: open interconnected rather than closed segregated Neuroscience, 63 , pp. 363-379

Joel, D., Weiner, I. (1997) The connections of the primate subthalamic nucleus: indirect pathways and the open- interconnected scheme of basal ganglia-thalamocortical circuitry. Brain Res.: Brain Res. Rev. 23, 62–78.

Johnson, T. N., Rosvold, H. E. 1971. Topographic projections on the globus pallidus and the substantia nigra of selectively placed lesions in the precommissural caudate nucleus and putamen in the monkey. Exp. Neurol. 33: 584-96

Jones EG, Coulter JD, Burton H, Porter R (1977) Cells of origin and terminal distribution of corticostriatal fibers arising in the sensory-motor cortex of monkeys. J Comp Neurol. 173:53–80.

Jurgens, U. 1983. Afferent fibers to the cingular vocalization region in the squirrel monkey. Exp. Neural. 80: 395-409

Kaas JH, Hackett TA. (2000) Subdivisions of auditory cortex and processing streams in primates. Proc Natl Acad Sci USA. 97: 11793–11799.

Kaneda K, Nambu A, Tokuno H, Takada M (2002) Differential processing patterns of motor information via striatopallidal and striatonigral projections. J Neurophysiol. 88:1420–1432.

Kawaguchi Y, Wilson CJ, Emson PC (1989) Intracellular recording of identified neostriatal patch and matrix spiny cells in a slice preparation preserving cortical inputs. *J Neurophysiol* 62: 1052–1068

Kawaguchi Y., Wilson C.J., Augood S.J., Emson P.C. (1995), Striatal interneurones: chemical, physiological and morphological characterization.Trends Neurosci., pp. 527-535

Kelly RM, Strick PL. (2004) Macro-architecture of basal ganglia loops with the cerebral cortex: use of rabies virus to reveal multisynaptic circuits. Prog Brain Res. 143:449-59.

Kemp JM, Powell TP. (1970) The cortico-striate projection in the monkey. Brain. 93:525-46.

Kim, R., Nakano, K., Jayaraman, A., Carpenter, M. B. (1976) Projections of the globus pallidus and adjacent structures : An autoradiographic study in the monkey. J. Comp. Neurol. 1 69: 263-90

Kincaid AE, Wilson CJ (1996) Corticostriatal innervation of the patch and matrix in the neostriatum. *J Comp Neurol* 374: 578–592

Kitai ST, Kocsis JD, Wood J (1976) Origin and characteristics of the cortico-caudate afferents: an anatomical and electrophysiological study. Brain Res. 118:137–141.

Kreitzer A.C. (2009) Physiology and pharmacology of striatal neurons Annu. Rev. Neurosci., 32, pp. 127-147, 10.1146/annurev.neuro.051508.135422

Krienen, F.M., Goldman, M., Zhang, Q., CHDR, R., Florio, M., Machold, R., Saunders, A., Levandowski, K., Zaniewski, H., Schuman, B., Wu, C., Lutservitz, A., Mullally, C.D., Reed, N., Bien, E., Bortolin, L., Fernandez-Otero, M., Lin, J.D., Wysoker, A., Nemesh, J., Kulp, D., Burns, M., Tkachev, V., Smith, R., Walsh, C.A., Dimidschstein, J., Rudy, B., SK, L., Berretta, S., Fishell, G., Feng, G., SA, McCarroll, (2020) Innovations present in the primate interneuron repertoire. Nature 586 (7828), 262–269

Künzle H. (1975) Bilateral projections from precentral motor cortex to the putamen and other parts of the basal ganglia. An autoradiographic study in Macaca fascicularis. Brain Res. 88:195-209.

Kunzle, H. 1977. Projections from the primary somatosensory cortex to basal ganglia and thalamus in the monkey. Exp. Brain Res. 30 : 481-92

Künzle H. (1978) An autoradiographic analysis of the efferent connections from premotor and adjacent prefrontal regions (areas 6 and 9) in macaca fascicularis. Brain Behav Evol. 15:185-234.

Kuo, J. S., Carpenter, M. B. (1973) Organization of pallidothalamic projections in the rhesus monkey. J. Camp. Neural. 151 : 201-36

Lanciego, J. L., Luquin, N., & Obeso, J. A. (2012). Functional neuroanatomy of the basal ganglia. *Cold Spring Harbor perspectives in medicine*, *2*(12), a009621.

Lanciego JL (2015) Retrograde Tract-Tracing "Plus": Adding Extra Value to Retrogradely Traced Neurons. In: Neural Tracing Methods: Tracing Neurons and Their Connections (Arenkiel BL, ed), pp67-84. New York: Humana Press.

Landry P., Wilson C.J.,. Kitai S.T (1984) Morphological and electrophysiological characteristics of pyramidal tract neurons in the rat Exp. Brain Res., 57,(1) pp. 177-190, 10.1007/BF00231144

Lee AT, Vogt c D, Rubenstein JL, Sohal VS (2014) A class of GABAergic neurons in the prefrontal cortex sends long-range projections to the nucleus accumbens and elicits acute avoidance behavior. J Neurosci. 34:11519–11525.

Lehéricy S, Bardinet E, Tremblay L, Van de Moortele PF, Pochon JB, Dormont D, Kim DS, Yelnik J, Ugurbil K. (2006) Motor control in basal ganglia circuits using fMRI and brain atlas approaches. Cereb Cortex. 16:149-61.

Levesque M., Charara A., Gagnon S., Parent A., Deschenes M. (1996)a Corticostriatal projections from layer V cells in rat are collaterals of long-range corticofugal axonsBrain Res., 709 (2)), pp. 311-315

Levesque M., Gagnon S., Parent A., Deschenes (1996) Axonal arborizations of corticostriatal and corticothalamic fibers arising from the second somatosensory area in the rat Cereb. Cortex, 6 (6), pp. 759-770

Levesque M., Parent A. (1998) Axonal arborization of corticostriatal and corticothalamic fibers arising from prelimbic cortex in the rat Cereb. Cortex, 8 (7), pp. 602-613, 10.1093/cercor/8.7.602

Liles SL, Updyke BV. 1985. Projection of the digit and wrist area of precentral gyrus to the putamen: relation between topography and physiological properties of neurons in the putamen. Brain Res. 339:245-55. doi: 10.1016/0006-8993(85)90089-7

Luppino G, Matelli M, Camarda RM, Gallese V, Rizzolatti G. (1991) Multiple representations of body movements in mesial area 6 and the adjacent cingulate cortex: an intracortical microstimulation study in the macaque monkey. J Comp Neurol. 311:463–482.

Luppino G, Rozzi S, Calzavara R, Matelli M (2003) Prefrontal and agranular cingulate projections to the dorsal premotor areas F2 and F7 in the macaque monkey. Eur J Neurosci 17:559–578.

Luppino G, Ben Hamed S, Gamberini M, Matelli M, Galletti C. 2005. Occipital (V6) and parietal (V6A) areas in the anterior wall of the parieto-occipital sulcus of the macaque: a cytoarchitectonic study. Eur J Neurosci. 21:3056–3076.

Luys J. (1868). Recherches sur le Systeme Nerveux Cérébro-Spinal; sa structure, ses fonctions, ses maladies; par, J. Luys, Médecin des Hôpitaux de Paris. Paris: Bailliére.

Matelli M, Luppino G, Rizzolatti G (1985) Patterns of cytochrome oxidase activity in the frontal agranular cortex of macaque monkey. Behav Brain Res 18:125–136.

Matelli M, Luppino G, Rizzolatti G (1991) Architecture of superior and mesial area 6 and the adjacent cingulate cortex in the macaque monkey. J Comp Neurol 311:445–462.

Muakkassa, K. F., Strick, P. L. 1979. Frontal lobe inputs to primate motor cortex : Evidence for four somatotopically organized 'premotor' areas. Brain Res. 177 : 176-82

McFarland NR, Haber SN (2000) Convergent inputs from thalamic motor nuclei and frontal cortical areas to the dorsal striatum in the primate. J Neurosci. 20:3798–813.

McFarland N.R, Haber S.N. (2002) Thalamic relay nuclei of the basal ganglia form both reciprocal and non-reciprocal cortical connections, linking multiple frontal cortical areas J. Neurosci., 22, pp. 8117-8132

McGeorge AJ, Faull RL (1989) The organization of the projection from the cerebral cortex to the striatum in the rat. Neuroscience. 29:503–37.

McGuire PK, Bates JF, Goldman-Rakic PS. (1991) Interhemispheric integration: II. Symmetry and convergence of the corticostriatal projections of the left and the right principal sulcus (PS) and the left and the right supplementary motor area (SMA) of the rhesus monkey. Cereb Cortex. 1:408-17.

Melzer S, Gil M, Koser DE, Michael M, Huang KW, Monyer H. (2017) Distinct corticostriatal GABAergic neurons modulate striatal output neurons and motor activity. Cell Rep. 19:1045–1055.

Middleton FA, Strick PL (2000) Basal ganglia and cerebellar loops: motor and cognitive circuits. Brain Res Brain Res Rev. 31:236–250.

Milardi D., Gaeta M., Marino S., Arrigo A., Vaccarino G., Mormina E., et al.. (2015). Basal ganglia network by constrained spherical deconvolution: a possible cortico-pallidal pathway? *Mov. Disord.* 30, 342–349. 10.1002/mds.25995

Mink J. W. (1996). The basal ganglia: focused selection and inhibition of competing motor programs. *Progress in neurobiology*, *50*(4), 381–425.

Mishkin, M., Manning, F. 1. 1978. Nonspatial memory after selective prefrontal lesions in monkeys. Brain Res. 143 : 313-23

Morecraft RJ, Cipolloni PB, Stilwell-Morecraft KS, Gedney MT, Pandya DN. (2004) Cytoarchitecture and cortical connections of the posterior cingulate and adjacent somatosensory fields in the rhesus monkey. J Comp Neurol. 469:37–69.

Naito A., Kita H. (1994). The cortico-pallidal projection in the rat: an anterograde tracing study with biotinylated dextran amine. *Brain Res.* 653, 251–257. 10.1016

Nambu A., Tokuno H., Hamada I., Kita H., Imanishi M., Akazawa T., et al.. (2000). Excitatory cortical inputs to pallidal neurons *via* the subthalamic nucleus in the monkey. *J. Neurophysiol.* 84, 289–300. 10.1152

Nambu A., Tokuno H., Takada M. (2002). Functional significance of the cortico-subthalamo-pallidal 'hyperdirect' pathway. *Neurosci. Res.* 43, 111–117. 10.1016

Nambu A (2004) A new dynamic model of the cortico-basal ganglia loop. *Prog Brain Res* 143: 461–466

Nambu A (2009) Dynamic Model of the Basal Ganglia Functions and Movement Disorders Systems Biology, 91:10.1007

Nambu A (2011) Somatotopic organization of the primate basal ganglia. Front Neuroanat. 5:26.

Napieralski JA, Butler AK, Chesselet MF. (1996) Anatomical and functional evidence for lesion-specific sprouting of corticostriatal input in the adult rat. J. Comp. Neurol. 373, 484–497.

Neumann W. J., Jha A., Bock A., Huebl J., Horn A., Schneider G. H., et al.. (2015). Cortico-pallidal oscillatory connectivity in patients with dystonia. *Brain* 138, 1894–1906. 10.1093/brain/awv109

Nauta, W. J. H., Mehler, W. R. 1966. Projections of the lentiform nucleus in the monkey. Brain Res. 1 : 3--42

Oguchi M, Tanaka S, Pan X, Kikusui T, Moriya-Ito K, Kato S, Kobayashi K, Sakagami M. (2021) Chemogenetic inactivation reveals the inhibitory control function of the prefronto-striatal pathway in the macaque brain. Commun Biol. 4:1088.

Oka H (1980) Organization of the cortico-caudate projections. A horseradish peroxidase study in the cat. Exp Brain Res. 40:203–208.

Pandya DN, Seltzer B. (1982) Intrinsic connections and architectonics of posterior parietal cortex in the rhesus monkey. J Comp Neurol. 204:196–210.

Parent, A., Bouchard, c., Smith, Y. (1984)a. The striatopallidal and striatonigral projections : Two distinct fiber systems in primate. Brain Res. 303 : 385-90

Parent, A., Smith, Y., Bellefeuille, L. (1984)b. The output organization of the pallidum and substantia nigra in primate as revealed by a retrograde double-labeling method. In The Basal Ganglia, Structure and Function, eds. J. S. McKenzie, R. E. Kemm, L. N. Wilcock, pp. 1 47-60. New York : Plenum

Parent M, Parent A (2006) Single-axon tracing study of corticostriatal projections arising from primary motor cortex in primates. J Comp Neurol. 496:202–213.

Parent A. (2013). The history of the basal ganglia: the contribution of Karl Friedrich Burdach. *Neurosci. Med.* 03, 374–379. 10.4236/nm.2012.34046

Parthasarathy HB, Schall JD, Graybiel AM. (1992) Distributed but convergent ordering of corticostriatal projections: analysis of the frontal eye field and the supplementary eye field in the macaque monkey. J Neurosci. 12:4468-88

Percheron G., Filion M. (1991) Parallel processing in the basal ganglia: up to a point TINS, 14 pp. 55-59 Perth CB, Kuhar MI, Snyder SH (1976) Opiate receptor: Autoradiographic localization in rat brain. *Proc Natl Acad Sci* 73: 3729–3733

Pettine WW, Steinmetz NA, Moore T (2019) Laminar segregation of sensory coding and behavioral readout in macaque V4. Proc Natl Acad Sci U S A. 116:14749–14754.

Ragsdale CW, Graybiel AM (1988) Fibers from the basolateral nucleus of the amygdala selectively innervate striosomes in the caudate nucleus of the cat. *J Comp Neurol* 269: 506–522

Reiner A., Medina L., Veenman C. L. (1998). Structural and functional evolution of the basal ganglia in vertebrates. *Brain Res. Rev.* 28, 235–285. 10.1016

Reiner A. , Jiao Y., Del Mar N., . Laverghetta A.V, Lei W.L. (2003) Differential morphology of pyramidal tract-type and intratelencephalically projecting-type corticostriatal neurons and their intrastriatal terminals in rats J. Comp. Neurol., 457 (4), pp. 420-440

Reiner A, Hart NM, Lei W, Deng Y (2010) Corticostriatal projection neurons - dichotomous types and dichotomous functions. Front Neuroanat. 4:142.

Reveley C, Gruslys A, Ye FQ, Samaha J, Glen D, Russ B, Saad Z, Seth A, Leopold DA, Saleem KS (2017) Three-dimensional digital template atlas of the macaque brain. Cereb Cortex 27: 4463-4477.

Rock C, Zurita H, Wilson C, Apicella AJ (2016) An inhibitory corticostriatal pathway. Elife. 9;5.

Royce GJ (1982) Laminar origin of cortical neurons which project upon the caudate nucleus: a horseradish peroxidase investigation in the cat. J Comp Neurol. 205:8–29.

Rozzi S, Calzavara R, Belmalih A, Borra E, Gregoriou GG, Matelli M, Luppino G (2006) Cortical connections of the inferior parietal cortical convexity of the macaque monkey. Cereb Cortex 16:1389 –1417.

Sadikot AF, Parent A, François C (1992)a. Efferent connections of the centromedian and parafascicular thalamic nuclei in the squirrel monkey: A PHA-L study of subcortical connections. *J Comp Neurol* 315: 137–159

Sadikot AF, Parent A, Smith Y, Bolam JP (1992)b. Efferent connections of the centromedian and parafascicular thalamic nuclei in the squirrel monkey: A light and electron microscopic study of the thalamostriatal projection in relation to striatal heterogeneity. *J Comp Neurol* 320: 228–242

Saga Y, Hirata Y, Takahara D, Inoue K, Miyachi S, Nambu A, Tanji J, Takada M, Hoshi E. (2011) Origins of multisynaptic projections from the basal ganglia to rostrocaudally distinct sectors of the dorsal premotor area in macaques. Eur J Neurosci. 33:285–297.

Saint-Cyr JA, Ungerleider LG, Desimone R (1990) Organization of visual cortical inputs to the striatum and subsequent outputs to the pallido-nigral complex in the monkey. J Comp Neurol. 298:129–156.

Saleem KS, Kondo H, Price JL. (2008) Complementary circuits connecting the orbital and medial prefrontal networks with the temporal, insular, and opercular cortex in the macaque monkey. J Comp Neurol. 506:659–693.

Saleem KS, Logothetis NK. (2012) A combined MRI and histology atlas of the rhesus monkey brain in stereotaxic coordinates. In: With horizontal, coronal, and sagittal series. 2nd ed. San Diego: Academic Press/Elsevier.

Saleem KS, Miller B, Price JL. (2014) Subdivisions and connectional networks of the lateral prefrontal cortex in the macaque monkey. J Comp Neurol. 522:1641–1690.

Seidler RD, Noll DC, Chintalapati P. (2006) Bilateral basal ganglia activation associated with sensorimotor adaptation. Exp Brain Res. 175:544-55.

Shepherd GM (2013) Corticostriatal connectivity and its role in disease. Nat Rev Neurosci 14:278-291

Sohur US, Padmanabhan HK, Kotchetkov IS, Menezes JR, Macklis JD. (2014) Anatomic and molecular development of corticostriatal projection neurons in mice. Cereb Cortex. 24:293-303.

Somogyi P, Bolam JP, Totterdell S, Smith AD (1981). Monosynaptic input from the nucleus accumbens-ventral striatum region to retrogradely labelled nigrostriatal neurones. *Brain Res* 217: 245–263.

Stephenson-Jones M., Ericsson J., Robertson B., Grillner S. (2012). Evolution of the basal ganglia: dual-output pathways conserved throughout vertebrate phylogeny. *J. Comp. Neurol.* 520, 2957–2973. 10.1002

Strick PL, Dum RP, Picard N (1995) Macro-organization of the circuits connecting the basal ganglia with the cortical motor areas. In: Models of information processing in the basal ganglia (Houk G, ed), pp117–130. Bost

Szabo, J. 1962. Topical distribution of the striatal efferents in the monkey. Exp. Neurol. 5 : 21-36

Szabo, J. 1967. The efferent projections ofthe putamen in the monkey. Exp. Neurol. 19: 463-76 on: MIT Press.

Takada M, Tokuno H, Nambu A, Inase M (1998) Corticostriatal projections from the somatic motor areas of the frontal cortex in the macaque monkey: segregation versus overlap of input zones from the primary motor cortex, the supplementary motor area, and the premotor cortex. Exp Brain Res. 120:114–128.

Takada M, Tokuno H, Hamada I, Inase M, Ito Y, Imanishi M, Hasegawa N, Akazawa T, Hatanaka N, Nambu A. (2001) Organization of inputs from cingulate motor areas to basal ganglia in macaque monkey. Eur J Neurosci. 14:1633–1650.

Takada M, Hoshi E, Saga Y, Inoue K, Miyachi S, Hatanaka N, Inase M, Nambu A. (2013) Organization of two cortico-basal ganglia loop circuits that arise from distinct sectors of the monkey dorsal premotor cortex. In: Barrios FA, Bauer C, editors. Basal ganglia—an integrative view. InTech. p. 103–116.

Tanaka D Jr (1987) Differential laminar distribution of corticostriatal neurons in the prefrontal and pericruciate gyri of the dog. J Neurosci. 7:4095–4106.

Tanaka K. (1996) Inferotemporal cortex and object vision. Annu Rev Neurosci. 19:109–139

Tepper J.M., Bolam J.P. (2004),Functional diversity and specificity of neostriatal interneurons. Curr Op Neurobiol, pp. 685-692

Tepper J.M., Tecuapetla F., Koos T., Ibanez-Sandoval O. (2010).Heterogeneity and diversity of striatal GABAergic interneurons Front. Neuroanat., p. 150, 10.3389

Thomson AM (2010) Neocortical layer 6, a review. Front Neuroanat. 4:13.

Tobias, T. J. 1975. AlTerents to prefrontal cortex from the thalamic mediodorsal nucleus in the rhesus monkey. Brain Res. 83 : 191-212

Tomioka R, Rockland KS (2007) Long-distance corticocortical GABAergic neurons in the adult monkey white and gray matter. J Comp Neurol. 505:526–538.

Uryu K, MacKenzie L, Chesselet MF. (2001) Ultrastructural evidencefor differential axonal sprouting in the striatum after thermocoagulatory and aspiration lesions of the cerebral cortex in adult rats. Neuroscience 105, 307–316.

Veening JG, Cornelissen FM, Lieven PA (1980) The topical organization of the afferents to the caudatoputamen of the rat. A horseradish peroxidase study. Neuroscience. 5:1253–1268.

Vogt, B. A., Rosene, D. L., Pandya, D. N. (1979) Thalamic and cortical afferents differentiate anterior from posterior cingulate cortex in the monkey. Science 204 : 205-7

Wall NR, De La Parra M, Callaway EM, Kreitzer AC (2013) Differential innervation of direct- and indirect-pathway striatal projection neurons. Neuron. 79:347–360.

Wilson C.J. (1987) Morphology and synaptic connections of crossed corticostriatal neurons in the ratJ. Comp. Neurol., 263 (4), pp. 567-580

Wymbs NF, Bassett DS, Mucha PJ, Porter MA, Grafton ST. (2012) Differential recruitment of the sensorimotor putamen and frontoparietal cortex during motor chunking in humans. Neuron 74, 936–946.

Yelnik J., Francois C., Percheron G. (1997) Spatial relationships between striatal axonal endings and pallidal neurons in macaque monkeys Adv. Neurol., 74, pp. 45-56

Yelnik J. (2002). Functional anatomy of the basal ganglia. *Movement disorders : official journal of the Movement Disorder Society*, *17 Suppl 3*, S15–S21.

Yeterian EH, Pandya DN (1993) Striatal connections of the parietal association cortices in rhesus monkeys. J Comp Neurol. 332:175–997.

Yeterian EH, Pandya DN (1994) Laminar origin of striatal and thalamic projections of the prefrontal cortex in rhesus monkeys. Exp Brain Res. 99:383–398.